Janis Michael Zoder, MSc

# Validation and Optimization of Determination Methods for Structural Carbohydrates and Lignin in Biomass

**MASTER'S THESIS**

to achieve the university degree of

Diplom-Ingenieur

Master's degree programme:

Advanced Material Science

submitted to

**Graz University of Technology**

**Supervisor:**

Univ.-Prof. Dipl.-Ing. Dr.techn. Ulrich Hirn

**Co-Supervisor:**

Dipl.-Ing. Roman Poschner, BSc

Institute of Bioproducts and Paper Technology

Graz, February 2024

Abstract (DE):

Analyseergebnisse von Biomasse unterliegen einer natürlichen Schwankung durch Herkunft und inhomogene Zusammensetzung. Ziel dieser Arbeit war es, aktuelle Analysemethoden zu testen und optimieren. Grundlage dafür war die NREL LAP 42618 – „Bestimmung von Strukturkohlenhydraten und Lignin“. Es konnte gezeigt werden, dass die gravimetrische Bestimmung des Klason Lignins durch unaufgelöste und unlösliche Probenbestandteile einen falsch höheren Lignin Gehalt verursachten. Bei der Hydrolyse entstandene Furan Derivate erschwerten die UV/Vis-Spektroskopie des säurelöslichen Lignins. Kohlenhydrate wurden mit zwei Flüssigchromatographen mit verschiedenen Detektoren (Brechungsindexdetektor (RID) und gepulster amperometrischer Detektor (PAD)) bestimmt. Ein Vergleich ergab, dass das bevorzugte RID-System bessere Linearität erzielte und eine Messung der unverdünnten Probenflüssigkeiten ermöglichte.

Ein Ringversuch zwischen TU-Graz (TUG), TU-Wien (TUW) und Celignis Analytical (CA) wurde an fünf Lignozellulose-Biomassen durchgeführt. Es zeigte sich, dass die Klason-Lignin Bestimmung mit großen Schwankungen und Fehlern behaftet war. Besonders für Lignin-arme Proben wie gebleichtes Papier (0,74 bis 11,08 m%). Für säurelösliches Lignin wurden durchgehend Konzentrationen zwischen 0,6 und 1,2 m% bestimmt, außer gebleichtes Papier (0,4 bis 0,7 m%). Ein Vergleich der Kappa-Zahlen führte zu dem Ergebnis, dass NREL in 11 von 15 Fällen einen bis zu 6,5 m% höheres Gesamtlignin ergab. Die Zucker Arabinose und Galactose (<1 m%) konnten nur von CA und TUW quantitativ nachgewiesen werden. Für TUG lagen diese beiden Zucker unterhalb der Nachweisgrenze. Die Summenparameter wurden zwischen 93 und 108 m% ermittelt.

Als mögliche Lignin Bestimmungsmethode wurde die L-Cystein-unterstützte Schwefelsäureauflösungsmethode (CASA) verwendet. Da derzeit keine Absorptionskoeffizienten verfügbar sind, eignet sich die CASA-Methode zur Schätzung und Relativierung von Kohlenhydraten und Lignin. Um eine quantitative Bestimmung des Gesamtlignins zu versuchen, wurde aus einer Klason-Lignin Probe ein Absorptionskoeffizient nach dem Lambert-Beer Gesetz ermittelt. Ein Wiederfindungstest ergab zufriedenstellende Wiederfindungen von 115 bis 116 %.

Abstract (EN):

Analysis results of biomass are subject to natural variation due to origin and inhomogeneous composition. The aim of this work was to test and optimize current analysis methods. The basis of this work was NREL LAP 42618 - "Determination of Structural Carbohydrates and Lignin". It could be shown that the gravimetric determination of Klason lignin caused a falsely higher lignin content due to undissolved and insoluble sample components. Furan derivatives formed during hydrolysis made UV/Vis spectroscopy of the acid-soluble lignin difficult. Carbohydrates were determined using two liquid chromatographs with different detectors (refractive index detector (RID) and pulsed amperometric detector (PAD)). A comparison showed that the preferred RID system achieved better linearity and allowed measurement of the undiluted sample liquids.

A round robin test between TU-Graz (TUG), TU-Vienna (TUW) and Celignis Analytical (CA) was carried out on five lignocellulose biomasses. It was found that the Klason lignin determination was subject to large fluctuations and errors. Especially for low lignin samples such as bleached paper (0.74 to 11.08 m%). For acid-soluble lignin, concentrations between 0.6 and 1.2 m% were consistently determined, except for bleached paper (0.4 to 0.7 m%). A comparison of the kappa number showed that NREL gave up to 6.5 m% higher total lignin in 11 out of 15 cases. The sugars arabinose and galactose (<1 m%) could only be quantitatively detected by CA and TUW. For TUG, these two sugars were below the detection limit. The sum parameters were determined to be between 93 and 108 m%.

The L-cysteine-assisted sulfuric acid dissolution method (CASA) was used as a possible lignin determination method. Since no absorption coefficients are currently available, the CASA method is suitable for estimating and relativizing carbohydrate and lignin. To attempt a quantitative determination of total lignin, an absorption coefficient was determined using a Klason lignin sample and Lambert-Beer law. A recovery test resulted in satisfactory recoveries of 115 to 116 %.

# Content:

# 1. Introduction

## 1.1. Biomass

The term biomass summarizes the sum of the material mass of all carbon-based living beings and organisms. This includes living, dead, moving and stationary organisms in the biosphere. The biosphere refers to the totality of all areas of a celestial body in which living organisms occur. For the Earth, it refers to the sum of all ecosystems or, more generally, the zones of life on Earth. The term biomass has different meanings in different areas and contexts. In biotechnology, for example, this term is used as the sum of all microorganisms that are used to manufacture products. In the energy industry, biomass is regarded as a raw material for energy production. The most general term for biomass is used in an ecological context. As defined above, the mass of living biological organisms is considered, but in a specific area or volume or ecosystem at a specific point in time. [7, 59, 85, 132]

Biomass can be typified based on three different criteria. These criteria and the respective types of biomasses result from the different ecological concepts of biomass. The three criteria are a) the water content, b) the origin of the biomass and c) the vitality of the biomass. [85]

- In a), the biomass is divided into fresh biomass, mass with water, and dry biomass, mass without water.
- For b), biomass is divided into biomass from plants (phytomass), biomass from animals (zoomass) and biomass from microorganisms (microbial mass).
- In c) the biomass is divided into two groups: the living biomass, where the mass is on or in living organisms, and the dead biomass, where the mass is on or in dead organisms or is dead.

The subunits or building blocks of biomass are limited to the three main groups of carbohydrates, lipids, and proteins. These three are the pillars of all living and dead organisms on earth. The predominant carbohydrates in biomass are simple molecules consisting of the elements carbon, oxygen, and hydrogen, which can be assembled in different ways to form complex structures with unique properties. For example, the simple monomeric unit glucose can be arranged into cellobiose (a water-soluble substance), starch (a moderately water-soluble substance) or cellulose (a water-insoluble substance). Carbohydrates are primarily used by animals and microorganisms

as a source of energy, while plants utilize them for energy storage and structure formation. [32, 90, 130, 135, 136]

The next group are the lipids. They have the same elemental composition as carbohydrates, but with a much lower oxygen content. They occur primarily as triglycerides, which are tri-esters consisting of a glycerol (a tri-ol) bound to three fatty acid molecules. These compounds are more soluble in water than the individual fatty acids (>5 C atoms), which are insoluble in water. In organisms, lipids are used as energy stores, energy sources and structural elements in cell membranes. [90, 110, 126]

The last group are proteins and enzymes. They are synthesized from their monomeric units, the amino acids. Amino acids are organic compounds that contain the elements carbon, oxygen, and hydrogen as well as nitrogen and sulfur. They contain an amino and a carboxylic acid group as well as a third group, the side chain, which ranges from non-polar (aliphatic, acyclic, and aromatic groups) to polar groups (hydroxyl, sulfur, amine and acid groups). They also have a wide range of electrical properties, as they can occur as cations, anions, neutral and zwitterionic species. These amino acids can be arranged to form proteins, which fulfil structural tasks in organisms, and enzyme complexes, which perform important functions in organisms for metabolism, synthesis, synthesis and degradation as well as signaling and regulation. [32, 41, 67, 71, 135]

Biomass is a renewable organic material that comes from plants and animals. As organisms have developed in such a way that they can survive under certain environmental conditions, there are major differences in the composition of the building blocks (at macro and micro level) and in the physical and chemical properties of biomass. [88, 132]

A major advantage of biomass is the unlimited and freely renewable capacity of these raw materials in the biosphere. This can reduce the need for fossil raw materials for human society. The wide availability of this biomass also enables independence and reduces the need for imports and exports as well as the risks. In addition to these advantages of biomass utilization, however, there are also the short-term economic disadvantages of building industrial plants to process biomass. There are also many gaps in the research needed to describe, understand and utilize biological products. [7, 85, 88, 132, 134]

## 1.2. Carbohydrates & Structural Carbohydrates

Carbohydrates are found in the metabolism of all living organisms on earth and are the most abundant biomolecules on the planet. In living organisms, they serve as a source of energy for biological activities or play a role in building structures. From a chemical point of view, carbohydrates are simple molecules consisting of carbon (C), hydrogen (H) and oxygen (O) atoms. Their empirical formula is a multiple (>2) of $C_x(H_2O)_y$ where x and y can be different. [42, 85]

The simplest carbohydrates are the sugars and saccharides with the empirical formula $(CH_2O)_n$, where n > 2. The class of sugars can be divided into three groups. The 1) monosaccharides, the 2) disaccharides and the 3) polyols. [26, 35, 98, 135, 136]

1) The subclass of monosaccharides describes the simplest sugars available for carbohydrates. This group of solids is (under standard conditions (25°C and 1.013 bar)) usually colorless, very soluble in water and crystalline. A well-known example of this group is the 6-carbon sugar glucose, which is also the most abundant monosaccharide on earth, as it is synthesized by plants and some algae through photosynthesis. Other important examples are fructose, xylose, and galactose visible in Figure 1. An overview of these monosaccharides is shown in Figure 1 & Figure 2. Monosaccharides are categorized according to the number of carbon atoms in their backbone. They are categorized as triose (3 carbon atoms), tetrose (4 carbon atoms), pentose (5 carbon atoms) and hexose (6 carbon atoms). In addition to this categorization according to the number of carbon atoms in the backbone, the position of the functional group is also a categorization criterion. In the following Figure 1 & Figure 2 the class of monosaccharides are shown. [81]

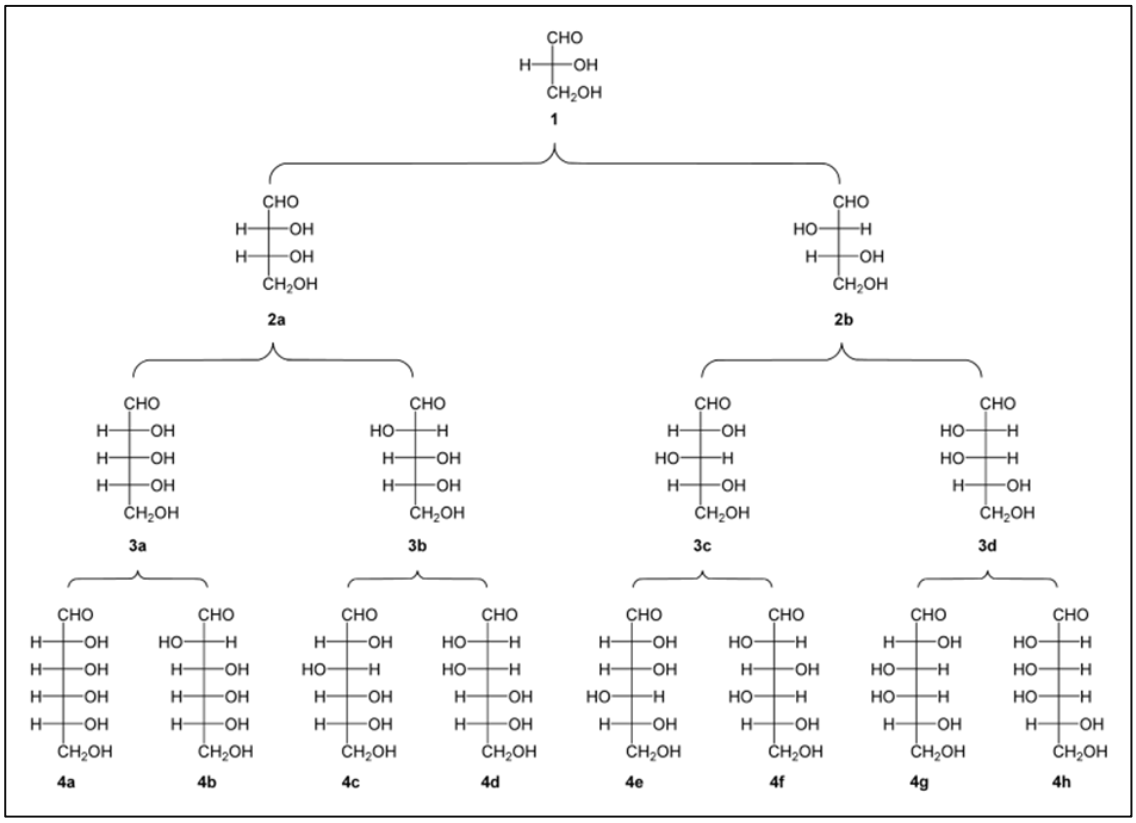


*Figure 1_Family tree of aldoses in Fischer projection; the simple aldosaccharide D-glyceraldehyde (**1**) (3 C atoms/triose), a derivative of glycerol; the basic structure is extended by adding CH-OH groups so that other sugars can be derived; Tetroses are D-erythrose (**2a**) and D-threose (**2b**); pentoses are D-ribose (**3a**), D-arabinose (**3b**), D-xylose (**3c**) and D-lyxose (**3d**); hexoses are D-allose (**4a**), D-altrose (**4b**), D-glucose (**4c**), D-mannose (**4d**), D-gulose (**4e**), D-idose (**4f**), D-galactose (**4g**) and D-talose (**4h**) (Wikimedia Commons)*

If the first carbon atom is functionalized with an aldehyde group (-H(C=O)), the saccharide is called aldose, shown in Figure 1. If the second carbon atom is functionalized with a ketone group (-C=O), the saccharide is called a ketose, which are shown in Figure 2. [81]

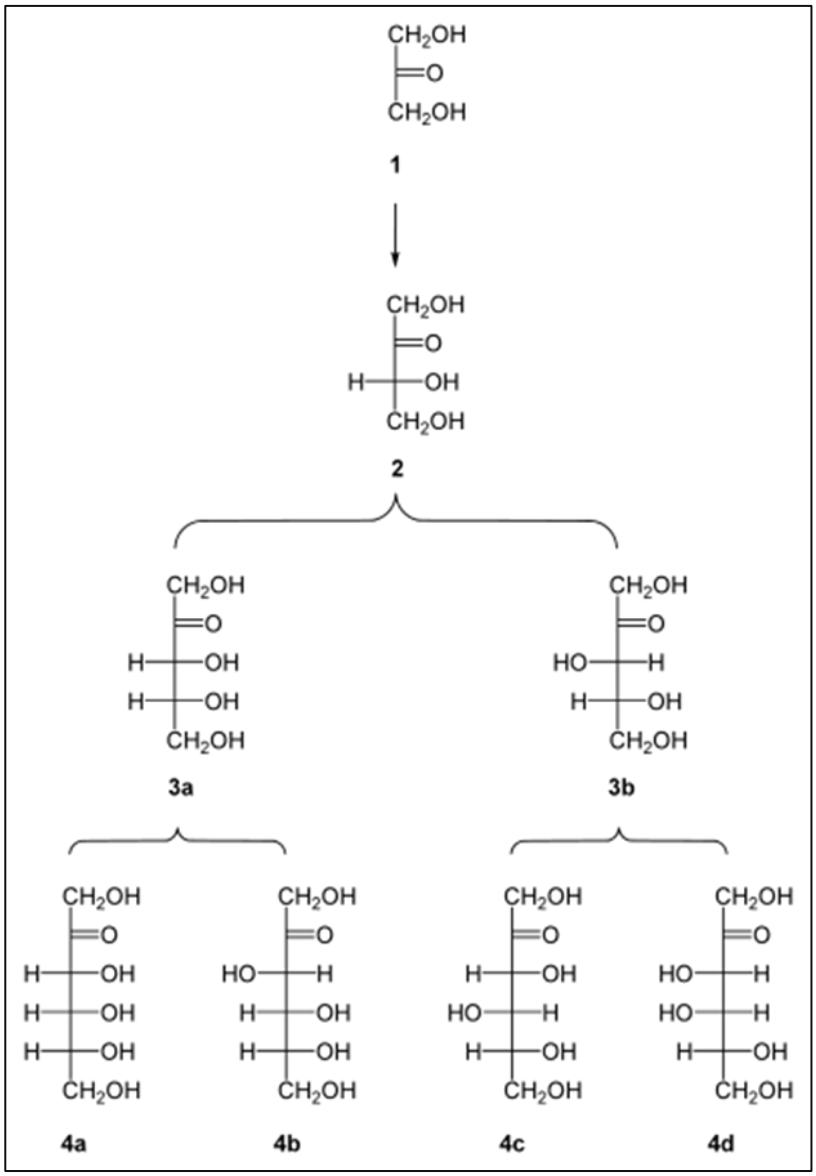


*Figure 2_Family tree of ketoses in Fischer projection; the simplest ketose dihydroxyacetone (**1**), a glycerol derivative; the addition of CH-OH groups expands the basic structure and leads to other ketoses; the tetrose D-erythrulose (**2**); the two pentoses are D-ribulose (**3a**) and D-xylulose (**3b**); hexoses are D-psicose (**4a**), D-fructose (**4b**), D-sorbose (**4c**) and D-tagatose (**4d**) (Wikimedia Commons)*

In addition to the chemical structure of monosaccharides, their physical properties are also used as a criterion. As monosaccharides are chiral molecules, demonstrated in Figure 3, which describes a property of asymmetry and means that they are distinguishable from their mirror image, they have a relative configuration known as the D or L configuration (they are optically active). [26, 28, 81, 90, 135, 136]

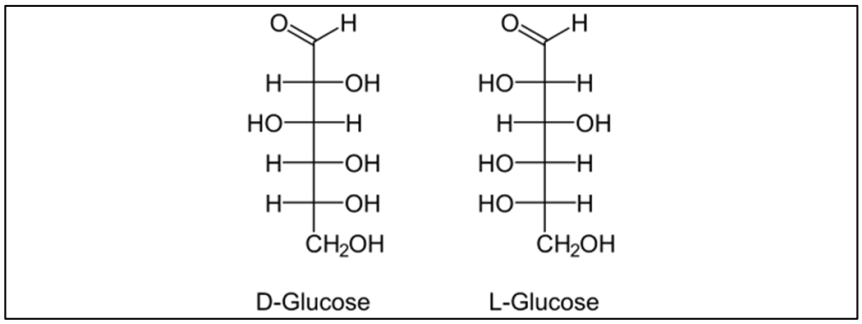


*Figure 3_The chirality of glucose; the penultimate C atom determines the D/L configuration; D- if the hydroxyl (-OH) is on the right-hand side and L- if -OH is on the left-hand side (Wikimedia Commons)*

When using linearly polarized light, these two configurations can be distinguished by optical rotation. The prefix (+) means clockwise rotation (rotates the polarization axis clockwise) and the prefix (-) means anti-clockwise rotation (rotates the polarization anti-clockwise). The device for determining the angle of rotation using polarized transmitted light is called a polarimeter. The structure of a polarimeter is shown in Figure 4. A summary example: D-(+)-glucose is a monosaccharide in which the penultimate carbon atom has its -OH group on the right-hand side, and the polarimetry experiment shows a clockwise rotation of the polarized light. [22, 43]

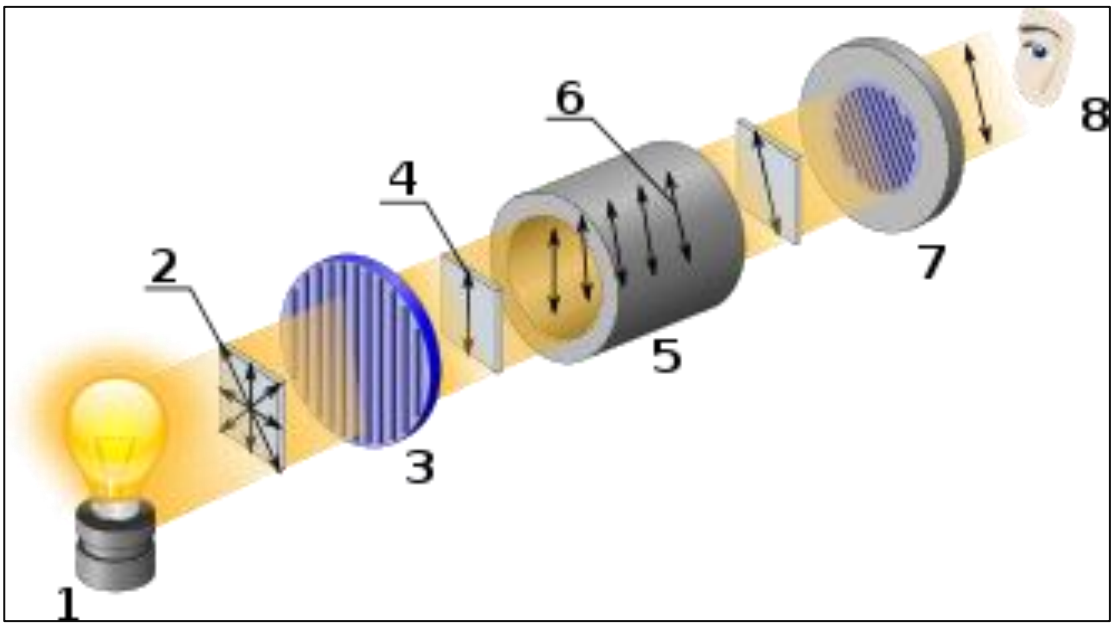


*Figure 4_ Operating principle of an optical polarimeter; the light source (1) generates unpolarized light (no orientation) (2); a linear polarizer (3) generates linearly polarized light (4); the sample tube (5) with optically active molecules rotates the polarized light (6); the angle of rotation is recorded and evaluated (7&8) (Wikimedia Commons)*

In addition to the open-chain D/L form, another possible orientation of the monosaccharides is the cyclic form with an α/β prefix. In the next Figure 5 several projections are shown for the same molecule. Here, a cyclisation reaction takes place through a nucleophilic addition reaction between the carbonyl group and a hydroxyl group of the same molecule. [26, 28]

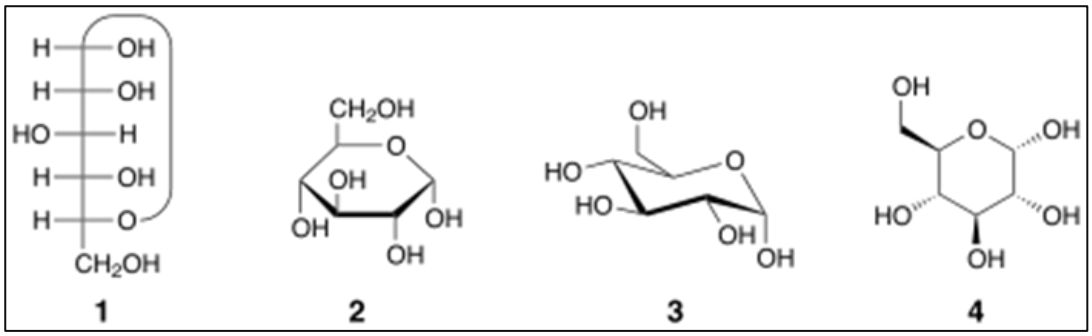


*Figure 5_Cyclisation of glucose to α-D-glucopyranose in the Fischer/Tollens projection (**1**), the Haworth ring projection (**2**), the conformational formula (chair conformation) (**3**) and the stereochemical view (**4**) (Wikimedia Commons)*

This leads to a ring system with C atoms and an O atom. If the linear form was an aldose, the cyclic molecule has a hemiacetal group; if the linear form was a ketose, the new molecule has a hemiacetal group. This reaction behavior and outcome is demonstrated in the following Figure 6. [26, 28, 90]

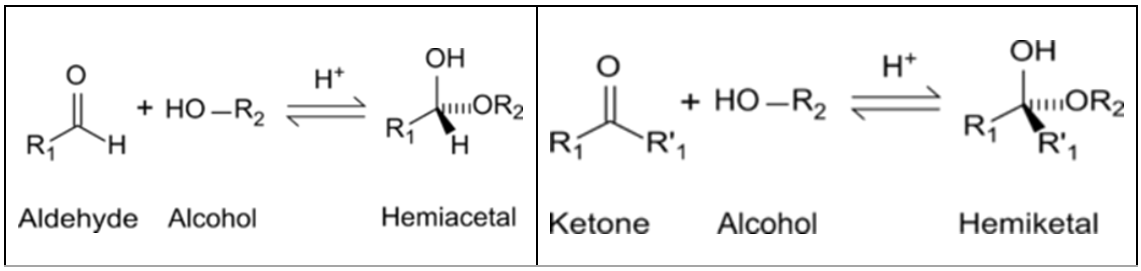


*Figure 6_The difference between hemiacetal and hemiketal in the cyclisation of monosaccharides; the hemiacetal has a hydrogen atom, while the hemiketal has an additional R' group (Wikimedia Commons)*

As a monosaccharide molecule has several -OH groups for cyclisation, two forms are possible. A ring molecule with five atoms, called furanose, and a ring molecule with six atoms, called pyranose, derived from molecule furan and pyran. These structures are demonstrated in the following Figure 7. [28, 90]

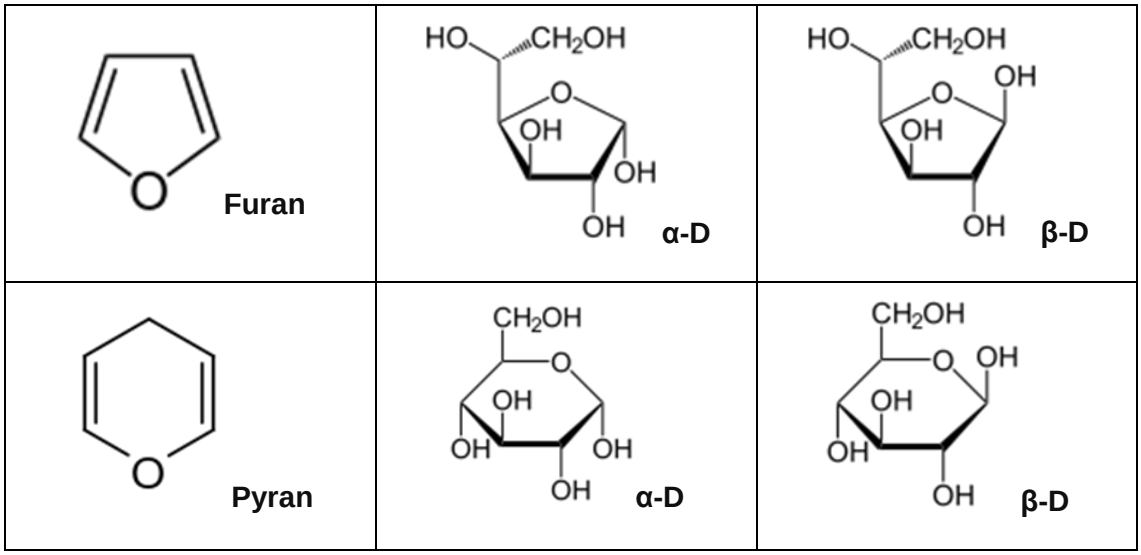


*Figure 7_Structure of glucose in 5-atom ring (glucofuranose) and 6-atom ring (glucopyranose) formation (Wikimedia Commons)*

This cyclic form is favored for many monosaccharides, either in solid form and/or in solutions. As two different positions of the -OH group are possible for ring closures, the prefixes α/β are used for separation. Most monosaccharides are synthesized in living plants by oxygenic photosynthesis. The monosaccharides are synthesized from $CO_2$ (carbon dioxide) from the air and the hydrogen atoms contained in $H_2O$ (water) with the help of solar energy. During the necessary water splitting, oxygen is released as a waste product. [26, 28, 90, 135]

2) A disaccharide is described by the glycosidic bond (ether bond) of exactly two monosaccharides shown in Figure 8 & Figure 9. They are also easily soluble in water and are colorless solids. Examples of this group are cellobiose (Figure 8**c**) (the disaccharide of cellulose by β-(1→4) linkage), lactose (or milk sugar, by linking galactose and glucose), maltose (Figure 8**m**) (or malt sugar, by linking glucose in an α(1→4) linkage) and the well-known sucrose (by linking glucose and fructose). [31]

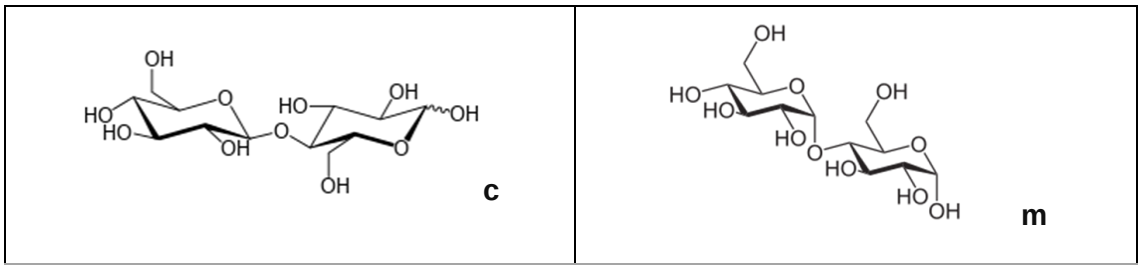


*Figure 8_Structure of cellobiose (**c**) and maltose (**m**) to see the difference in linkage; C is β-(1→4) linked and M is α(1→4) linked (Wikimedia Commons)*

In chemistry, the binding process is known as condensation which is demonstrated in Figure 9 for glucose forming maltose. In a condensation reaction, two molecules (monosaccharides) react and form a new molecule (disaccharide). In this synthesis pathway, a water molecule is formed during condensation, which is released as a by-product. The reverse reaction, in which this bond is broken, is called hydrolysis. Water and a catalyst (enzyme or acid) are required for this step. [26, 31, 135, 136]

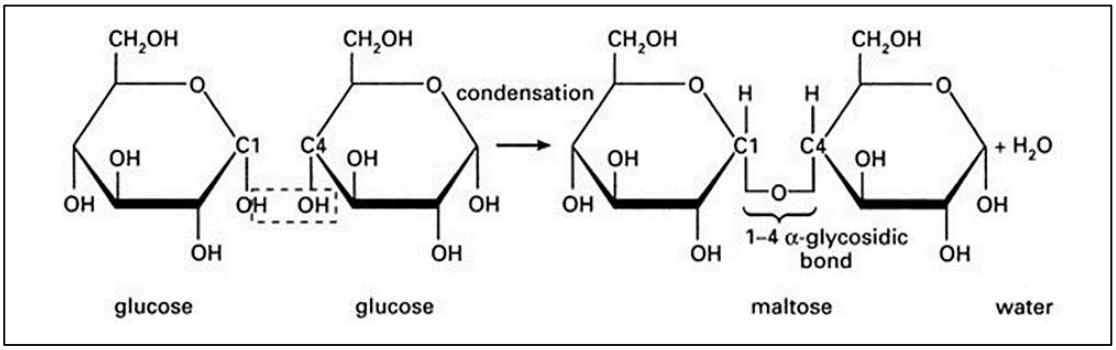


*Figure 9_Condensation reaction of two glucose monomer by forming maltose and a single water molecule [125]*

3) The subgroup of polyols, or sugar alcohols in this case, describes hydrogenated sugar molecules. These modified sugar molecules are exemplary visible in Figure 10 and are formed by a reduction reaction (addition of hydrogen atoms) in which certain oxygen-containing functional groups are converted into an -OH group. Compared to the other two groups, the properties of sugar alcohols are different. For example, they are not broken down by oral bacteria. Compared to sucrose, they also have a lower nutritional value and a lower sweetness and do not caramelize when heated. In the food industry, these sugar alcohols are used as sweeteners and sugar substitutes. [35, 65, 78, 124]

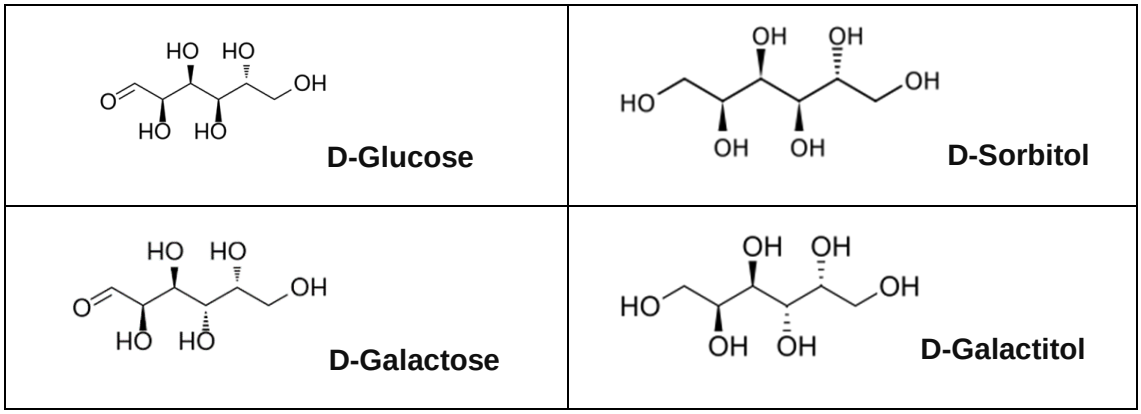


*Figure 10_The monosaccharides glucose and galactose with their reduced sugar alcohols sorbitol and galactitol (Wikimedia Commons)*

In addition to the class of sugars (monosaccharides), carbohydrates contain the two other classes of saccharides, namely a) oligosaccharides and b) polysaccharides. They differ in their degree of polymerization, which is equal to 1 for sugars, <9 for oligosaccharides and >9 for polysaccharides. For the sake of completeness, it should be mentioned that the degree of polymerization (DP) for homopolymers (only a single monomeric unit) is defined as the number of monomeric units in a macromolecule or polymer. Mathematically, the DP is calculated as the ratio of the average molecular weight $M_n$ divided by the molecular weight of the monomer unit $M_0$. If the DP is equal to 1, the sample molecule is a monomer. As the DP increases, the physical properties also change. For example, the easily soluble monomer glucose (DP=1) becomes completely insoluble in any solvent when it polymerases to the cellulose polymer (DP~3000) of cotton. [5, 46, 90]

a) Oligosaccharides are polymers of monosaccharides with a monomer repeat of <9. This leads to the fact that disaccharides are a type of oligosaccharide.

b) Polysaccharides are long-chain polymeric carbohydrates. They consist of monosaccharide units that are linked together by glycosidic bonds. Compared to other sugars with a DP < 9, polysaccharides can form micro- and macrostructures that can be linear and/or branched which is demonstrated in Figure 11. A well-known example of a linear polysaccharide is the cellulose in wood. It consists only of glucose monomers and forms structures ranging from small fibrils to complex hierarchical wood structures. Glycogen, the polysaccharide used to store energy, is an example of highly branched polymers. [36, 74]

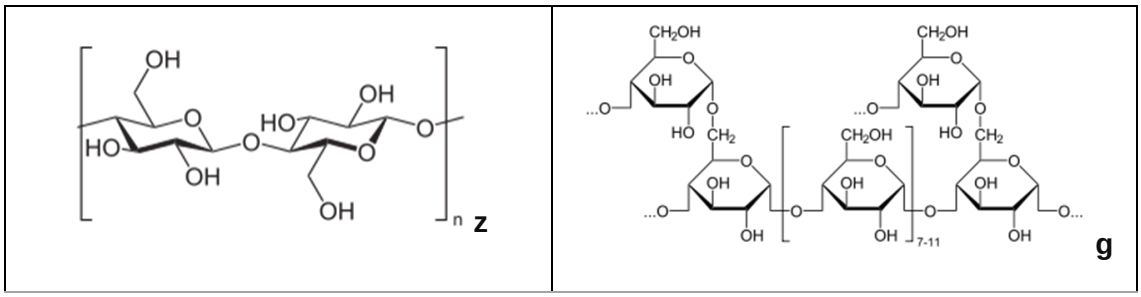


*Figure 11_The linear structure of the structural polysaccharide cellulose (11**z**) and the highly branched structure of the storage polysaccharide glycogen (11**g**) (Wikimedia Commons)*

The degradation of polysaccharides is called hydrolysis and requires water and the presence of a catalyst (acid or enzymes). This reaction produces monosaccharides, oligosaccharides, and other degradation products such as furfurals, depending on which polymer is hydrolyzed. Compared to their monomeric unit, polysaccharides exhibit a

wide range of physical and chemical properties. Glucose, for example, is highly soluble in water, whereas cellulose is insoluble in water and other solvents. In addition, cellulose cannot be melted. [26, 74, 90, 135, 136]

As these biopolymers are often natural products, they also exhibit heterogeneity in that they contain a different monomer as a modification of the repeating unit. Such a polymer is called a heteropolysaccharide. If only the monomeric unit is the repeating unit, such a polymer is called a homopolysaccharide. As a biological biopolymer, they fulfil a variety of functions. Depending on their function in living organisms, two main groups can be distinguished: (1) structural and (2) storage-related functions. [35, 48, 74, 133]

1) Structural polysaccharides are used in living organisms to build up, resist and protect against environmental influences. The biopolymers arabinoxylans (**a**), cellulose (11**z**), chitin (12**i**) and pectin (13**p**) are listed in this group.

Arabinoxylan (12**a**) is a hemicellulose, a heteropolysaccharide containing arabinose and xylose as a repeating monomeric unit. The structure of arabinoxylan is shown in Figure 12**a**. The monomer chain is composed of 1,4-linked β-D-xylopyranosyl units, which may be substituted with up to two α-L-arabinofuranosyl units. Its main purpose is to be used as a structural component in plant cells and as a carrier for various acids for defense against fungal attack. [115]

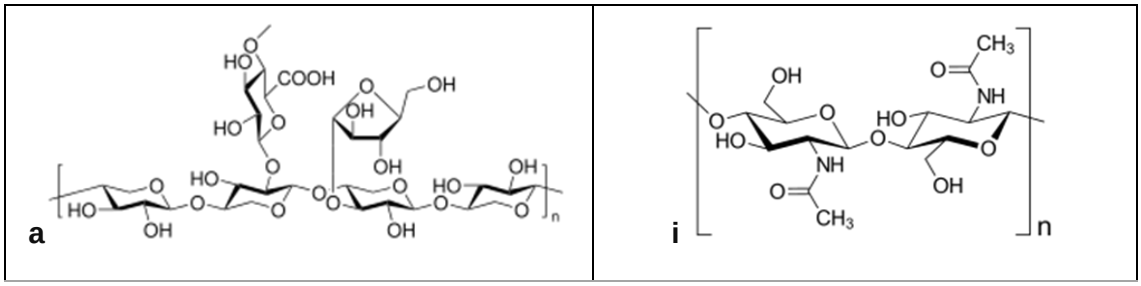


*Figure 12_The structure of arabinoxylan (**a**) and chitin (**i**) (Wikimedia Commons)*

Cellulose (11**z**) is the most important structural component of plants. Their structure is shown in Figure 11**z**. While cotton is almost pure cellulose, wood is a composite of cellulose, hemicellulose, and lignin. As already mentioned, it consists only of β-linked glucose monomers (homopolysaccharides). The biopolymer cellulose is discussed in more detail in the next section. [74]

The protective structural compound of insects and other animals with an exoskeleton is chitin (12**i**). As demonstrated in Figure 12**i**, it consists of N-acetylglucosamine

monomers, an amide derivative of glucose. It is probably the second most abundant polysaccharide on earth. It has similar properties to cellulose, as both have a linear structure, are insoluble in water and both materials provide the organism with structure, strength and protection. [91]

The homopolysaccharides of pectin (**p**) are linear chains of α- and β-(1-4)-linked D-galacturonic acid (**GA**). These two chemical structures are visible in Figure 13. In the heteropolysaccharides of pectin, the scaffold molecules are replaced by various monosaccharides. They are present in most primary cell walls and in the non-lignified parts of land plants. [83]

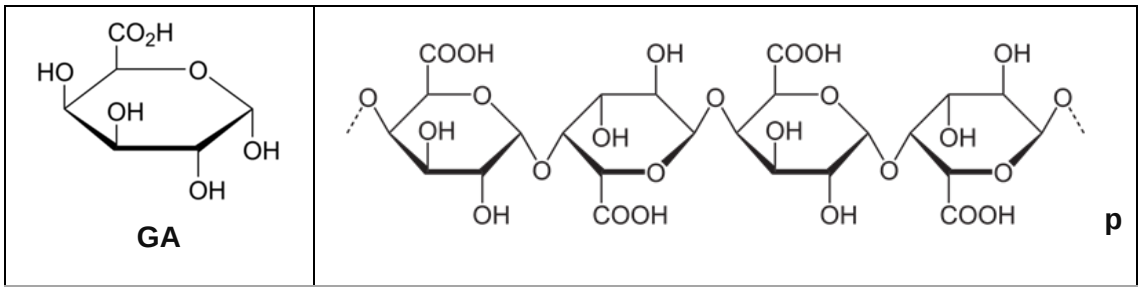


*Figure 13_Structure of homopolymer pectin (**13p**) and their monomeric unit galacturonic acid (**GA**) (Wikimedia Commons)*

2) Storage polysaccharides are used for energy storage and /or energy source. This group contains starch (amylose (**AS**) and amylopectin (**AP**)), glycogen (11**g**), galactogen (**s**) and inulin (f) which are visible in Figure 11**g**, 14 and 15.

The well-known starch is a pure glucose polymer. It is synthesized by most plants to store glucose and is an important source of energy for animals and humans. In its pure form it is a white powder with no taste or odor. As a polymer, it is insoluble in cold water, like cellulose, but it is possible to physically bind water with heat. This leads to so-called starch gelatinization, an irreversible process in which the intermolecular bonds of the starch molecules are broken, and hydrogen bonds can form with water. This is made possible by the two subunits of starch shown in Figure 14, amylose (**AS**) (linear α(1→4) glycoside bonds) and amylopectin (**AP**) (linear α(1→4) glycoside bonds and branched α(1→6) glycoside bonds). [138]

Glycogen (**g**) is defined as the starch analogous in animals. It is shown in Figure 11**g** and is the energy store in animal cells and is mainly synthesized in liver and muscles tissue. The glucose structure is more closely related to amylopectin, but it is more branched and compact. [108]

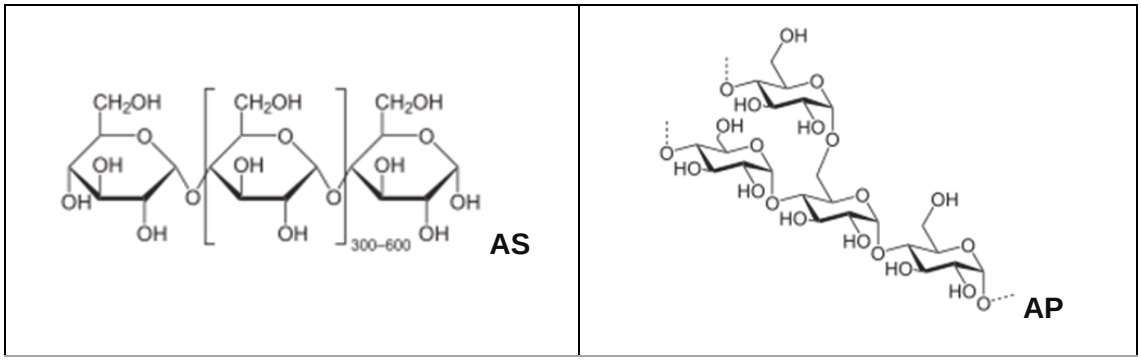


*Figure 14_Structure of amylose (**AS**) and amylopectin (**AP**) the subunits of the biopolymer starch (Wikimedia Commons)*

The exotic energy store galactogen (15**s**) is a polysaccharide made up of galactose monomers demonstrated in Figure 15**s**. It is the energy store in some snails and is used exclusively for reproduction and is therefore only found in female snails. It also serves as an energy reserve for developing embryos and hatchlings and is replaced by glycogen at a later stage. As it is a relatively unknown polysaccharide, some facts and uses are unclear. So far, it is known to be a linear and branched D-galactose biopolymer with predominant β (1→3) and β (1→6) linkages. In some snail species, β (1→2) and β (1→4) binding is also observed. [139]

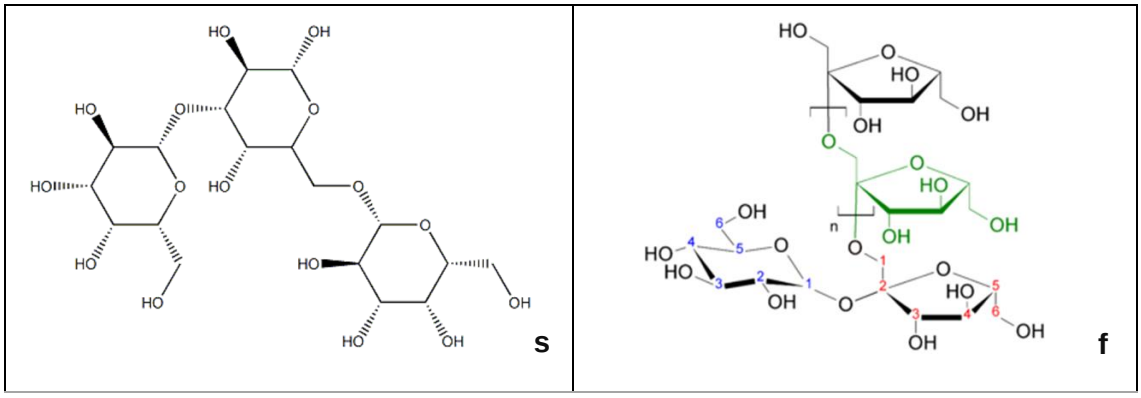


*Figure 15_Structure of the energy store of galactogen (**15s**) and inulin (15**f**) (Wikimedia Commons)*

Figure 15**f** shows inulin (15**f**), a complex biopolymer based on fructose. Like pectin, it is a plant fiber product that is not digestible by humans. It belongs to the class of fructans, which are polymer chains made up of fructose molecules. Inulin is a structural composition of linear fructans (β-2,1-linkage) with a terminal α-D-glucose with 1→2-linkage. For grass plants, inulin plays an important role in energy storage as it gives them a certain frost tolerance. In addition, this polysaccharide is water-soluble and has an osmotic effect in the plant anatomy. [105]

## 1.3. Wood, Cellulose, Hemicellulose & Lignin

As one of the most important and oldest materials in the history of mankind and with limitless application possibilities, wood in all its diversity is worth mentioning here. [100]

A tree, as a living and continuously growing plant construct, can continue to grow steadily through water and light in the photosynthesis reaction, which is shown in Figure 16. Photosynthesis is a process in which light energy from the sun (or similar), water and carbon dioxide are converted into chemical energy and stored as carbohydrates such as sugar, starch, and other more complex constructs. As a waste product of photosynthesis, oxygen is released into the environment and is the reason for the oxygen in the air we breathe. [34, 95]

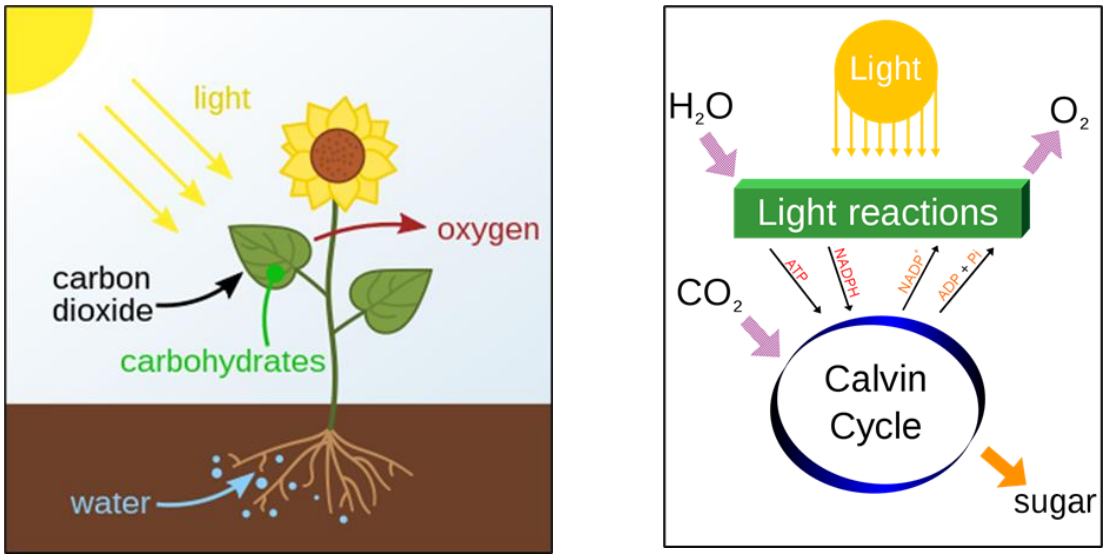


*Figure 16_The photosynthesis cycle, in which light, carbon dioxide and water are converted into carbohydrates and oxygen in the Calvin cycle (Wikimedia Commons)*

To be able to photosynthesize, light energy must be absorbed. This is done by leaf proteins that contain the green pigment chlorophyll. In the next step, the chloroplasts are activated by this light-dependent synthesis reaction. A chloroplast is a membrane-bound, specialized cell subunit (organelle) that carries out photosynthesis. In a first step, it produces adenosine triphosphate (ATP) and nicotinamide adenine dinucleotide phosphate (NADPH) from the absorbed energy, which provide the energy for the removal of oxygen from the water molecules and release it into the environment. ATP and NADPH are organic cell molecules that provide energy for processes and reactions in a cell. NADPH is the reduced form of NADP and acts as a reducing agent in the cells by providing hydrogen atoms. These two molecules are used together with carbon

dioxide to synthesize sugars in the Calvin cycle (Figure 16). Put simply, the Calvin cycle is a series of biochemical redox reactions in which carbon dioxide molecules are bound with the help of ATP and NADPH to produce sugars, a process known as carbon fixation. These reactions lead to the end products sugars, which are utilized by plants as energy stores. [10, 17, 95, 103, 113, 117]

The sugars synthesized in the Calvin cycle are generally used as structural material in plants. For this purpose, the monomeric sugar molecules are linked to form a polymer chain or network. In nature, glucose is the predominant monosaccharide. More precisely, D-glucose achieve these structures demonstrated in Figure 17. During plant evolution, various combinations of this monomer have been developed to form a polymer. This is achieved by enzymatic biosynthesis in the cell. In the case of cellulose, the enzyme cellulose synthase (a transferase), which is located on the plasma membrane, synthesizes the various cellulose polymers for the plant. [18, 48, 74, 97]

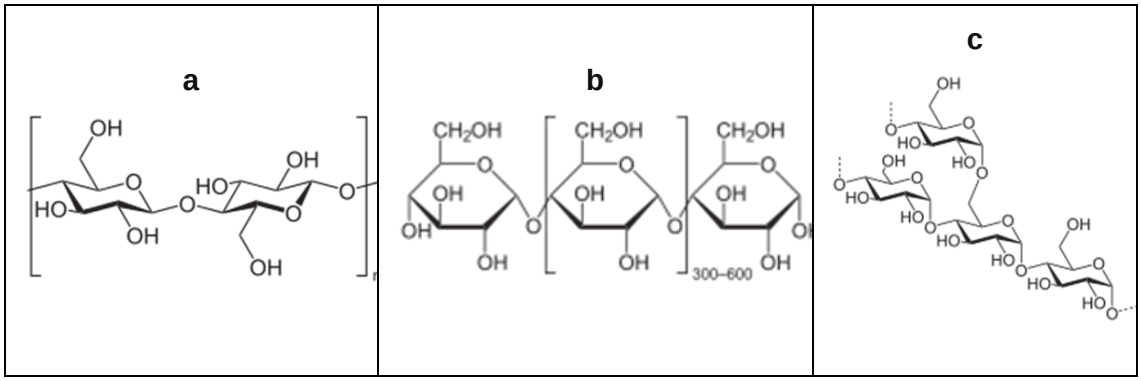


*Figure 17_Possible structures of cellulose linkage for different use and properties in plants; (17**a**) linear β(1→4) D glycosidic bond chain of cellulose, (17**b**) linear but coiled α(1→4)-D glycosidic bond chain of amylose and (17**c**) the branched α(1→6)-D glycosidic linked polymer of amylopectin (Wikimedia Commons)*

For structural reasons, the D-glucose monomer units are linked together in a linear β(1→4)-D-linked glycosidic chain of several thousand to tens of thousands of glucose units called cellulose (Figure 17**a**). These cellulose chains can be arranged in such a way that they become cellulose microfibrils and combine in further steps to form cellulose fibers. This assembly from a monomeric compound at the atomic level to fibers at the macro level is called a hierarchical structure and is the reason for the mechanical strength of plants and wood. [18, 74, 99, 104]

As an energy store, the glucose monomer may be linked in a glycosidic α(1→4)-D linkage chain, which is a linear but coiled structure called amylose (Figure 17**b**), or it may

be an α(1→6)-D glycosidically linked polymer with a branched structure called amylopectin (Figure 17**c**). The combined structure of amylopectin and amylose is called starch and is the most used carbohydrate for energy in the human diet. The largest amount of starch is found in wheat, potatoes, maize, and rice. Cellulose, on the other hand, can only be fed to ruminants such as cows, sheep and goats, as these mammals have special enzymes in their stomachs that break down the cellulose network into glucose monomers and utilize them. [74, 99, 138, 143]

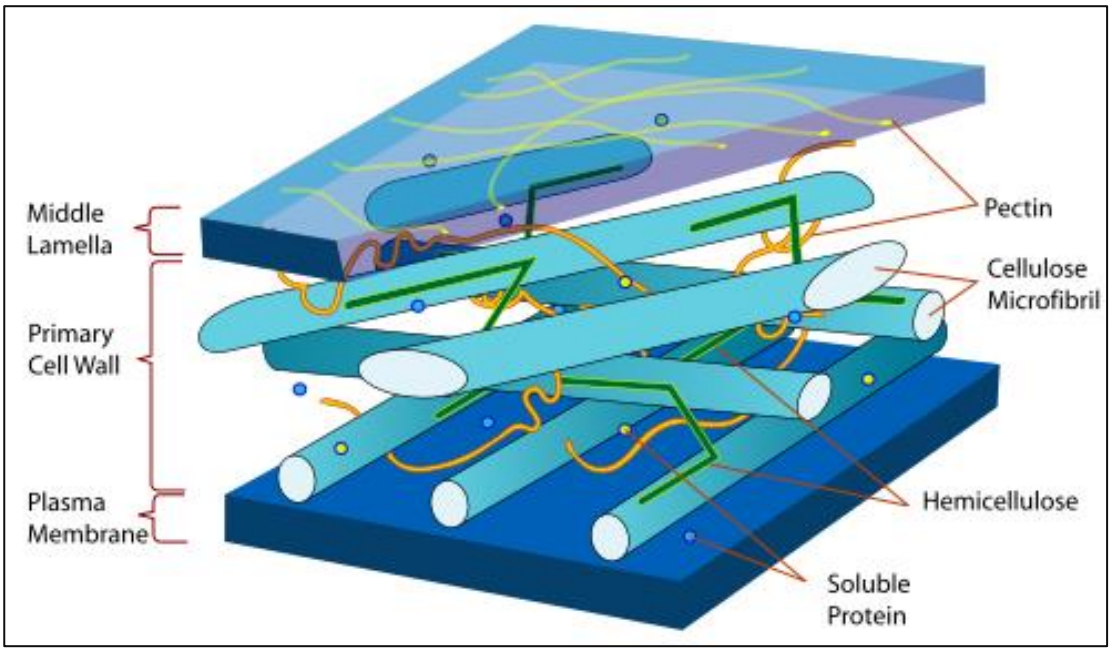


*Figure 18_Overview of a non-lignified plant cell wall; hemicellulose in green and cellulose fibrils as staggered rods on top of each other (Wikimedia Commons)*

Wood is defined as a biological hard tissue and structurally consists of three main components, namely cellulose, lignin and hemicellulose. In Figure 18 these three main components are demonstrated in their complex structural composition. In addition to these structural polymers, wood also contains a variety of non-structural components known as extractives. As already mentioned, the polymer cellulose serves as a structural component to reinforce the primary cell walls of plants, whose monomers consist of D-glucose. [38, 100]

Hemicellulose (or polyose), on the other hand, is a polysaccharide with a structure like cellulose, but consisting of multiple sugars (a heteropolymer). It supports cellulose in its task of reinforcing the cell walls of plants. This is achieved by acting as a cross-linker between the cellulose microfibrils. It also interacts with the third main unit, lignin, to provide better structural support for the tissue. In addition to glucose (a six-carbon sugar)

as the monomer unit, the polymer also utilizes the five-carbon sugars (pentose) xylose and arabinose and the six-carbon sugars (hexose) mannose, galactose and rhamnose. Another difference to cellulose is the possible branched structure of the shorter (hundreds to thousands of monomers) polymer chains compared to the linear and longer polymer chains of cellulose. This variation of the monomer units also leads to a great variety of hemicelluloses and is also a kind of characteristic for certain plant genera. [33, 45, 50, 112, 120]

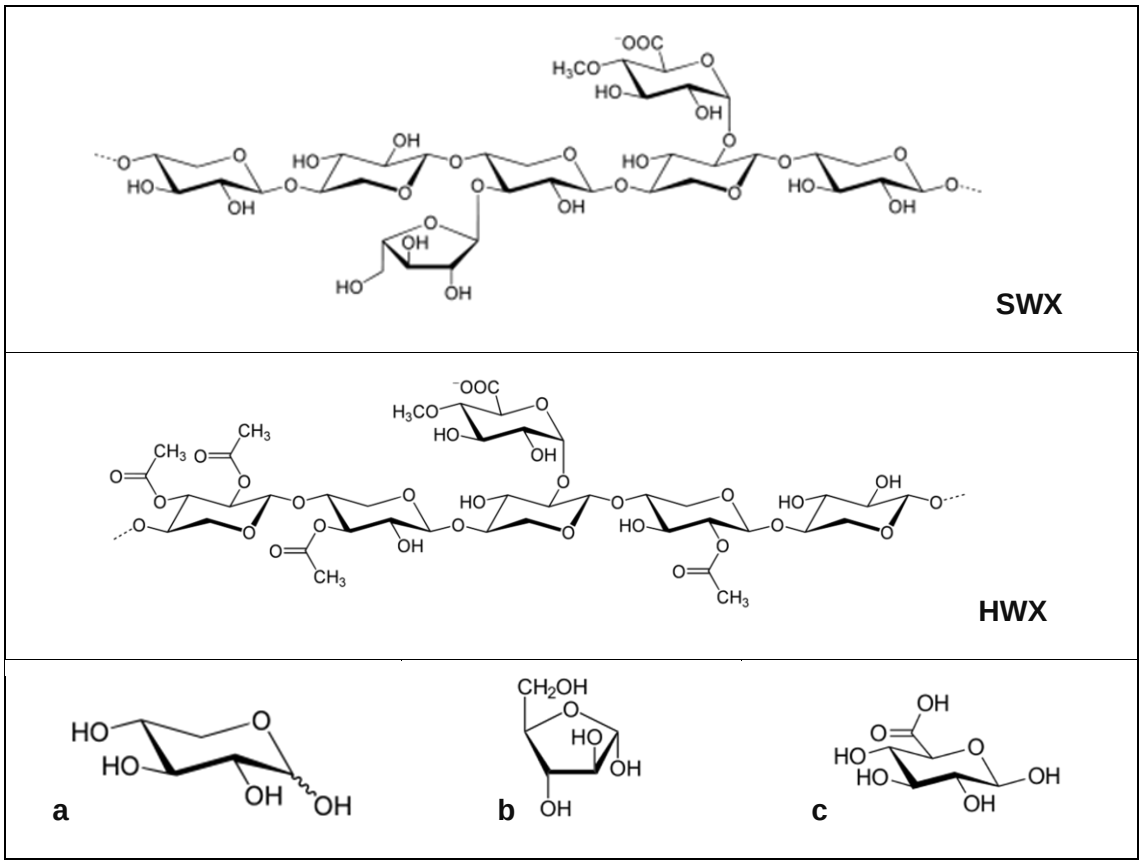


*Figure 19_A softwood xylan structure (**SWX**) and a hardwood xylan structure (**HWX**) with their building blocks of xylopyranose (xylose) (19**a**), α-arabino furanose (19**b**) and α-glucuronic acid (19**c**) (Wikimedia Commons)*

Figure 19 shows the different structures of the hemicellulose xylan (**SWX** & **HWX**). Xylan is a polysaccharide consisting of β-(1→4)-linked xylose monomers (19**a**) with side branches. In softwood, the xylose chain has the side branches of α-arabinofuranose (19**b**) and/or α-glucuronic acids (19**c**). In hardwood, the xylan chain has fewer side branches compared to softwood xylan but is much more acetylated. The hemicellulose mannan is shown in the following Figure 20. Here the mannose units (20**a**) are β-(1→4)-linked with a galactose (20**b**) side branch. [33, 50, 112, 120]

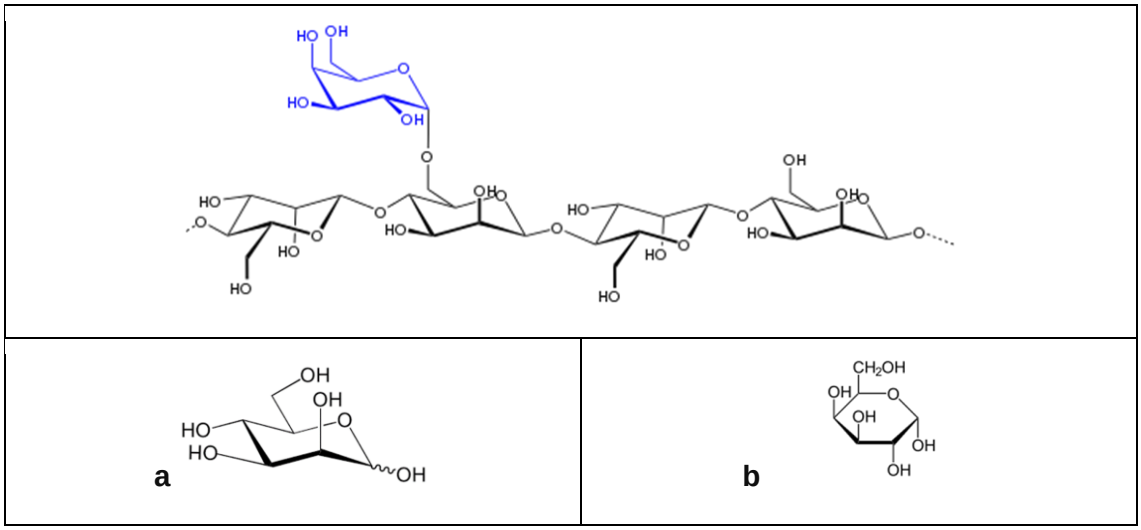


*Figure 20_A mannan (up) hemicellulose structure with their building blocks of mannopyranose (mannose) (20**a**) and α-galactose (20**b**) branches (Wikimedia Commons)*

The hemicelluloses shown are just three examples of the different types of heteropolymer linkages and branching of hemicelluloses that have not yet been structurally resolved, as each plant has its own unique blueprint for these structures. [97, 99, 112]

As a natural sugar source distinct from glucose, hemicellulose is used in biorefinery to process platform chemicals from furan and furan derivatives or alcohols. [19, 96]

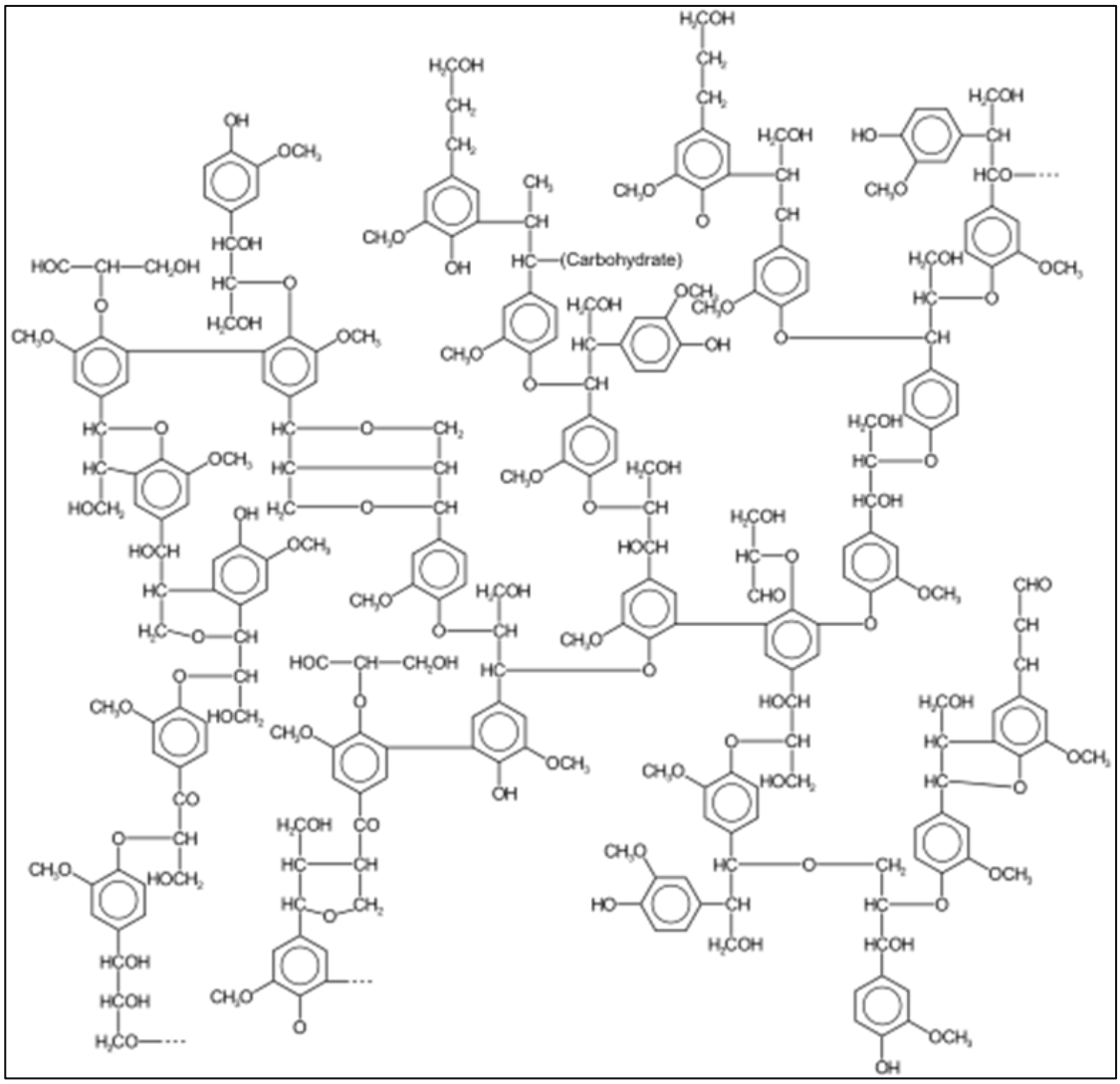


*Figure 21_Simplified lignin structure to visualize their cross-linked aromatic monomers (Wikimedia Commons)*

The last main building block of wood is lignin. Lignin is a complex macromolecule that is synthesized by plants and acts as a structural reinforcing element. The complexity of lignin is demonstrated in Figure 21. It ensures the compressive strength and durability of the plant tissue and fills the space in the cell walls between the cellulose, hemicellulose and pectin components. [12, 66]

The macromolecule lignin is composed of various cross-linked phenolic monomers, the so-called monolignols, which are phenylpropanoids. They have the structure of an aromatic phenyl group with a three-carbon propene tail, which refers to the compound of the same name phenylpropane (Figure 22**a**). [63, 68, 82]

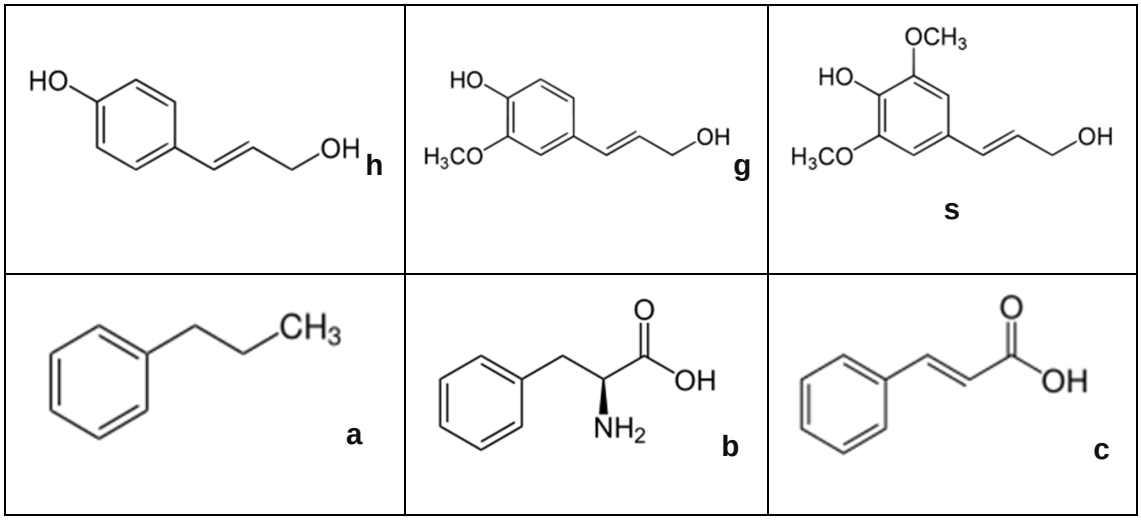


*Figure 22_The monolignols paracoumaryl alcohol (22**h**), coniferyl alcohol (22**g**) and sinapyl alcohol (22s) as well as the amino acid precursor phenylalanine (22**b**), the eponymous compound phenylpropane (22**a**) and the intermediate structure of cinnamic acid (22**c**) for coumaroyl alcohol. (Wikimedia Commons)*

There are three common monolignols, namely paracoumaryl alcohol (22**h**), coniferyl alcohol (22**g**) and sinapyl alcohol (22**s**). These monomeric units of lignin are shown in Figure 22 and are similar to each other because their precursor is the amino acid phenylalanine (Figure 22**b**). [15, 66, 68]

Via phenylpropanoid biosynthesis, an enzymatic synthesis pathway in plant cells, this amino acid is first converted into the monolignol paracoumaryl alcohol (22**h**) and then further processed into coniferyl alcohol (22**g**) and sinapyl alcohol (22**s**). The site of this synthesis reaction is in the cytosol, the cytoplasmic matrix, which is an intracellular fluid (ICF). An ICF combines all the fluids contained in the cells. The cross-linking reaction takes place in the apoplast, the space outside the cell membrane into which the material can diffuse freely (extracellular space). These three monolignols differ only in the number of methoxylations of the phenyl ring ($H_3CO$- group). [15, 68]

The ratio and linkage of these three monolignols to the complex organic polymer lignin is unique for each plant species, as is the structure of hemicellulose. [12, 97, 99]

The properties of lignin are similar to those of cellulose, as both have a high molecular mass, are insoluble in water and other solvents and therefore have a hydrophobic character. Compared to other biopolymers such as cellulose or proteins, lignin is very resistant to natural degradation (biodegradation) and acid- or base-catalyzed hydrolysis processes. This resistance protects and minimizes the accessibility of cellulose and

hemicellulose, which leads to a lower digestibility of the biomass. This resistance complicates the digestion and degradation of wood in the environment and in industry. As a result, wood and lignin degradation in nature takes a very long time and the industry requires harsh acids (concentrated sulfuric acid), solvent mixtures in combination with harsh conditions for the digestion of raw materials from wood, which in many cases leads to sugar degradation products such as furfurals. [12, 15, 66, 68, 87, 111, 123]

The following Table 1 provides an overview of various biomass plants and their composition in hexoses, pentoses and lignin.

*Table 1_Composition of different biomass plants in hexoses, pentoses and lignin [53]*

| | **Hexoses [%]** | **Pentoses [%]** | **Lignin [%]** |
|---|---|---|---|
| **Softwood** | 57-60 | 7-11 | 27-32 |
| **Birch wood** | 45-47 | 21-27 | 19-20 |
| **Beech wood** | 50-54 | 19-24 | 22-23 |
| **Wheat straw** | 35-39 | 22-24 | 18-25 |
| **Corn cobs** | 37-44 | 32-35 | 15-19 |
| **Bagasse** | 42-50 | 29-42 | 16-21 |

In addition to the structural polymer cellulose, hemicellulose and lignin, non-structural substances, known as extracts, are also important. This group mainly includes organic compounds with a low molecular weight. These compounds can be easily extracted with a neutral solvent such as acetone, ethanol or water. They can be found in the extracellular fluid (ECF) of the cell. [51]

Most of these extracts are lipophilic (fat-loving) in nature. Only a small proportion is hydrophilic (water-loving). The largest amount of lipophilic material is wood resin, which is mainly found in softwood. In nature, wood resin is secreted by trees and plants for protective purposes. It protects the plant or tree from further damage and attacks by insects and pathogens. It is a highly viscous substance with a color ranging from transparent to brown, which is very non-polar and highly flammable. Chemically, wood resin consists of terpenes, a group of chemical compounds that contain the monomer of a five-chain molecule with an unsaturated (double) bond called isoprene. This chemical

is shown in following Figure 23 (23**a**). Another important product that plants produce from isoprene is natural rubber (polyisoprene) (Figure 23**b**). [51, 61, 116, 118]

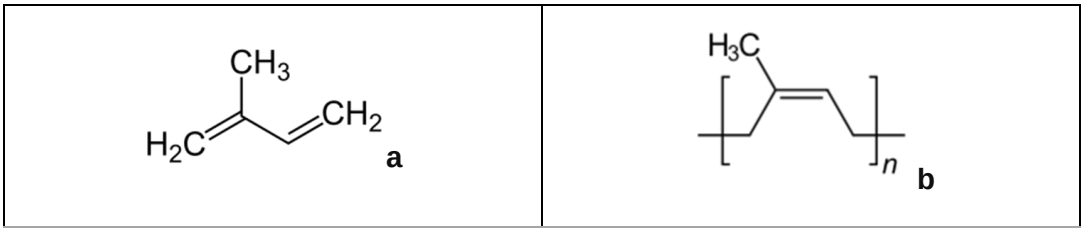


*Figure 23_Structure of an isoprene molecule (left), the monomeric unit of terpene and other isoprenoids; right the polymeric repeating unit of natural rubber where the monomer isoprene is used for (Wikimedia Commons)*

In addition to the use of pure isoprene units in the resins, these monomeric units can be chemically functionalized to obtain various alcohols, solvents, acids, oils and much more using only hydrocarbons or functionalized chemicals. Compared to the solid matrix compounds in wood, this raw material exhibits an enormous range of variation. More than 55,000 different compounds have been found and registered for terpenes and terpenoids alone. [23, 58, 73, 116]

The phenolic compounds are mainly found in hardwood and bark. These compounds act as fungicides (they protect the wood from biodegradation by fungi) and as colorants (they influence the color of the wood). [56, 73, 108]

Of these extractive compounds, phenolic compounds and resin acids are the most important toxic contaminants in raw pulping effluents. [53, 101, 127]

## 1.4. Chromatography

Chromatography is a separation and/or purification process based on the laws of diffusion and interaction (attraction and repulsion). The sample components to be separated are removed by complete dissolution in a mobile phase (eluent), which can be a gas, a liquid, or a supercritical fluid (SCF). The classifications of chromatography are summarized in Figure 26. The mobile phase is usually moved in one direction by pressure (pump, gas pressure) (Figure 24**c**), gravity (Figure 24**b**), capillary force (Figure 24**a**), or electrical voltage. In the following Figure 24 a comparison of different chromatography systems is demonstrated. The sample mixture is separated on or in the stationary phase, demonstrated in Figure 25. It is the immobile part in which the interactions between the individual sample components take place, while the mobile phase constantly transports the sample components. Due to the selected nature of the stationary phase, certain sample components are attracted more strongly than others. This leads to an enrichment process (equilibrium state) for some components. As a result, sample components that do not interact with the stationary phase drift with the mobile phase, while components with greater affinity remain in the stationary phase for longer. This process results in different sample components leaving the stationary phase at different times. This is used in many areas of chemistry, medicine, biology, pharmacy and many more for the separation, extraction, determination and further processing of pure substances from sample mixtures (analytical and preparative chromatography). [20, 25, 47, 62, 119]

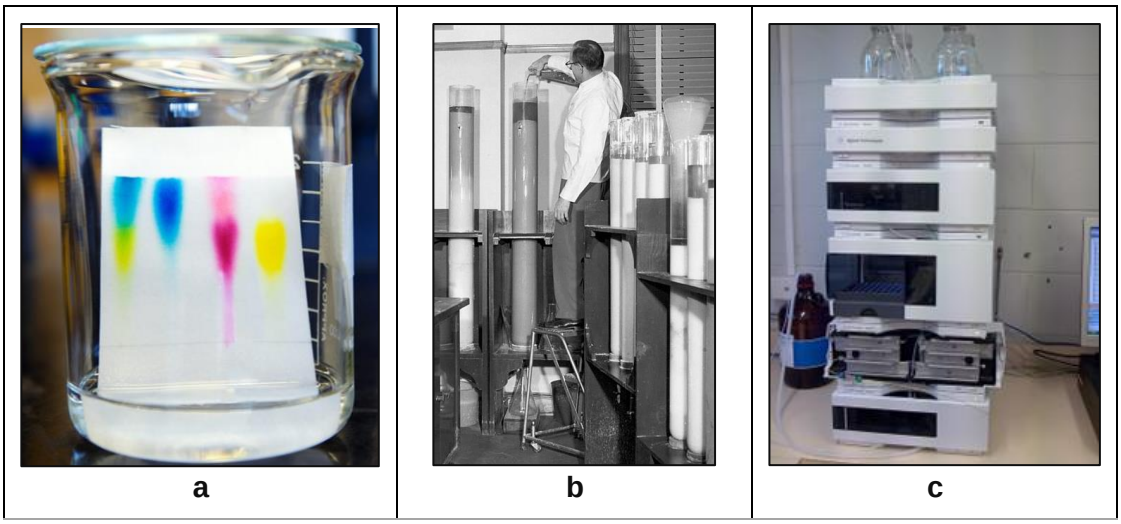


*Figure 24_Evolution of liquid chromatography; from simple thin layer chromatography (**a**) using a planar stationary phase [106], over preparative chromatography (**b**) [140], to modern analytical chromatography systems (Agilent 1200 HPLC) (**c**) using increasingly smaller and more efficient columns as stationary phase [141]*

The time required for a sample component (analyte) to pass through the stationary phase is referred to as the retention time. It is a characteristic time value that is used for comparison and identification. The individual sample components that emerge from the stationary phase are referred to as eluate. [16, 25, 47, 119]

It is important to know that chromatography is only a separation method. For quantitative applications, so-called standards (pure substances) of the desired compounds and a calibration (pure substances with precisely known concentrations) must be used and applied. A detector downstream of the stationary phase is used to detect these and the individual eluates. A detector is a device for the qualitative and quantitative detection of analytes after separation. A detector can range from the simple human eye (visible range of the electromagnetic spectrum) to physical measurement signals (temperature, refractive index, current) to highly complex devices (mass spectrometry, radioactivity detector, electrochemical detectors). The result of a chromatographic measurement is a chromatogram (Figure 25**b**). This is a visual representation where the x-axis represents the retention time and the y-axis represents a signal corresponding to the reaction generated by the analytes leaving the system and passing through a detector. [20, 25, 47, 119]

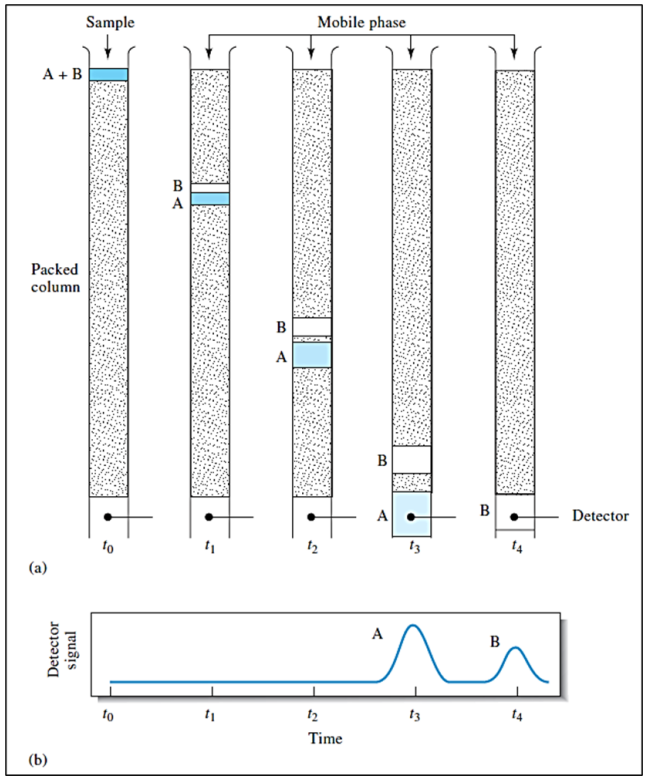


*Figure 25_Sketch of a chromatographic separation; (a) shows the separation step of a mixture of components A and B by column chromatography; (b) shows the corresponding chromatogram recorded by a detector at various time stages [119]*

As a variety of applications have been developed for chromatography, it can be classified according to several criteria, shown in Figure 26. The first criterion is the mobile phase used, which, as already mentioned, can be gaseous, liquid or a supercritical fluid. Depending on the choice of phase, a distinction is made between gas chromatography (GC), liquid chromatography (LC) and supercritical fluid chromatography (SFC). [20, 25, 47, 119]

In GC, carrier gases are used as the mobile phase. These are inert gases consisting of small atoms/molecules, such as hydrogen, helium, or nitrogen. In LC, all types of liquids can be used, which must be adapted to the properties of the stationary phase, the solubility of the analyte, polarity, availability, purity, molecular size, stability, and other physical and chemical properties in order to achieve optimal flow properties and separation of the analytes. In SFC, the mobile phase is a substance that is above and relatively close to its critical temperature and pressure. These substances in this state are referred to as supercritical fluids. This is a substance whose temperature and pressure are above its critical point, in which there are no separate liquid and gaseous phases, but which is below the pressure required to compress it into a solid. SCFs are far superior to gases in their ability to dissolve substances such as liquids or solids, but generally have properties intermediate between those of a gas and a liquid. In addition, small changes in pressure or temperature near the critical point result in large changes in density, so many properties of a supercritical fluid can be customized. [20, 119]

A further classification is based on the type of stationary phase. A distinction is made between planar chromatography (paper chromatography and thin-layer chromatography), in which the stationary phase is a film or plate, and column chromatography. In most applications of planar chromatography, a liquid is used as the mobile phase and mass transfer is based on capillary forces. [62, 119]

Depending on the application, column chromatography is further subdivided into GC or LC. In GC, a distinction is made between packed columns (the inside of a column is filled with a fine-grained material) and capillary columns (only the column wall is covered with a layer). In LC, the stationary phases are divided into normal phase (polar stationary phase) and reversed phase (non-polar stationary phase). The choice of mobile phase must therefore be matched to the column and the sample so that the stationary phase is not dissolved. [62, 119]

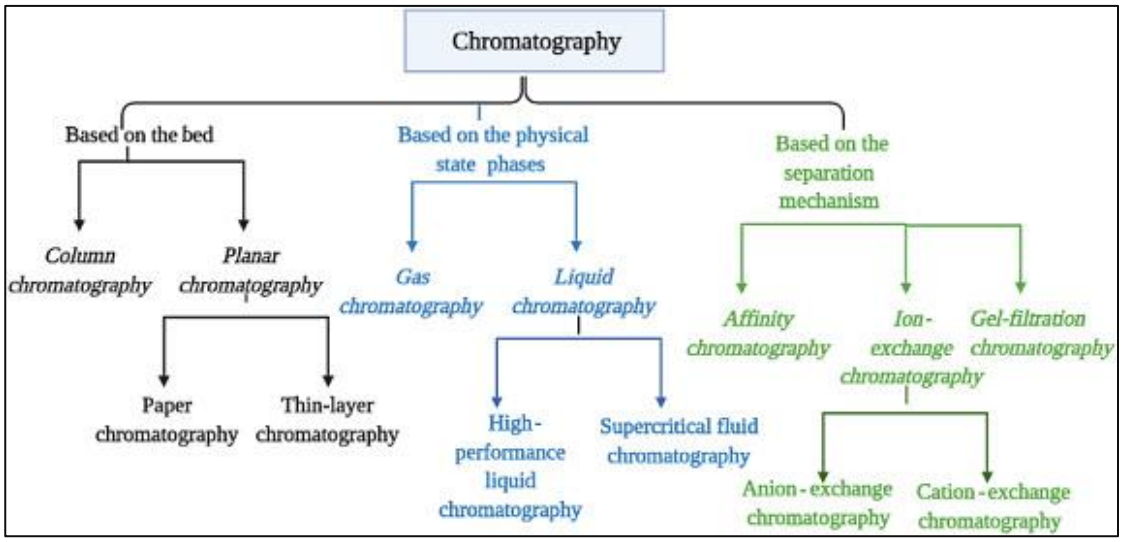


*Figure 26_Classification of the different chromatographic methods [62]*

The last classification criterion is based on the separation principle, i.e. the way in which the equilibrium between the stationary and mobile phases is achieved. The best known are adsorption (separation by adsorptive bonds of different strengths to the stationary phase), participation (utilizes different solubility of the components to be separated, second solvent is applied to the carrier material in the stationary phase), ion exchange (stationary phase is a solid ion exchanger, which forms differently stable bonds between the different ions of the mobile phase), size exclusion (separation by size, whereby in LC processes the larger components elute first while the smaller components settle in the filter pores) and affinity chromatography (the stationary phase is a chemical compound that is specific for each analyte and causes the separation by non-covalent forces). [20, 62, 119, 142]

### 1.4.1. High Performance Liquid Chromatography & Detectors

An improved and more powerful application of column LC is high-performance liquid chromatography (HPLC). In contrast to conventional column LC, which is mostly used for preparative applications and utilizes gravity as a force for mass transport, HPLC uses a pump that can reach a pressure of up to 1000 bar to push a sample through a column. A schematic of a HPLC system is shown in Figure 27**a**. Another difference lies in the type of stationary phase. Preparative LC columns usually consist of a solid glass tube with lengths in the meter range (m) and several centimeters (cm) in diameter, which is filled with silica gel or aluminum oxide. In HPLC, the columns are usually metal or plastic tubes with a length of a few decimeters (dm) and a diameter of a few millimeters (mm), which are filled with various materials. Modified silica gels are usually used for adsorption

and particle chromatography, and coated quartz glasses or resins with functional groups are usually used for high-performance anion exchangers (HPAE). An advantage and disadvantage of HPLC compared to column LC is the small sample volume (max. 1000 µl) required for accurate but non-preparative analysis. [20, 25, 47, 62, 119]

A HPLC system consists of at least six parts. A solvent reservoir (mobile phase), a solvent degasser, one or more high-pressure pumps, mixing vessels for solvents, a sample injector, a switching valve (≥ 6-port valve), in most cases a guard column, the analytical column (stationary phase), a detector, a computer for data acquisition and a waste container. In Figure 27**b** some examples some examples of what a chromatographic column for HPLC looks like. [20, 47, 119]

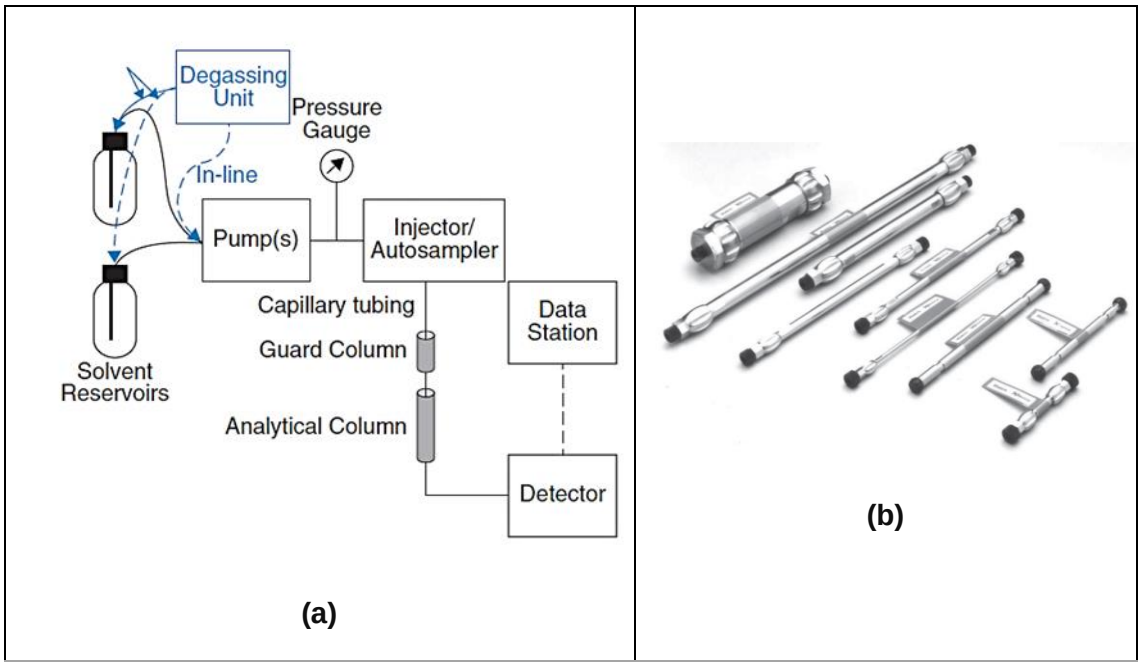


*Figure 27_(27**a**) Schematic of a basic structure of an HPLC system; (27**b**) variety of columns for HPLC applications [25]*

There are various detectors for HPLC. As described above, a detector has the task of detecting the eluates from the stationary phase. This is usually done by measuring a characteristic physical and/or chemical quantity of the sample, which in some cases is very specific (molecular and atomic weight, radiation, absorption, conductivity, ...). They can be categorized into two groups: destructive and non-destructive eluent detectors. Destructive detectors in LC include mass spectrometry (MS), the charged aerosol detector (CAD) and the evaporative light scattering detector (ELSD). Non-destructive detectors include the UV/Vis detector (CCD, DAD or PDA), the fluorescence detector, the refractive index detector (RID), the conductivity detector, the radioactivity detector,

the chirality detector and the electrochemical amperometry detector (single-potential amperometry and pulsed amperometry (PAD)). [20, 25, 119]

The PAD is an electrochemical detector based on the principles of amperometry. The Amperometric method is characterized by the measurement of an electrolysis current at a working electrode while a constant electrochemical potential is applied. The measured electrolysis current is directly proportional to the concentration of the reacted substance. This means that unknown concentrations can be determined using a calibration function. Commonly used materials for working electrodes are platinum, gold, carbon, mercury, and silver. It is used to detect ions in a solution based on the electric current or changes in the electric current and is therefore suitable for certain electrochemically active ions such as cyanide, sulfite, and iodide. Any analyte that can be oxidized or reduced is a candidate for detection. In contrast to single-potential amperometry, in which there is a constant DC potential between two electrodes, pulse amperometry has a working potential and a cleaning potential. The working potential arises in the same way as in single-potential amperometry, but only for a few hundred milliseconds. After the measurement, a cleaning potential is applied, which cleans and regenerates the metal surface of the electrode. This makes PAD ideal for analytes such as carbohydrates, which contaminate the electrode surface and lead to a reduction in the signal. The reason why PAD is considered a non-destructive detector is the very short application time of the potential to the sample and the resulting barely measurable sample consumption due to oxidation. [25, 57]

The RID is a detector based on the principles of refractometry and refractive index (RI). It is a simple refractometer that is connected to an LC system. The RI is an optical material property and a dimensionless number. It provides information about the ability of the medium to diffract light and is defined as the ratio of the wavelength of light in a vacuum to the wavelength in the material. Light is refracted and reflected at the interface between two media with different refractive indices. The medium with the higher refractive index is considered optically denser. The concept of RI applies to the entire electromagnetic spectrum, from X-rays to the visible spectrum and radio waves. Refractometry uses the behavior of light (diodes) at the interface between a prism with known properties and the material to be examined. At the interface between the measuring prism and the sample medium, the light propagates at different angles. The unknown refractive index of the sample medium is measured via the light deflection. If the composition of a liquid is known, the concentration can be measured with a refractometer. The disadvantage for the application is that the refractive index of a

sample varies for almost all materials at different wavelengths and the temperature has a very large influence on the refractive index. Refractometers are traditionally used to determine the sugar content in aqueous solutions. [20, 25]

The most used and most popular detector is the UV-Vis spectroscopy detector. This is a simple spectrophotometer that is connected to an LC system. A photometer is an instrument that measures the strength of electromagnetic radiation. It covers the range from ultraviolet to infrared and the visible spectrum. The design of a photometer comprises a lamp, a slit, a monochromator, a sample cuvette (with dual-beam photometers a second cuvette as a reference) and a detector (diode array detector (DAD), photodiode array (PDA) or charge-coupled device (CCD)). Photodiodes or a combination of a deuterium lamp (for the UV range) and a tungsten halogen lamp (for the visible and near IR range) can be used as the lamp. The slit and the monochromator are used to focus the beam and generate a specific wavelength (monochromatic light) that hits the cuvettes. When the sample is optically active (chromophores), a certain amount of radiation is absorbed by the sample, resulting in a decrease in beam intensity. The initial and reduced beam intensity is recorded by a semiconductor detector. This semiconductor element generates a current when photons are absorbed on the surface. This electrical response is used for comparison and is assumed to be proportional to the concentration. To obtain results, the response of the device to the unknown analyte must be compared to the response to a standard. A calibration curve is used to obtain accurate results. [25, 47, 70, 94]

## 1.5. Ultraviolet-Visible Spectroscopy

As part of spectroscopy, ultraviolet-visible spectroscopy (UV/Vis) also deals with the electromagnetic spectrum and its interactions and effects with matter and with absorption processes. The electromagnetic spectrum, which is demonstrated in Figure 28, is the totality of all electromagnetic waves of different wavelengths (λ; unit is meter (m)). The light spectrum (color spectrum) is the part of the electromagnetic spectrum visible to humans (range from 380nm (violet) to 780nm (red)). In UV/Vis spectroscopy, wavelengths between 180nm and 1100nm are used for analysis. [20, 25, 47, 52, 70, 94, 119]

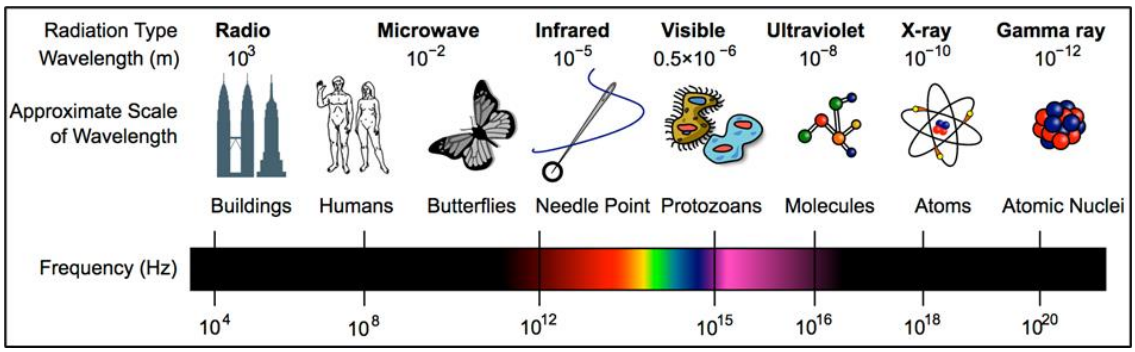


*Figure 28_Overview of the electromagnetic spectrum; wavelength is inverse proportional to frequency and energy (Wikimedia Commons)*

As already mentioned, the device used to carry out UV/Vis spectroscopy is called a photometer. This spectroscopy method can only be used for molecules and substances that are optically active in this range of the electromagnetic spectrum. So-called chromophore groups are responsible for the color in the visible range. They are a part of a molecule that is responsible for its color. Color can be created by light absorption, but also by light reflection, light scattering or light refraction. [20, 25, 94, 119]

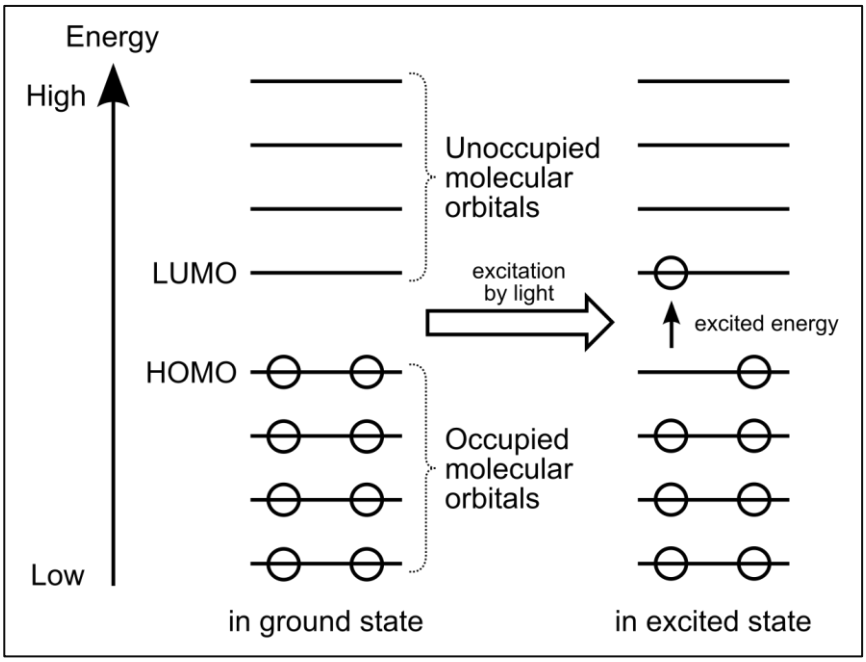


*Figure 29_Diagram of HOMO and LUMO of a molecule (each circle represents an electron; when an electron in the HOMO absorbs light at a sufficiently high frequency (energy), it jumps to the LUMO, resulting in an excited state) (Wikimedia Commons)*

In most cases, the process of optical activity is due to the electron configuration of a molecule. In principle, optical activity requires an electron transition from the highest occupied molecular orbital (HOMO) to the lowest unoccupied molecular orbital (LUMO). This electron movement is demonstrated in the above Figure 29. The molecular orbitals are described by molecular orbital theory (MO), which is one way of describing the electronic structure of a molecule. In organic molecules, the free or delocalized electrons are responsible for the color. Typical organic chromophores include molecules with multiple bonds between atoms, aromatic ring systems, organic compounds containing nitrogen, and others. The same laws of HOMO and LUMO occupation also apply to inorganic chromophores, but the mechanism is different. Depending on the electron configuration, the color is due to charge transitions or the excitation of electrons in the inner electron shell. [20, 47, 52, 94]

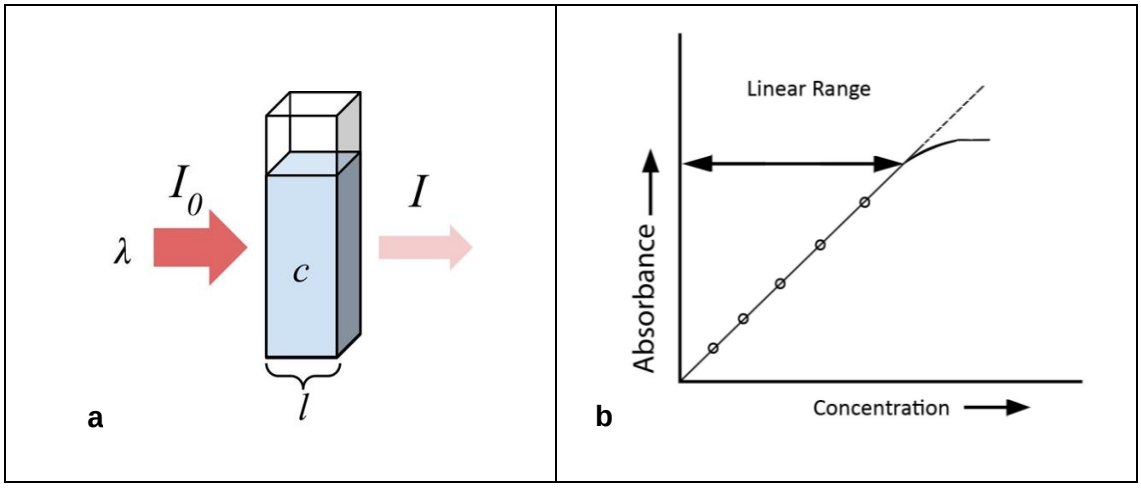


*Figure 30_(**a**) Scheme of attenuation of an incident light beam (λ) by a cuvette of length l containing a solution of concentration c (power of the incident radiation ($I_0$) and the emerging radiation (I)) [55]; (**b**) Calibration diagram of the Beer-Lambert law equation, where the x-axis is the concentration (c), the y-axis is the absorbance (A) and the slope is the optical path length (l) and the absorptivity (ε) (the Beer-Lambert law only applies to dilute solutions (below 10 mM), as at higher concentrations physical interactions come into play and affect the absorptivity measurements, leading to deviations from the linear behavior shown in the diagram above) [64]*

UV/Vis spectroscopy is based on the measurement of the absorbance ($A$) (or transmittance ($T$)) of visible and ultraviolet light through a sample. Absorbance is defined as the logarithm of the ratio between the power of the incident radiation ($I_0$) and the radiant power transmitted through a sample ($I$). This relationship is known as the Beer-Lambert law and shown in Figure 30**a**. In addition, the optical attenuation of a physical material containing a single attenuating species at a uniform concentration ($c$) is related to the optical path length ($l$) through the sample and the absorptivity ($\varepsilon$) of the species. This leads to the equation of the Beer-Lambert law:

$$\boldsymbol{A = \varepsilon l c = \log\left(\frac{I_0}{I}\right) = -\log T} \qquad \textbf{(1)}$$

The absorptivity or molar attenuation coefficient is a measure of how strongly a chemical substance absorbs and thus attenuates light of a certain wavelength. It is an intrinsic property of the species and is given as the inverse mole (M) times centimeter [$M^{-1}cm^{-1}$]. The Beer-Lambert law states that the absorption of a solution is directly proportional to the concentration of the absorbing species in the solution and the path length. This means that the concentration of the absorber in a solution can be determined using UV/Vis spectroscopy with a fixed path length. A calibration curve like in Figure 30**b** can be used to determine an unknown concentration of a chemical species in a sample. [20, 47, 52, 119]

As already mentioned, a photometer consists of one or more lamps, a slit, a monochromator, a sample cuvette (a second cuvette as a reference for dual-beam photometers) and a detector. A schemata of a simple double beam spectrophotometer can be found in Figure 31. In a single-beam spectrophotometer, only one cuvette is used in the system. The original photon beam ($I_0$) is first measured in a run without a cuvette or only with solvent in the cuvette and then compared with the sample ($I$) in a further run. The logarithmic ratio gives the absorbance value ($A$) according to the Beer-Lambert law. A simple double-beam spectrophotometer represents an improvement. The light is split into two beams before it reaches the sample. One beam (reference cell) serves as a reference, while the other beam penetrates the sample (sample cell). Complete (100 %) transmission (or zero absorption) is assumed for the intensity of the reference beam, and the measured value displayed is the ratio of the two beam intensities. [20, 47, 70, 119]

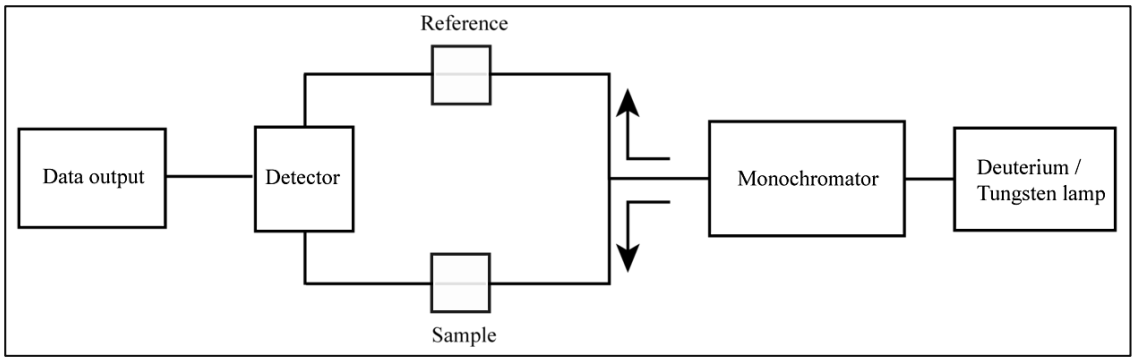


*Figure 31_Schemata of a double beam spectrophotometer (Wikimedia Commons)*

A cuvette is a one-sided closed vessel with plane-parallel sides that is usually used for the optical examination of liquids and solutions (a simple cuvette is shown in Figure 30**a**). In principle, cuvettes can be made from any material that is transparent in the desired wavelength range. They are usually made of glass or plastic. For wavelengths below 250 nm, cuvettes made of quartz glass are required, as normal glass strongly absorbs light at wavelengths below 250 nm. [25, 47]

## 1.6. Determination Methods for Lignin

The determination of lignin is an analysis that is routinely used to characterize lignocellulosic material. It is also used to assess the effects of chemical, physical and biological treatments of wood and pulp, as well as for wastewater monitoring in the wood processing industry and, in the case of pulp, to estimate the need for bleaching chemicals. When considering the various methods for the determination of lignin, it is important to note that none of them can be considered completely satisfactory. This is because lignin has not yet been isolated in a pure or unmodified state. Therefore, there is currently no definitive structural formula for lignin based on which a rational and quantitative measurement could be developed or the validity of currently available methods could be accurately assessed. In addition, many of the methods commonly used for lignin determination have fundamental shortcomings that significantly affect their accuracy. The methods are divided into two groups. One deals with the analytical methods that can be applied to lignin when it is initially present as a component of a solid (biomass) mixture. The second focusses on the determination of lignin in solution. The first group can also be divided into two groups, namely direct and indirect methods. In contrast to direct lignin determination, no lignin residue is isolated in indirect methods. Instead, it is calculated by measuring a characteristic structural functionality, property or chemical reaction and the result is linked to the concentration. [4, 69]

### 1.6.1. Analytical direct methods

The most used and best-known method for determining lignin in lignocellulose samples is acid hydrolysis with sulfuric acid. In this method, the sample is almost completely dissolved by hydrolysis. In an ideal sample, the carbohydrate components dissolve completely, while the main component, lignin, remains as a poorly acid-soluble residue (Klason) and can be determined gravimetrically. The small proportion of (acid-soluble) lignin is determined in the supernatant from the hydrolysis step using UV/Vis spectroscopy. [69]

The disadvantage of this acid hydrolysis method is the influence of extractable sample components (ash, resins, ...), which can lead to an increased lignin content. To avoid this, the sample must be extracted with a suitable solvent. Another disadvantage concerns the carbohydrate components of the samples. Rearrangement and degradation reactions are catalyzed using concentrated mineral acids (72% sulfuric

acid). In some cases, these reactions lead to various furfurals, which influence the lignin signal in the UV/Vis spectrum due to the aromatic ring system. [69]

### 1.6.2. Analytical indirect methods

In contrast to direct determination methods, indirect methods do not isolate the lignin as a residue. Here, the lignin content is calculated as the difference between 100 % and the saccharide content or by measuring a certain characteristic structural functionality, property or chemical reaction and the result is converted into a concentration. These indirect methods also include the determination of acid-soluble lignin using UV/Vis spectroscopy. As already mentioned, the signal generated by the aromatic ring system of the lignin molecules is measured. In addition to the lignin molecules, furfurals, and resin components with an aromatic character, which have a higher lignin content, are also measured. A better determination method is based on the complete dissolution of a sample and the measurement of the UV absorbance of this solution. Suitable solvents mentioned in the literature are nitric acid, sodium chlorite solution, cadoxene (cadmium oxide in ethylenediamine) and acetyl bromine in acetic acid, with the latter solvent being the most promising. [52, 69]

Other spectroscopic methods applicable to solid samples include internal reflectance spectroscopy (IRS), UV micro-spectrophotometry and solid-state cross-polarization magic angle spinning carbon-13 nuclear magnetic resonance (CP/MAS $^{13}$C-NMR). Another indirect method for the determination of lignin is the bromination (chemical conversion) of lignin. The bromine uptake is then proportional to the lignin content and is determined using scanning or transmission electron microscopy (SEM or TEM) in combination with energy dispersive X-ray analysis (EDXA). [25, 52, 69]

The last method is based on the consumption of oxidizing agents. The most common method to quickly estimate the lignin content for quality control is to determine a Roe-Chlorine number or a Kappa number. These numbers can be converted to Klason lignin and are expressed as the amount of oxidizing agent consumed per weight of sample. These methods are based on the principle that lignin consumes the oxidizing agent faster than the carbohydrate components of a sample. The two most used oxidizing agents for determining the number are chlorine and potassium permanganate. In the history of the determination of the Roe-Chlorine number, this method was replaced by the determination of the hypo number (chlorine number). In this method, the sample is reacted with acidified sodium or calcium hypochlorite and the chlorine consumption is

measured titrimetrically. Compared to these methods, the traditional determination of the kappa number has the advantage that potassium permanganate easily oxidizes lignin and leaves carbohydrates relatively unreacted. In contrast, the determination of the kappa number can only be used for semi-bleached and unbleached pulp samples. [69]

### 1.6.3. Analytical methods for lignin in solution

One advantage of lignin in solution is the possibility of online monitoring. For this purpose, several methods for the real-time determination of lignin have been developed. Most of these methods are based on the formation of derivatives (chemical conversion), the absorption or emission of radiation or the modification of lignin by a specific chemical reaction. [69]

One of these methods is the aforementioned determination of acid-soluble lignin, in which a small amount of complete lignin is detected using UV/Vis spectroscopy. A similar spectroscopic determination method is fluorescence spectroscopy. This more sensitive method (2-3 orders of magnitude) is used to determine the radiation emission of the sample (fluorescence). Another spectroscopic method for online determination is (Fourier transform) infrared spectroscopy ((FT)IR). In contrast to UV/Vis and fluorescence spectroscopy, in which electronic excitation and relaxation are used and measured, in IR spectroscopy the molecule is excited to vibrate by absorbing frequencies characteristic of its structure, so-called resonance frequencies. In an IR spectrum, certain functional groups exhibit certain oscillation frequencies. In this way, aromatic molecules can be easily and quickly identified as lignin. [25, 52, 69]

One method based on a chemical reaction is the determination of lignin using the modified Pearl-Benson method (Nitrosation). The phenolic unit of the lignin is modified with acidified sodium nitrite, which leads to the formation of a nitroso phenol. The addition of alkali then leads to tautomerization (same molecular formula, different atomic arrangement) to an intensely colored quinone monooxime compound. This compound can then be determined by spectroscopy at 430 nm (colorimetry). Here too, as already mentioned for acid-soluble lignin, other flavoring substances can have an interfering effect and lead to a false lignin content. [69]

## 1.7. Determination Methods for Carbohydrates

As carbohydrates are of great importance for living organisms, progress, research, and utilization have always been widespread and are constantly evolving. The limitless variety, creativity and importance of carbohydrates becomes clear when you look at nature. As carbohydrates are found in every corner of the living world, there are a multitude of methods of analysis. The limits of the analytical methods lie with the carbohydrate monomers, as their chemical structure and behavior are very similar. All monosaccharides are soluble in water, occur in D and L configurations and can combine into polymers or be converted into other chemical compounds by condensation or other chemical reactions. As discussed in section 1.2. a monosaccharide is a molecule with the molecular formula $C_n(H_2)_nO_n$ ($n \geq 3$) and consists of a carbon backbone chain with hydrogen or hydroxyl side groups and a carbonyl group. [26, 28, 65, 90, 109, 136]

The analysis methods for carbohydrates can be divided into two classes: the classic detection reactions and the modern methods. Most classical detection reactions have in common that they are only suitable for qualitative analyses. Modern methods are more attractive and better suited for quantitative analyses.

### 1.7.1. Classic Detection Reactions for Carbohydrates

A classic detection reaction for carbohydrates, which has been known since 1849, is the Fehling test. The Fehling solution can be used to differentiate between functional aldehyde and ketone groups. Aldehydes are oxidized to carbonic acids, which leads to a positive result, while ketones do not react. The Fehling's solution is prepared by combining two separate solutions. Fehling's A, a deep blue aqueous solution of copper(II) sulphate, and Fehling's B, a colorless solution of aqueous potassium sodium tartrate made strongly alkaline with sodium hydroxide. After combining equal volumes of both Fehling's solutions, the Fehling's reagent has a characteristic dark blue color. In the presence of reducing groups, the copper(II) ions are first reduced to yellow copper(I) hydroxide (CuOH) and then dehydrogenated to copper(I) oxide (Cu2O), which precipitates as a reddish-brown precipitate. The Fehling test can be used to analyses urine for glucose and thus detect diabetes. Another application is the breakdown of starch to convert it into glucose syrup and maltodextrins and measure the amount of reducing sugar. [26, 37, 54, 86]

Another detection reaction that is like the Fehling test is the Tollens test or silver mirror test. Like the Fehling test, it is used to detect aldehydes or reducing functional groups and is used to differentiate between these and ketones. Tollens' reagent is an ammoniacal silver nitrate solution. This is added to an aqueous solution of the substance to be analyzed in a test tube and heated for detection. The test is positive if the solution turns black due to the precipitation of elemental silver and silver is deposited on the inner wall of the test tube, forming a reflective coating (silver mirror). Both Tollens' reagent and Fehling's reagent give positive results with formic acid. [93, 129]

Another shortcoming of these tests is the ketol-enediol tautomerism (the Lobry de Bruyn-Van Ekenstein transformation, which is demonstrated in Figure 32). This is the base-catalyzed conversion of an aldose into the ketose isomer and/or vice versa. For example, D-glucose (an aldose) is converted into D-fructose (a ketose), which in turn can be converted into glucose or into the epimer D-mannose (epimerization). The product is a state of equilibrium between D-glucose, D-fructose, and D-mannose. In an alkaline environment, this can lead to the formation of endiolate ions, which have the same reducing effect as aldehydes. This also leads to a positive test result. [26, 40, 90]

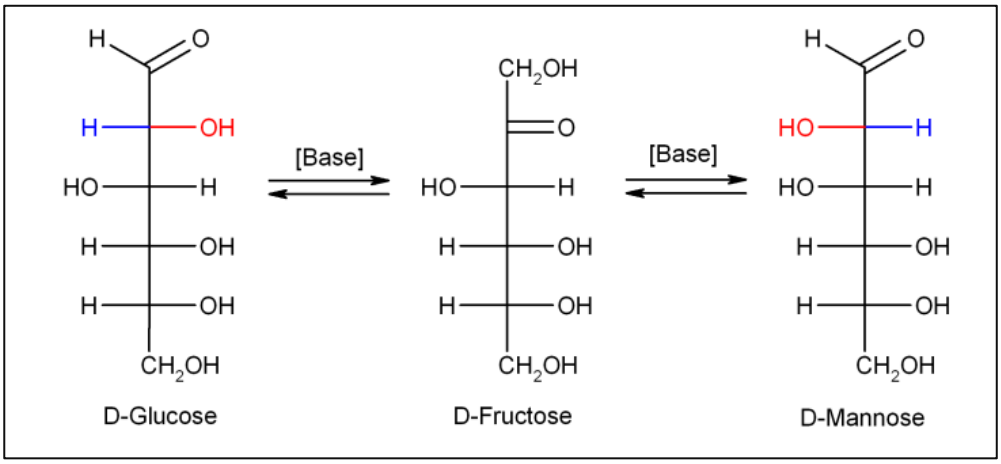


*Figure 32_ Equilibrium state between D-glucose, D-fructose, and D-mannose in the Lobry de Bruyn-van Ekenstein rearrangement (Wikimedia Commons)*

A sensitive classic detection reaction for ketose sugars is the Seliwanoff test. It can differentiate between aldose and ketose sugars by producing a red color in the presence of ketose sugars such as fructose, but also sucrose. In this case, the aldose group reacts much more slowly, resulting in only a weak color. A sugar solution is acidified with concentrated hydrochloric acid, an ethanolic resorcinol solution is added and heated. A furfural intermediate reacts further with resorcinol (benzene-1,3-diol) and atmospheric oxygen to form a strongly colored solution. [60, 114]

One test for the presence of pentoses is the Bial test. This test was originally developed for the diagnosis of Pentos Uria, a congenital metabolic disorder in which the pentose xylitol is present in high concentrations in the urine. The Bial reagent is a solution of orcin (5-methylbenzene-1,3-diol) and $FeCl_3$ in concentrated hydrochloric acid. The test is positive if a green-blue coloration occurs after adding Bial reagent to the test solution and heating. Here too, furfural is formed as an intermediate product, which reacts with orcinol to form a colored iron complex. Hexoses require a longer heating time for a similar color reaction. [13, 14, 39]

A more sensitive test for the presence of carbohydrates is the Molisch test (ring test). It is based on the dehydration of the carbohydrate by sulfuric acid or hydrochloric acid, which produces an aldehyde. The aldehyde (a furfural derivative) condenses with two molecules of a phenol (α-naphthol), producing a dye. A positive reaction is indicated by the appearance of a colored ring at the interface between the acid and the test layer. When added, the pentose arabinose forms a yellow dye, the deoxy sugar rhamnose an orange dye and the hexose glucose a salmon-colored dye. [84, 92, 102]

The Barfoed test is presented as the last detection reaction for monosaccharides. It is a method for differentiating monosaccharides from di-, oligo- or polysaccharides. The reagent for this test is a solution of copper(II) acetate in 1% acetic acid. It is based on the reduction of copper(II) acetate to copper(I) oxide ($Cu_2O$), similar to the Fehling test, and also leads to a red precipitate if the result is positive. As with the previous tests, the reaction is much slower with the other components, but in this case with disaccharides. [9, 137]

A classic detection reaction is also available for the polymers starch and cellulose. For starch, the classic solution of potassium iodide with iodine in water (Lugol's iodine) is used. The detection of starch is based on a characteristic and very sensitive color reaction (iodine-starch test). Depending on the type of starch and the concentration of the reactants, the color of the iodine-starch inclusion compound appears reddish, violet, blue or black. The polyiodine ions can be incorporated into the interior of the spiral-shaped starch molecules. Typically, a stronger branching of the molecular chain leads to a reddish color (20-30 glucose units to the next branching) and a less branched chain (over 45 units to the next branching) leads to a blue appearance. [27, 75, 107, 131]

A wet-chemical detection reaction for cellulose is the chlorine-zinc-iodine test. It is comparable to the iodine test (detection of starch). As cellulose forms a β-sheet structure

and not a spiral-shaped molecule (α-helix) like starch, direct detection with iodine alone is not possible here. The addition of zinc chloride causes the cellulose structure to swell and enables a color reaction with iodine. As zinc chloride is a harmful chemical, this method was modified with calcium chloride. If the result is positive, the test shows a characteristic blue-black discoloration, which indicates the presence of cellulose. [24, 49, 107]

### 1.7.2. Modern Detection Methods for Carbohydrates

In contrast to these wet-chemical detection reactions, modern detection methods generally use a chromatographic separation technique. As mentioned in chapter 1.4, chromatography is merely a separation method. A high-purity sample must be available as a reference for the determination. Since a separation technique is not suitable for detection, a detector is also required to obtain a signal from a sample compound. These facts lead to the conclusion that, in contrast to the simple and fast preparative wet-chemical detection, these complex analyzers, a trained user and sufficient space must be available. In this case, however, the use of analyzers offers the advantage of qualitative and quantitative determination of carbohydrates. [25, 62, 119]

Size exclusion chromatography (SEC) is used to differentiate between carbohydrates of different sizes. SEC is a type of liquid chromatography in which dissolved molecules can be separated based on their size (hydrodynamic volume). Porous polymers (cavities) serve as the stationary phase. Through diffusion, small molecules enter the many pores of the stationary phase and remain there. Large molecules penetrate fewer or no pores and therefore flow faster through the column. Therefore, large molecules are in the first fractions of the eluate, while smaller molecules elute later. All molecules that do not fit into the pores elute at the very beginning, and molecules that fit very well into all pores elute at the very end. The separation effect in SEC is not based on a filtration process, but on diffusion processes. [119, 122]

Ion chromatography (IC) is commonly used for carbohydrates. It is used in the form of an HPLC system in which the column is an ion exchanger. The separation process is based on the different interactions and binding strengths of the various carbohydrates. As explained in Chapter 1.4, there are various detectors. Varying from destructive to non-destructive detectors. Of this selection of detectors, the RID is a solid gold detector for carbohydrate mixtures and applicability (concentrations in the mg/ml range). For samples containing very small amounts of carbohydrates, the PAD is recommended

(concentrations in ng/ml). Mass spectrometry of varying complexity is used for high-end determinations. As most carbohydrates are water-soluble, HPLC is currently the most important chromatographic method, as it enables fast, specific, sensitive and precise measurement. [25, 57, 119]

For gas chromatography (GC), a sample must be brought into the gas phase undecomposed (must be volatile). To achieve this, carbohydrates can be derivatized to change their probertites. Another method for detecting derivatized carbohydrates is electrophoresis. To do this, the carbohydrates must be modified so that they have an electrical charge. In an electric field, charged particles in solution migrate to the pole with the opposite charge. For this purpose, the sample solution is applied to a carrier medium (liquids, gels or solids). If a gel is used as the medium, this is referred to as gel electrophoresis. Such an advice is shown in Figure 33**a**. The driving force for the separation is a voltage potential that is applied between two opposite edges of the gel and attracts or repels the charged molecules. In addition to the electrical potential, the size and mass of a molecule also play a role due to the diffusion process through the gel. A small molecule with a strong charge moves faster than a molecule of the same size with a weak charge. One advantage of this separation method is that the isolated compounds can be reused, as the gel can be cut open and the desired compound extracted. [25, 60, 77, 119, 135]

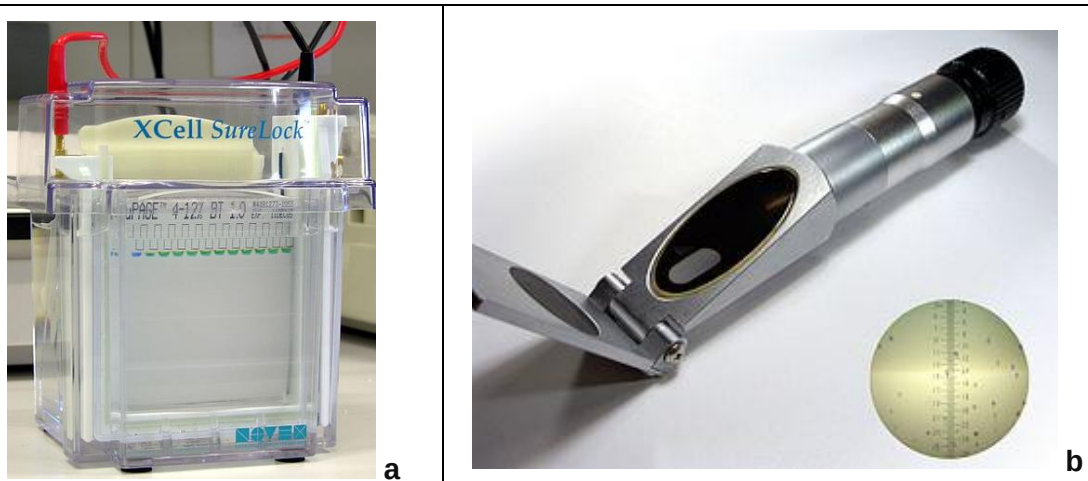


*Figure 33_On the left, a modern gel electrophoresis system with a vertical tank, the sample chambers are the green and blue dots. When an electric field is applied, the sample molecules move in a certain direction at different speeds depending on their charge, mass, and size. On the right, a typical handheld refractometer with an open measuring prism used to measure the sugar content. In the bottom corner, a view through the eyepiece of the handheld device, where a built-in scale, which can be read by eye, serves as a detector. (Wikimedia Commons)*

A classic instrumental field method for carbohydrates is the (hand-held) refractometer, shown in Figure 33**b**. It is a device for measuring the refractive index (refractometry) of a liquid. It is used to determine the degree of ripeness during the grape harvest, to measure the original wort when brewing beer and in beekeeping to determine the water content of honey. Refractometry can also be used to determine the sugar and alcohol content in aqueous solutions as well as acid concentrations in batteries and the purity of organic solvents. [25, 44, 121]

## 1.8. National Renewable Energy Laboratory

The National Renewable Energy Laboratory (NREL) is recognized as the leading laboratory in the United States for research and development in the field of renewable energy and energy efficiency. It specializes in the research and development of renewable energy, energy efficiency, energy system integration and sustainable transportation. NREL is home to the National Center for Photovoltaics, the National Bioenergy Center and the National Wind Technology Centre. NREL works with private partners to bring technological developments in renewable energy, energy efficiency and technology to the marketplace and society. NREL develops laboratory analytical procedures (LAPs) for the standard analysis of biomass. These methods help scientists and analysts to learn more about the chemical composition of biomass raw materials and intermediate process products. [1–4, 8, 89]

## 1.9. Kappa Number

The kappa number is an indirect analytical method and a parameter that describes the residual lignin content. The kappa number can be used to estimate the intensity of the pulping process and the amount of bleaching chemicals required. As the amount of bleaching agent required depends on the lignin content of the pulp, the kappa number can be used to monitor the effectiveness of the lignin extraction phase of the pulping process. It is roughly proportional to the residual lignin content of the pulp. Chemically, it measures the amount of easily oxidizable double bonds in the pulp. This leads to the reaction of double bonds and aromatic structures as well as resins and hexuronic acids (HexA). HexAs are formed from the hemicelluloses during the chemical pulping process. [29, 80, 128]

The kappa number is determined according to ISO 302 or TAPPI T 236 and applies to all types of chemical and semi-chemical pulps and results in a kappa number in the range of 1-100. The kappa number for bleachable pulps is in the range of 25-30, for sack paper pulps in the range of 45-55 and for corrugated board pulps in the range of 60-110. As a rule of thumb, the kappa number is approximately proportional to 6.57 times the lignin content in per cent. [29, 79, 80]

## 1.10. CASA Method

The cysteine-assisted sulfuric acid dissolution method (CASA) for lignocellulosic samples was first described by Lu et al. in 2021 and is an analytical method for lignin in solution. In this method, a mixture of sulfuric acid and the amino acid L-cysteine is used to completely dissolve the lignocellulosic biomass. The schematic flow is shown in the following Figure 34. In the lignin determination methods described so far, only small amounts of lignin are dissolved, while the majority remains as insoluble Klason lignin. Since the CASA method can completely dissolve a lignocellulosic sample and lignin has an aromatic character, UV/Vis spectroscopic applications can be used for the determination. Lu et al. have published that the solution of fully dissolved loblolly pine powder becomes homogeneous and purple in color within 60 minutes after stirring at 24 °C. The exact mechanism behind the dissolution of lignocellulosic biomass in cysteine-containing sulfuric acid is not yet clear, but offers potential for methods to measure lignin content, as mild conditions are sufficient and only a few milligrams of sample are required. [72]

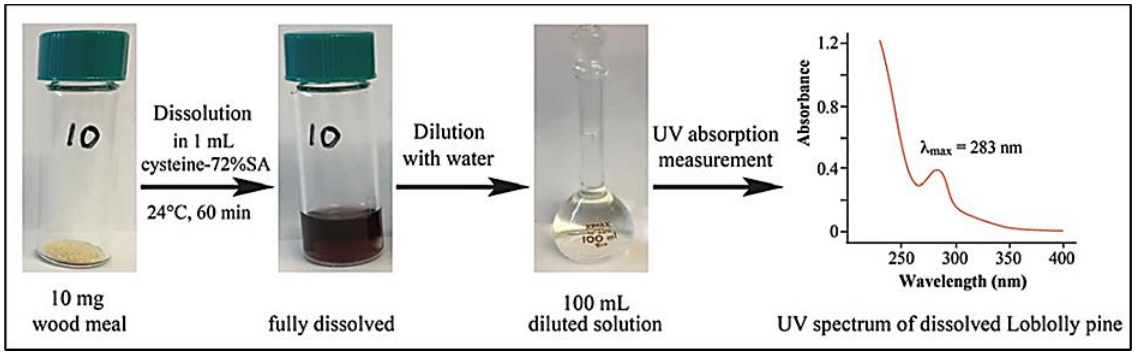


*Figure 34_Scheme of the dissolution of wood meal in CASA solution for lignin quantification using UV/Vis spectroscopy [72]*

Dilution with deionized water at a ratio of 1:50 or 1:100 resulted in colorless solutions that can be measured at 283 nm UV/Vis. Here, the UV absorption spectrum of the dissolved loblolly pine wood showed a local absorption maximum, which indicates the aromatic properties of the lignin. When this method is applied to samples containing only cellulose or hemicellulose (no lignin), the signal disappears, confirming that only the aromatic character of lignin generates a signal. As a spectrophotometric method, the CASA method also requires standards for meaningful quantification. Since biomass is a material produced by nature, there are large differences even within a single plant part, making it difficult to find one. To make matters worse, lignin itself consists of three different molecules, which also have different biological compositions and properties.

This circumstance makes it impossible to obtain a standard material (certified reference material (CRM)) for quantification. To circumvent this problem to a certain extent, synthetic lignin, commonly referred to as DHPs (dehydrogenation polymers) from monolignols, were used as lignin standards. [72]

Lu et al. use these DHPs to develop calibration curves for quantification. DHPs have the advantage that they are pure and can be easily produced in sufficient quantities as they are laboratory-produced products. Thus, different ratios of monolignols can be determined to create a biomimetic system that is close to the biomasses used in nature. [72]

Figure 35 shows the verification of the CASA method and the comparison with established methods. To verify the reliability of his CASA method for lignin quantification, Lu et al. used different samples of lignocellulosic biomass, including 7 softwoods, 6 hardwoods and 6 grasses. Their results were compared with the results of the NREL protocol (NREL/TP-510-42618). This correlation between the lignin determination methods is shown in the Figure 35 below. All 19 samples were correlated with the acid-insoluble lignin content (Klason lignin). 9 samples were compared with the total lignin content (sum of acid-insoluble and acid-soluble lignin). Both plot functions have a slope of almost 1 and correlate very well with the classical determination methods. [72]

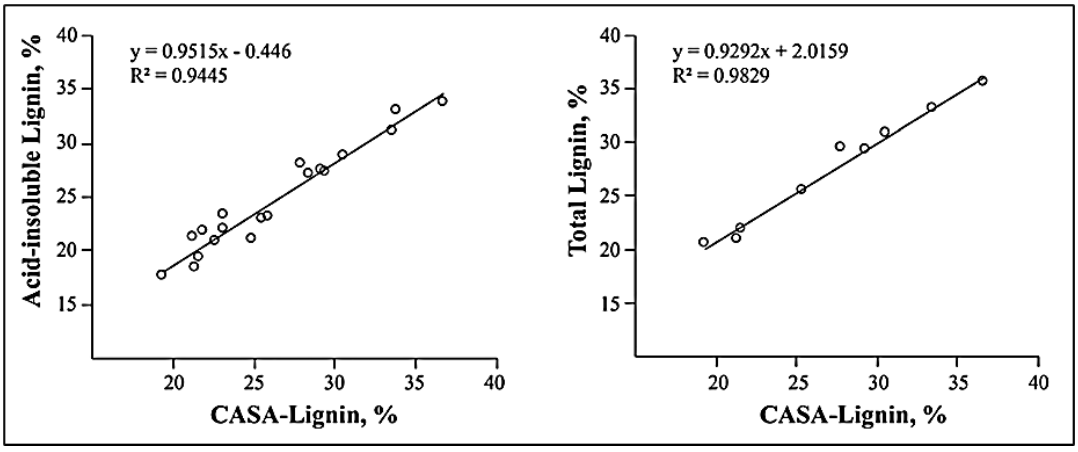


*Figure 35_Comparison and correlations between the lignin contents measured using CASA method and Klason method (NREL protocol); total lignin is defined as sum of acid-insoluble and acid soluble [72]*

Further advantages of this method are the lower preparative effort and the single analysis step compared to classical methods, in which two different determinations have to be carried out to obtain the total lignin. [72]

# 2. Experimental

In this work the NREL LAP 42618 - "Determination of Structural Carbohydrates and Lignin in Biomass" was tested, optimized and implemented. For the determination of total lignin, the direct analysis method of acid hydrolysis (72% sulfuric acid) was used to produce Klason lignin and the indirect analysis method of UV/Vis spectroscopy was used to determine acid-soluble lignin. Two different HPLC systems were used and compared to analyze carbohydrates. [4, 57, 76] For a Round Robin test the six different lignocellulose biomass samples shown in the following F were used.


*Figure 36_Centrifugal mill milled lignocellulose biomass samples used for a Round Robin test; samples were CD-1 (**a**) and CD-4 (**b**), both kraft paper, CD-6 (**c**), a recycled paper, CD-168 (**d**), a fully bleached paper, and MonoX (**e**), a pulp sample*

In addition to the NREL LAP lignin determination, kappa numbers were determined to compare the total lignin content. For the last experiment, the recently published CASA method was used as a potential lignin determination method.

## 2.1. Pretreatment

The aim of the pre-treatment was to bring the biomass samples to be analyzed into a more uniform and homogeneous form to ensure a better representation of the population and easier accessibility for extraction and reaction agents. This pre-treatment had included the steps of grinding and extraction of the organic and water-soluble components. These steps were based on NREL LAPs 42619 - "Determination of Extractives in Biomass" and 42620 - "Preparation of Samples for Compositional Analysis". [3, 8]

### 2.1.1. Milling

For wood-based biomass or samples that were difficult to grind, a certain amount (approx. 500 g) of the sample was prepared for a pre-grinding step. For this purpose, they were dried in a well-ventilated place at room temperature for a certain time to reduce the moisture content (<10 % is recommended) (approx. 3 weeks at 30 °C with daily stirring and turning). Alternatively, drying could also take place in a muffle oven at 105 °C or in an oven at 40 °C with circulating air. A random sample of 100 g was taken from this air-dried mass and ground in accordance with NREL LAP 42620 using a laboratory knife mill with a 2 mm sieve. [8]

For easily comminuted lignocellulosic biomass samples with a low moisture content (<10 %) such as maize, paper or fibers, pre-shredding with shears, knives, shredders or hand mills was sufficient. The final comminution is then carried out with the centrifugal mill (the Retsch centrifugal mill ZM 200 used is shown in the following Figure 37).

*Figure 37_Picture of an open RETSCH ultra centrifugal mill ZM 200 with accessories in circles; yellow circle a DR 100 vibration distribution device (used for even, continuous dispensing and conveying of free-flowing bulk materials and fine powders); blue circle a cyclone with dust filter and stainless-steel collection container*

From these pre-comminuted sample parts (diameter approx. 2-6 mm), 50 g of sample also taken at random, were comminuted in a centrifugal mill (Retsch ZM 200). This was done in three stages, starting with the 2.00 mm sieve, continuing with the 0.75 mm, and ending with the 0.20 mm sieve at a speed of 18,000 rpm of the 12-tooth plug-in rotor. From this point onwards, the biomass samples had a cotton-like consistency and a high surface area to volume ratio. After final comminution, the biomass sample was collected and stored in a polyethylene (PE) freshness bag with a double zipper.

Due to the increased development of fine dust, attention had to be paid to the carcinogenic and irritant hazards of fine dust and sample components. Suitable protective clothing should be worn (respiratory protection, face protection and closed clothing are strongly recommended).

### 2.1.2. Solvent Extraction

The uniformly sized biomass samples were further processed based on NREL LAP 42619. [3]

For this purpose, the extraction was carried out using a Soxhlet apparatus. First, a Soxhlet extraction thimble made of cellulose was prepared by drying it for several hours (>4 h) in a muffle furnace at 105 °C and then determining its mass to the nearest 0.1 mg. A certain amount of ground biomass was filled into the tared extraction thimbles. The moisture content and dry mass of this specific amount of biomass had to be determined. The total weight of the filled thimble with the biomass (both in the dry state) was then also determined to the nearest 0.1 mg.

The filled and weighed thimble was placed in the Soxhlet apparatus, which was connected to a reflux condenser. The extraction was carried out in two steps. For the first extraction step, 200 ml of deionized water (DI $H_2O$) was used as extraction solvent. Then 200 ml of ethanol (EtOH) was used for a second extraction step. The reflux time was between 12 and 24 hours, depending on the sample, sample volume and solvent cycle time. Towards the end of the extraction, a clear liquid must accumulate in the Soxhlet siphon.

Between the individual steps and at the end, the apparatus was cleaned. While the glass apparatus was burned out and cooled down, the extract obtained was evaporated and determined gravimetrically. After the extraction process, the total mass of thimble with biomass was determined and the extraction loss was calculated in relation to the total extract balance.

In addition to Soxhlet extraction, NREL LAP 42619 also includes instructions for using an Accelerated Solvent Extraction (ASE) system, which significantly reduces extraction times and provides greater efficiency.

The biomass sample obtained was theoretical free of water-soluble components such as salts and minerals, free sugars and easily accessible organic substances such as resins, fats, waxes and colorants (removal of all non-structural materials).

## 2.2. Ash Content

The ash content is defined as the total content of all inorganic components, both soluble and insoluble. This primarily includes metals, minerals and rocks that were absorbed or adsorbed by organisms or are introduced as impurities during processing. In this step, the heat-resistant and insoluble components of the biomass were determined. In accordance with NREL LAP 42622 - "Determination of Ash in Biomass", the biomass sample was incinerated at 575 °C in a muffle furnace for n times 12 hours (where n is the number of 12-hour ash cycles). [2]

For this purpose, depending on the number of samples, several porcelain crucibles were prepared with a blank sample (crucible without sample). The crucibles were annealed at 575 °C for >4 hours, cooled to room temperature in a desiccator over silica gel and weighed to the nearest 0.1 mg.

A dry sample quantity of 2 to 5 g was weighed into the prepared crucibles. Air-dried samples can also be weighed but must then be dried in the crucible at 105 °C and their dry weight determined. The result had to be the sum of the dry weight of the crucible and the biomass.

The porcelain crucible containing the sample and the empty crucible were then placed in the muffle chamber and heated to 575 °C. Incineration takes place at this temperature for 12 hours. After this time, the crucibles were cooled in the desiccator over silica gel and weighed. (= a single cycle) These steps were repeated until the change in weight was within the weighing error of the balance (n was between 2 and 3 cycles (24 to 36 hours of ashing)).

This process was carried out for each sample at least twice.

## 2.3. Sample Preparation for Determination

The sample preparation for the determination of the lignin and carbohydrate content was carried out in accordance with NREL LAP 42618 - "Determination of Structural Carbohydrates and Lignin in Biomass" and ISO/FDIS 21436 "Pulps - Determination of lignin content". [4]

### 2.3.1. Moisture Content

In a first step, a certain amount of the pre-treated biomass sample was dried and weighed as described in NREL LAP 42621 "Determination of Total Solids in Biomass and Total Dissolved Solids in Liquid Process Samples" to determine the moisture content. For this purpose, a certain amount of the sample was weighed into a dried and tared self-folded paper tray. This tray was then placed in a muffle furnace at 105°C overnight, cooled to room temperature in a desiccator and weighed to calculate the moisture content. [1]

### 2.3.2. Sulfuric acid hydrolysis

Approximately 300 ± 10 mg of the pretreated and specified biomass sample was weighed into a plastic weighing boat and transferred via a funnel into 100 ml pressurized containers. Then 3 ml (4.92 g) of 72% sulfuric acid was added and the mixture was homogenized while stirring with glass rods. The concentration of the sulfuric acid was double checked by its density (1.6338 g/ml at 20 °C) and a neutralization titration with sodium hydroxide.

The pressure vessels were then placed in a water bath set at 25 °C and incubated for 60 minutes, with the liquid sample mixture being stirred for 30 to 60 seconds every 10 minutes.

After 60 minutes of hydrolysis with sulfuric acid, the pressure vessels were removed from the water bath and diluted with 84.0 ml (84.0 g) of deionized water to a sulfuric acid concentration of 4 %. The vessels were sealed with Teflon screws, shaken vigorously and then autoclaved in an autoclave (CertoClav MultiControl 2) at 121°C for 60 minutes. After autoclaving, the pressurized containers were cooled to room temperature.

## 2.4. Determination of Lignin

For the determination of lignin in lignocellulosic biomass, the lignin content had to be divided into two fractions, the smaller acid-soluble lignin fraction and the larger insoluble (Klason) lignin fraction. To avoid errors due to incorrect excess quantities (insoluble non-lignin components), solvent extraction and ash content were recommended, as these contain or were insoluble sample components (resins and metals).

### 2.4.1. Klason Lignin (Acid Insoluble Lignin)

During autoclaving, several glass microfibre filters (Whatman; GF/A 9.00 cm diameter) for vacuum filtration were dried in a muffle furnace at 105 °C for 2 hours and their dry weight determined (one filter for each sample plus blank).

The cooled sample solutions were then vacuum filtered through one of the glass-microfibre filters using a Buechner funnel assembly, and the filtrate was collected in a vacuum flask (Buechner flask). After filtration, the pressure tube was rinsed with deionized water to quantitatively transfer all remaining solids to the filter and to wash the residue on the filter acid-free. The loaded glass microfibre filters were then dried overnight at 105 °C in a muffle furnace. The filters were then cooled to room temperature in a desiccator and weighed. The difference in weight was defined as acid insoluble (Klason) lignin.

The pure filtrate was transferred to 50 ml centrifuge tubes for storage to use in further steps for the determination described in section 2.4.2. Acid Soluble Lignin and 2.5. Determination of Carbohydrates. For longer storage (>2 days) the samples were stored at -18°C.

### 2.4.2. Acid Soluble Lignin

The acid-soluble lignin was determined using the filtrate from the lignin determination according to Klason, a UV/Vis spectrophotometer (Shimadzu UV-1900i) and high-precision quartz cuvettes (Hellma Analytics; 1 cm path length). For the measurement, a baseline correction was first performed, followed by a background run with deionized water.

A spectrum from 190 to 400 nm was recorded for each sample. In the 200 to 300 nm range, the absorbance must be in the range of 0.7 to 1.0. For this purpose, the samples

were diluted with deionized water. The blank sample serves as a reference and was also diluted in the same way as the samples.

The acid-soluble lignin was determined according to the Lambert-Beer law, Eq. (1). Letter $A$ is the absorbance of a sample resulting from the recorded spectrum at a wavelength of 205 nm with an absorption constant ($\varepsilon$) of 110 l/(g*cm) (ISO/FDIS 21436). The path length $l$ (cm) was determined using the cuvettes used for spectroscopy and the concentration $c$ was calculated.

## 2.5. Determination of Carbohydrates

The carbohydrates were also determined from the filtrate obtained in step 2.4.1 Klason Lignin. A distinction must be made between the total carbohydrate determination, which is carried out with non-extracted samples, and the determination of the structural carbohydrates, which requires step 2.1.2 Extraction.

### 2.5.1. Reagents and Materials

Based on NREL LAP 42618, there were five different monosaccharides commonly used for analyzing and quantifying biomass. These sugars were L-(+)-arabinose, D-(+)-galactose, D-(+)-glucose, D-(+)-mannose and D-(+)-xylose. The sugar alcohol xylitol (ISX) was used as the internal standard for HPLC-RID, while the hexose deoxy sugar L-(-)-fucose (ISF) was used for HPAE-PAD. In both LC systems, the mobile phase was pure water.

As two different LC systems were used, the type of sample preparation was also different for the two systems.

### 2.5.2. HPLC-RID

Carbohydrate analysis using a HPLC-RID system is an integral part of NREL LAP 42618. [4]

The LC system used consists of Agilent 1100 instruments and is shown in the following Figure 38. A degasser unit G1322A (Figure 38**b**), an iso pump unit G1310A (Figure 38**c**), an injector unit ALS G1313A (Figure 38**d**) and a refractive index unit G1362A (Figure 38**e**) were used. The column oven was a Knauer Jetstream column thermostat (Figure

38**f**). A BioRad HPLC carbohydrate analysis column Aminex HPX-87P (300 x 7.8 mm; catalogue 125-0098) with guard column BioRad Micro-Guard Carbo-P (30 x 4.6 mm; catalogue 1250119) was used as the stationary phase. In the following Table 2 the operation conditions for measurement are listed. The full HPLC-RID system is pictured in the following Figure 38.

*Table 2_System conditions for HPLC-RID measurement (US…Ultrasonic); * due to hardware problems, the column oven set at 80°C never reached more than 60°C*

| | |
|---|---|
| **Injection volume** | 15 µl |
| **Mobile phase** | Pure water (15 min US treated) |
| **Flow rate** | 0.6 ml/min |
| **Column oven temperature** | 80°C * |
| **RI detector unit temperature** | 35°C |
| **Run time** | 60 min |

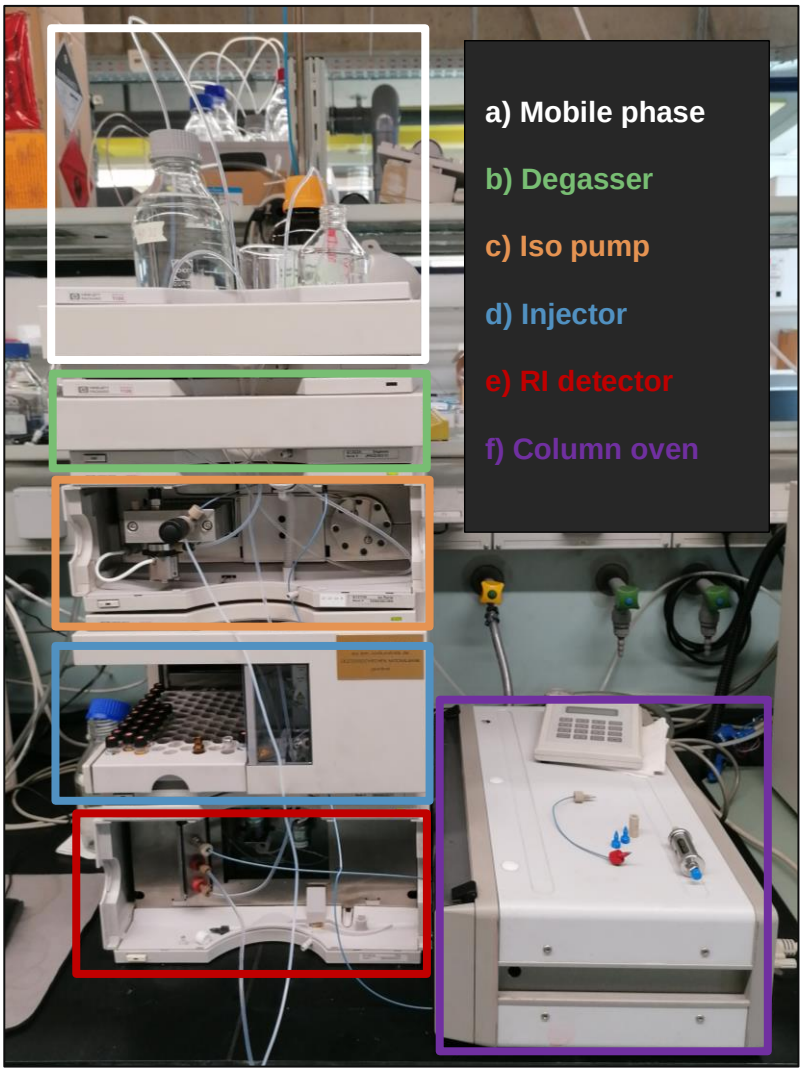


*Figure 38_Picture of the HPLC-RID system used for carbohydrate determination; mobile phase was pure water; column oven was limited to 60°C due to hardware problems*

A standard mixture containing all five sugars relevant for quantification must be prepared for calibration. A calibration curve with at least four points with different concentrations between 0.1 g/l and 4.0 g/l must be created from this sugar standard mixture to check the linearity as well as the LOQ and LOD of the LC system. In addition, a calibration verification standard (CVS) must be prepared with the same five sugars but from a different source (manufacturer or batch). The concentration of the CVS must be chosen in the middle of the linear range and must not correspond to a calibration point (1.33 g/l and 2.5 g/l). It was used to check the quality and stability of the calibration curve throughout the measurement run. Xylitol was used as an internal standard (ISX). A starting stock solution of 150 g/l was prepared, and 20 µl/ml was added to the prepared 1 ml samples with a piston pipette prior to measurement to achieve a final concentration

of 3 g/l. The run time of 30 minutes specified in the NREL LAP was extended to 60 minutes, as xylitol elutes at minute 53.

To prepare the sample, 10 mL of the Klason lignin hydrolysis liquid obtained in section 2.4.1. Klason Lignin (Acid Insoluble Lignin) was used and transferred to a 20 mL glass vial. Pure calcium carbonate powder was used to neutralize the remaining 4 % sulfuric acid to a pH of 5-7. By slowly adding calcium carbonate powder to avoid over-foaming and stirring with a magnetic stirrer, the pH was increased and checked with pH paper. As soon as a pH value of about 6 was reached, stop adding calcium carbonate and allow the gypsum ($CaSO_4$) formed to settle. A full 5 ml syringe was collected from the supernatant and filtered through a syringe filter (PTFE; hydrophilic; 0.20 µm pore size) into a 4 ml glass vial. The result is a clear liquid. From this 4 ml glass vial, 1 ml was transferred into a 1.5 ml HPLC glass vial using a piston pipette. Now 20 µl ISX was added to each HPLC vial (calibration, CVS, and samples) using a piston pipette. The vials were sealed with perforated screw caps with a Teflon seal and homogenized.

The Agilent ChemStation Revision B.01.03 software (Agilent Technologies) was used to analyze the obtained HPLC-RID data.

### 2.5.3. HPAE-PAD

The ion exchange (IE)-LC system used consisted of a Dionex Integrion ion chromatography system (Thermo-Fisher Scientific, Waltham, USA) with a Dionex AS-DV autosampler. The system was equipped with a Thermo Scientific ED solid gold working electrode and a Dionex pH-Ag/AgCl reference electrode connected to the pulsed Amperometric detection (PAD) cell. The mobile phase (KOH and pure H2O) was automatically generated by the system from a Dionex EGC 500 KOH eluent generator cartridge and high purity water (conductivity <0.055 µS cm-1 and TOC <2 ppb). The removal of impurities and the regeneration of the eluent were carried out with a continuously regenerated Dionex CR-ATC 600 anion capture column. A Thermo Scientific Dione CarboPac PA20 (150 x 3 mm) IC analysis column with a Dionex CarboPac PA20 (30 x 3 mm) guard column was used for chromatographic separation. Special 5.0 ml Dione AS-DV Autosampler PolyVials with corresponding caps were used as bottles for the autosampler. The operating conditions for the measurement are listed in the following Table 3. [21, 76]

*Table 3_System conditions for HPAE-PAD measurement (Run time consists of 45 min measurement plus 15 min detector surface regeneration) [76]*

| | |
|---|---|
| **Injection volume** | 10 µl |
| **Mobile phase** | KOH & pure $H_2O$ |
| **Flow rate** | 0.4 ml/min |
| **Column oven temperature** | 30°C |
| **PAD detector unit temperature** | 20°C |
| **Run time** | 45 + 15 min (60 min) |

A run initially consisted of a 10-minute column equilibration with 2 mM KOH, followed by the injection of 10 µL of sample and a separation phase (25 minutes, 2 mM KOH). This is followed by a 10-minute regeneration with 100 mM KOH as eluent and a further 10-minute run-on. After each sample measurement, a sample of ultrapure water was injected and eluted with 100 mM KOH for 7 minutes to regenerate and equilibrate the system. [76]

Compared to the HPLC-RID, this system works with lower concentrations in the range from 0.1 mg/l to 20 mg/l. Therefore, the calibration curve for the sugar standards between 0.1 and 5 mg/l and for the internal standard fucose (ISF) must be validated over the entire range.

As approximately 300 mg of biomass was mixed with 86.72 ml of liquid, a maximum concentration of 3459.41 mg/l (3.46 g/l) was possible when analyzing a single pure sugar. This means that the samples must be diluted in order not to overload the HPAE system. A two-stage dilution was carried out. Firstly, a 1:10 dilution was carried out and then a further 1:10 dilution to achieve an actual dilution of 1:100. In addition, a second dilution of 1:100 was made from the first 1:10 dilution to achieve a total dilution of 1:1000.

These dilution steps were required for each measurement point. Therefore, each sample was measured with two dilution concentrations (1:100 and 1:1000). In comparison to HPLC-RID, no neutralization step needs to be carried out here, as the acid concentration was already in the pH range of 5 to 7 due to the strong dilution. The filtration step with the syringe filter was unavoidable and the ISF was added before the filter step (PTFE

syringe filter; hydrophilic; 0.20 µm pore size). The PolyVials bottles were sealed with special caps and are now ready for measurement.

The software Chromeleon 7 (Thermo-Fisher Scientific) was used for data evaluation. [76]

## 2.6. Kappa Number

The kappa number of milled untreated and pre-treated lignocellulosic biomass samples was determined according to ISO 302:2015 "Pulps - Determination of Kappa number".

## 2.7. CASA Method

The cysteine-assisted sulfuric acid (CASA) dissolution method was performed as described in the work of Lu et al., 2021. [72]

An L-cysteine stock solution of 0.1 g/ml in 72% sulfuric acid was prepared by dissolving 5 g of L-cysteine in 50 ml of 72% sulfuric acid. 5 to 10 mg of a dried lignocellulosic sample was weighed into a 4 ml glass vial with a screw cap. 1 ml of the stock solution was added and the vial was sealed with a Teflon-coated screw cap. The reaction starts immediately with the addition of the CASA solution. To improve the reaction conditions, the vial was heated to 60 °C and stirred with a magnetic stirrer. A reaction time of at least 60 minutes was required to completely dissolve the lignocellulose sample.

After the reaction time, the colored sample solution was measured using UV/Vis spectroscopy. The selected wavelength for lignin was 283 nm, and to achieve an absorbance value between 0.7 and 1.0, the solution must be diluted with deionized water. Common dilutions for this were between 1:50 and 1:100. The same diluted CASA stock solution was used as a reference.

# 3. Results & Discussion

## 3.1. Pretreatment

As already mentioned, the aim of pre-treatment was to bring the biomass into a more uniform and homogeneous form to ensure better visualization of the population and easier accessibility for extraction and reaction agents.

### 3.1.1. Milling

The pre-treatment step of comminution was of utmost importance, as the following Figure 40 shows the gravimetric lignin determination of Klason lignin from the same maize sample but with different comminution pre-treatment show. In this step, all unreacted or insoluble sample components (resins) and insoluble metals (ash) were included in the calculation of the insoluble lignin content (Klason lignin). In Figure 40, incompletely hydrolyzed sample components were visible as black pieces of different sizes on the filter discs. These black pieces simulate a falsely high Klason lignin content. In addition, the sample images show that the samples were not homogeneous and the sampling for analysis is also subject to a large source of error, as different fractions were recognizable to the naked eye. These facts led to a further, but final pre-treatment step with a RETSCH Ultra Centrifugal Mill ZM 200. By grinding down to the 0.2 mm filter screen, the biomass samples became homogeneous and uniform with a cotton-like appearance, as shown in the following Figure 39.

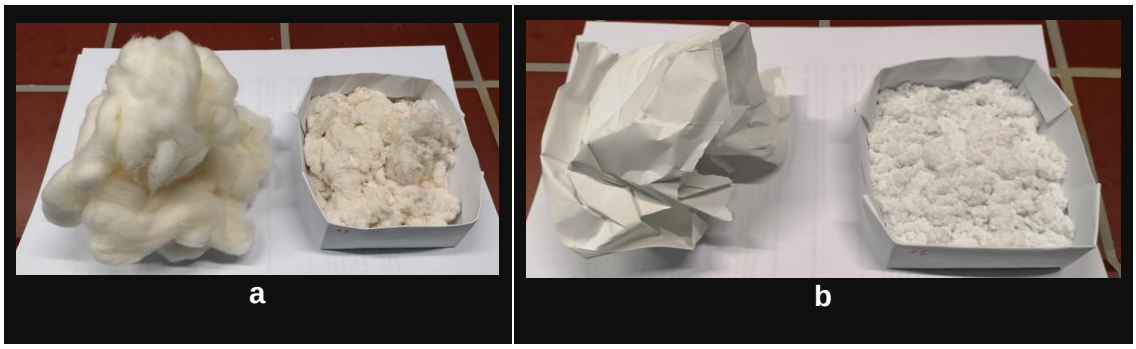


*Figure 39_Raw and milled samples of cotton (a) and copy paper (b) using a RETSCH ultra centrifugal mill ZM 200; starting with 2.00 mm sieve down to 0.20 mm sieve*

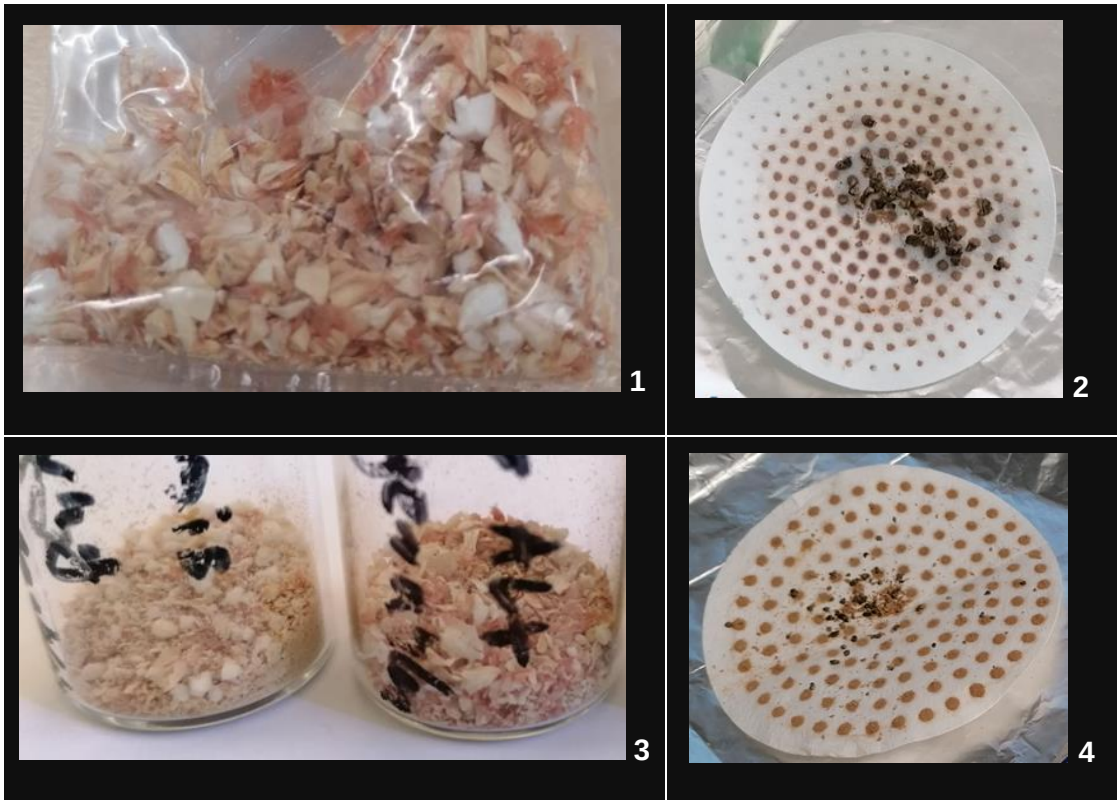


*Figure 40_Pictures of Klason lignin determination using corn samples of different pretreatment; 1 & **2** were corn samples with only knife chopping as pretreatment; **3** & **4** were corn samples pretreated according to NREL LAP 42620 using a knife mill; the filter discs shows black pieces of incompletely hydrolyzed sample components, which simulate an excessively high Klason lignin content*

The next Figure 41 shows a filter disk of a completely pre-treated pulp sample. Compared to the filter discs shown previously, no residue and an even color can be seen.

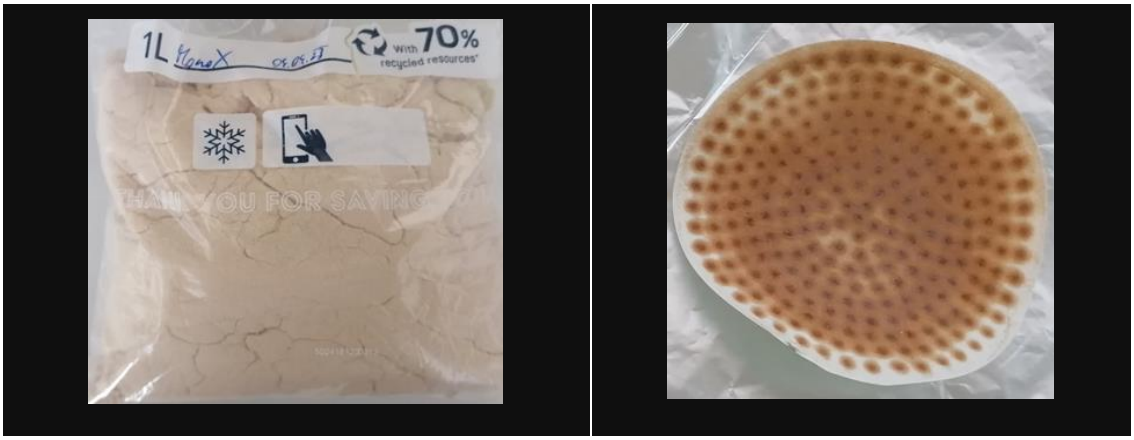


*Figure 41_For comparison a picture of the Klason lignin determination step of a full pretreated pulp sample and their filter disk residues, showing no residues of incomplete hydrolysis*

### 3.1.2. Solvent Extraction

Once the sample has reached a homogeneous and uniform consistency, organic sample components and non-structural material must be separated. These were components of a sample and can only be reached and dissolved using organic solvents. Common and largely harmless solvents for removing organic substances from biomass are alcohols (methanol, ethanol, isopropanol) and acetone. According to NREL LAP 42619, extraction with organic solvents (ethanol) and subsequent aqueous extraction is recommended. The extraction process was demonstrated in the following Figure 42, Figure 43 & Figure 44 using a spruce wood sample ground with a 0.2 mm sieve.

In the following Figure 42, the extraction step was carried out using only acetone as the extraction solvent (two Soxhlet extractions with acetone only). The solvent-free extract solid was a brownish and brittle film with a resinous odor that can be completely dissolved in acetone.

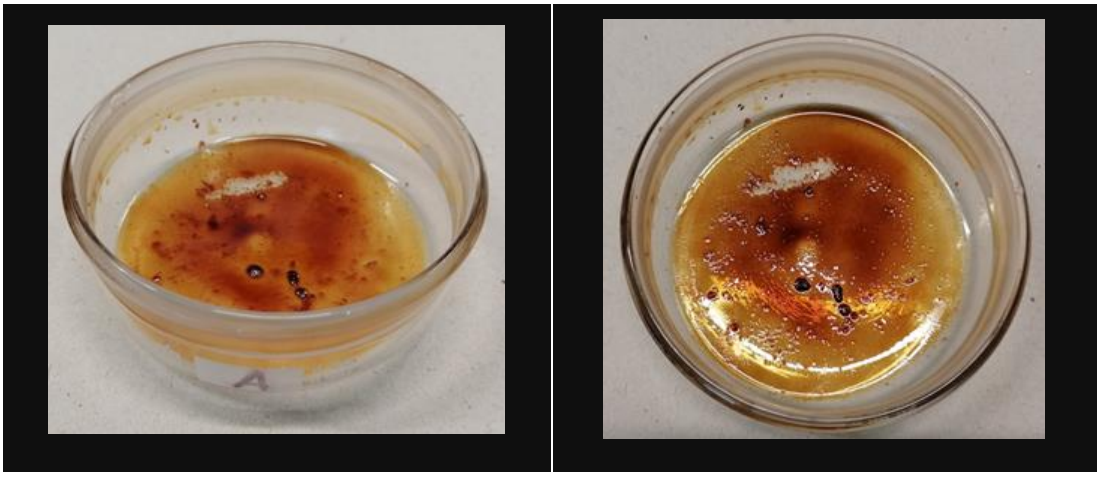

*Figure 42_Evaporated residual solids from a double acetone Soxhlet extraction of a spruce sample*

The next Figure 43 shows the residues of a Soxhlet extraction according to NREL LAP 42619. Deionized water was used in the first extraction stage and ethanol in the second extraction stage. A very dark-colored residue can be seen in glass beaker A in Figure 43, which was also very brittle and breaks up into shell-shaped pieces. A brownish residue can be seen in beaker 5 (also in Figure 43), which has similar properties to the previous acetone film, but is less shiny.


*Figure 43_ Evaporated residual solids from Soxhlet extraction according to NREL LAP 42619 of a spruce sample (first $H_2O$, then EtOH); beaker A (left) was the residue from the water extraction and beaker 5 (right) contains the residue from the ethanol extraction*

In the following Figure 44, the order of the solvents was reversed. Ethanol was used as the first extraction solvent and deionized water as the second solvent. This process was referred to as inverse Soxhlet extraction. The extraction with organic solvents also leads to a film residue like the acetone film with the same surface appearance. The scratch test again shows a brittle behavior as with the other films. The water extraction film, on the other hand, had a completely different surface appearance. When the water evaporates, a cracked film was formed that does not adhere to the bottom of the beaker.

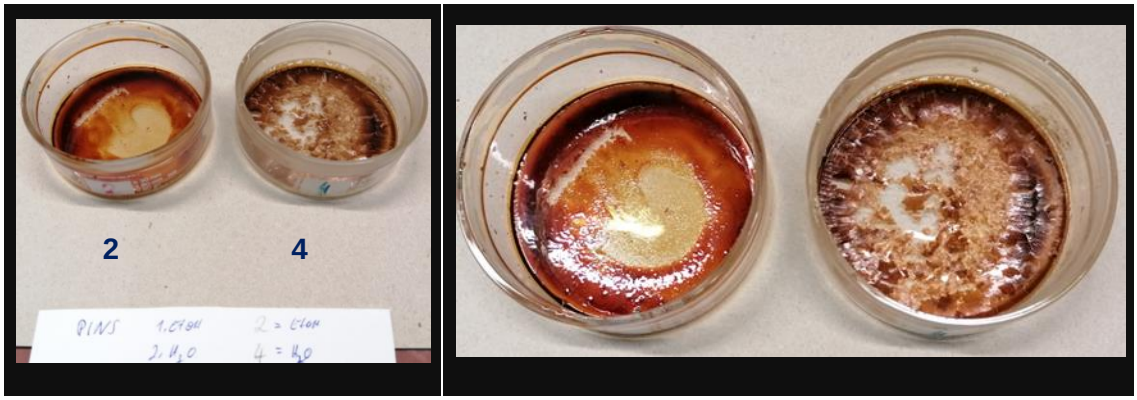


*Figure 44_Evaporated residual solids from inverse Soxhlet extraction according to NREL LAP 42619 of a spruce sample; "inverse" means reverse solvent order (first EtOH, then $H_2O$); beaker 2 (left) contains the residues from the ethanol extraction, while beaker 4 (right) contains the residues from the water extraction*

A visual and odor comparison made it clear that only resin components were removed during acetone extraction in the three extraction methods. In the other two methods, more material was extracted from the spruce sample, which explains the change in color, scratch behavior, and quantity. A graphical comparison of quantities was shown in the next Figure 45. There, the mass differences between the initial and final weights were

compared. As already mentioned, the acetone extraction again shows the small amount of resin extracted from the spruce sample at 2.37 m%. The other two extracted materials are 7.59 m% for the NREL order ($H_2O$+EtOH) and 6.36 m% for the reverse order (EtOH+$H_20$). This results in a 2.7 to 3.2 times higher amount of extracted material compared to the use of acetone alone.

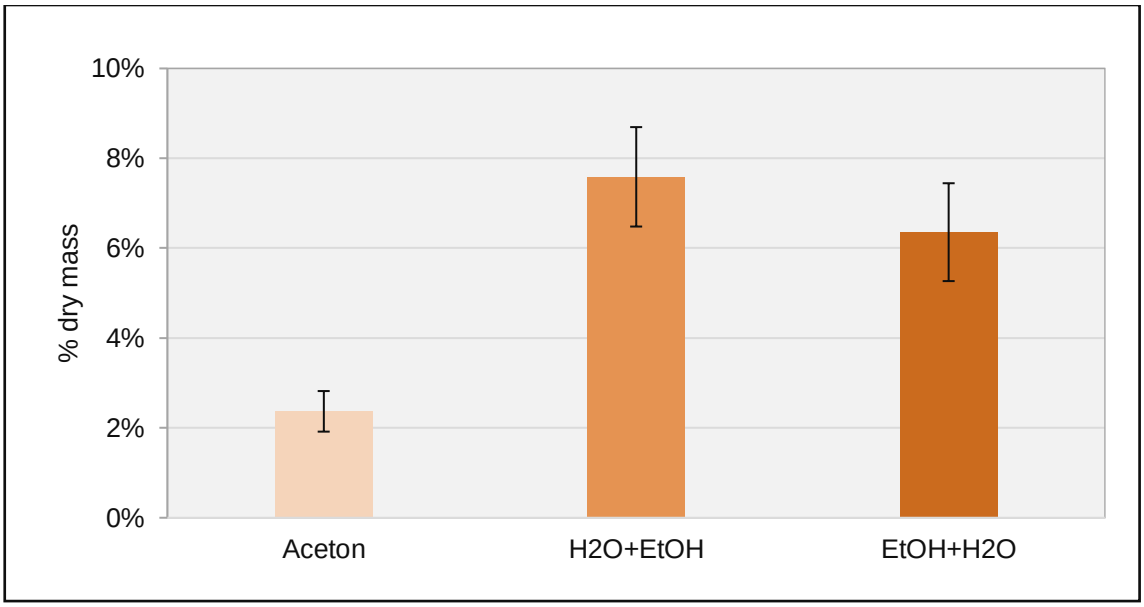


*Figure 45_Comparison of the extractable fraction of different Soxhlet extraction methods on a spruce sample; orange bar with standard deviation ($n_{(acetone)}$=4, otherwise n=2); calculation based on initial dry spruce mass*

Based on these results, the sequence of extraction solvents described in the NREL LAP was used for extractions on real samples. These results were shown in Table 4, in which five real samples were extracted according to the NREL LAP 42620 protocol. These five samples (see Figure 36) were samples of lignocellulosic biomass, where CD-1, CD-4 and MonoX were unbleached pulp, CD-6 was an unbleached recycled pulp and CD-168 was a fully bleached paper. Table 4 shows that the majority was extracted in the first extraction step, while <1 m% was extracted in the second extraction step for all samples. It also showed that sample CD-6 had the highest extractables content (7.3 m%) of these five samples, while CD-168 had the lowest extractables content (1.1 m%). The other three pulp samples had a similar extractable content of 1.5 to 2.4 m%.

*Table 4_Results from an extraction of five different real samples; the amount of extractables is reported as a mass percent based on the initial dry matter; the extraction was carried out first with water as the extraction solvent and then with ethanol as described in NREL LAP 42620*

| Probe | Extractables $H_2O$ [m%] | Extractables EtOH [m%] | $Sum_{Extract}$ [m%] |
|---|---|---|---|
| **CD-1** | 1.037 | 0.417 | 1.454 |
| **CD-4** | 1.623 | 0.376 | 2.000 |
| **CD-6** | 6.656 | 0.687 | 7.343 |
| **CD-168** | 1.002 | 0.083 | 1.085 |
| **MonoX** | 2.213 | 0.169 | 2.382 |

### 3.1.3. Summary -Pretreatment

The two pre-treatment steps of milling and extraction had a major influence on the analysis results, especially the grinding step. All unreacted or insoluble (extractives and ash) sample components were going to be included in the calculation of the insoluble lignin content (Klason lignin). As a result, the sample preparation according to NREL LAP 42620 only using a knife mill was insufficient for the biomass samples of interest used as demonstrated in Figure 40. A final grinding pre-treatment must be carried out using a RETSCH ZM 200 ultra-centrifugal mill. This gaves the samples a cotton-like appearance with high homogeneity and uniform shape by grinding them down to the 0.2 mm filter sieve, which can be seen in Figure 39.

The choice and sequence of solvents was also important in the further pre-treatment of the extraction process. The use of only one organic solvent only leads to the extraction of resinous and easily soluble organic compounds from the wood. According to NREL LAP 42619, the use of two different solvents was recommended to achieve the highest possible extraction amount from a sample. In addition, the order of solvents used for extraction was important. It had been shown that up to 15% more non-structural material can be extracted if deionized water was used first and ethanol was used as the second extraction solvent, compared to using solvents in reverse order.

The extraction of five real samples showed that most of the extractable material was obtained in the first extraction stage. In the second stage, less than 1 m% was extracted from these samples.

## 3.2. Ash Content

Three common temperatures were used to determine the ash content. In TAPPI T211 and T413, temperatures of 525 °C and 900 °C are used, while NREL LAP 42622 uses a temperature of 575 °C for ashing. The following Figure 46 & Figure 47 shows the results of ashing at these three temperatures with different extraction treatments of the same spruce sample.

An initial observation shows that the non-extracted and acetone-extracted spruce samples had the same ash content at all three temperatures. At an ashing temperature of 525/575/900 °C, the non-extracted (raw) spruce had an average ash content of 0.50/0.44/0.33 m%, based on the dry mass of the initial sample. The extracted acetone had an average ash content of 0.52/0.45/0.33 m%, based on the dry matter of the initial sample. In contrast, the NREL-extracted sample had an ash content that was three to two times lower. The NREL-extracted sample (H+E) had an average ash content of 0.24/0.17/0.13 m%, while the reverse NREL extraction (E+H) had an average ash content of 0.31/0.24/0.18 m%. This shows that the lowest ash content was determined for the NREL-extracted sample, followed by the inverse NREL extraction. Further, a constant difference of 0.07 m% between 525 °C and 575 °C could be observed for all samples, while between 575 °C and 900 °C the m% difference varies. The raw spruce wood sample and the acetone sample shows a difference of 0.11 m%, the H+E sample a difference of 0.04 m% and the E+H sample a difference of 0.06 m%.

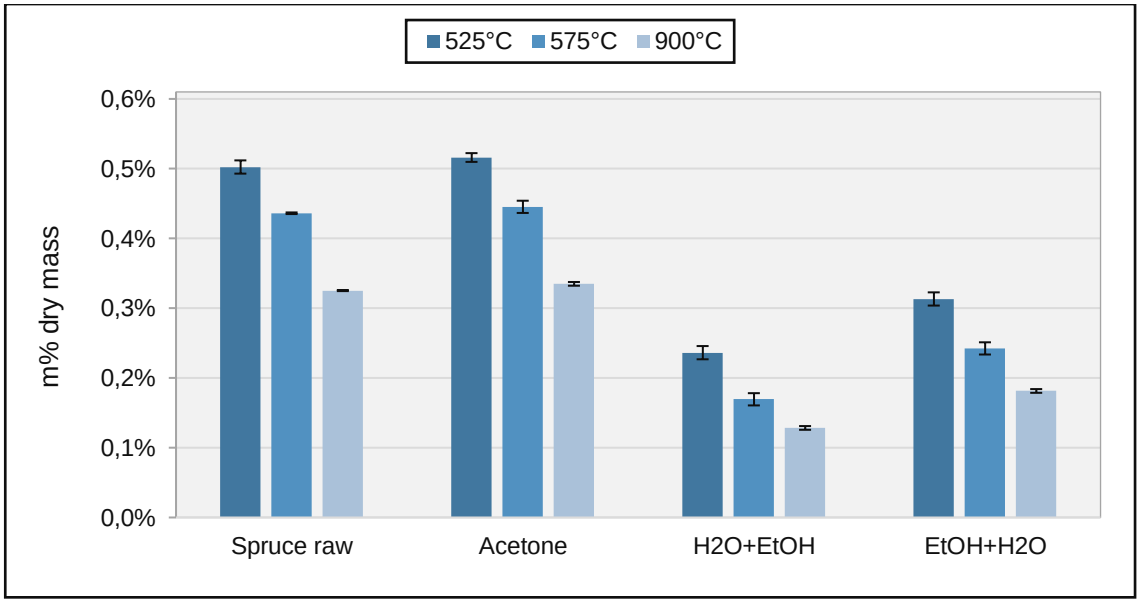


*Figure 46_Comparison of ash content at different temperatures for extracted and unextracted spruce sample with standard deviation (n=2) as error bars*

In the next Figure 47, the ash contents were normalized to the highest ash content values (at 525 °C) and shows the relative ash content in the spruce samples. Here it can be seen that at 900 °C the standard deviation (SD) for all three samples was the smallest (±0.003 m% / 0.8%). At the other two temperatures, 525°C (±0.009 m% / 1.84%) and 575°C (±0.009 m% / 1.97%), the relative SDs were twice as large (three times as large for the absolute proportion (m%)).

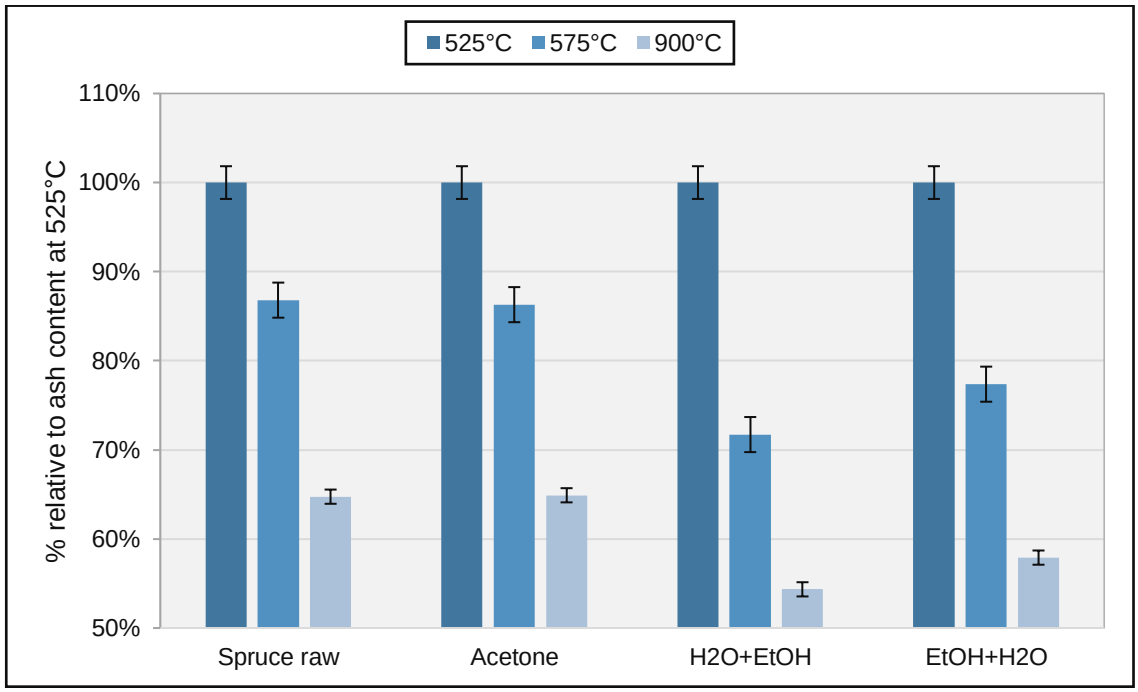


*Figure 47_Comparison of normalized ash content (normalized to ash content at 525°C) at different temperatures for extracted and unextracted spruce sample with SD (n=2) as error bars*

A comparison of ash and extractables with Figure 46 and Figure 45 shows that a reverse trend was observed for the ash content. While the lowest amount of extractables was found for the sample extracted with acetone, the ash content as the highest. In contrast, the lowest ash content was determined for the sample extracted with $H_2O$+EtOH, while the most extractables were extracted here.

The following Figure 48 and Table 5 shows an incineration test at 575°C over five incineration cycles (a total incineration time of 60 hours). About 2 g of different biomass samples were used for this purpose (the individually numbered samples are pulp (1, 4, 6), while 168 was a bleached paper). The absolute ash content was summarized in Table 5 below, and Figure 48 shows the relative ash content as a function of the number of ashing cycles.

*Table 5_Different wood-based samples with their initial dry weight and their ash content in m% (dry) over several ashing cycles (one ashing cycle takes 12 hours at 575°C followed by a cooling and weighting step)*

| Sample | Initial dry weight [g] | Ash content [m%] after n-time ashing cycles | | | | |
|---|---|---|---|---|---|---|
| | | 1 | 2 | 3 | 4 | 5 |
| **CD-1** | 1.93579 | 0.972 | 0.966 | 0.977 | 0.963 | 0.951 |
| **CD-4** | 1.96749 | 2.606 | 2.541 | 2.529 | 2.472 | 2.459 |
| **CD-6** | 1.91810 | 9.472 | 8.792 | 8.419 | 8.142 | 7.941 |
| **CD-168** | 1.88799 | 0.275 | 0.268 | 0.274 | 0.265 | 0.252 |

Figure 48 shows that red and blue curve had a similar trend and do not fall below 90 %. Sample 6 (orange line) shows a weakly square falling behavior. Over the course of 60 hours of ashing, this sample loses 1.5 m% (16.2%) of material, with a tendency towards even greater losses. The blue lines showed a similar behavior over time, with sample 4 showing more losses (5.6%) than sample 1 (2.2%). In contrast, sample 168 (red line) shows a particular behavior over time with a total loss of 8.3%.

Finally, the number of ashing cycles was limited to 2 to 3 (24- and 36-hours ashing) for further determinations, as a constant ash content can be achieved for most samples (3 out of 4).

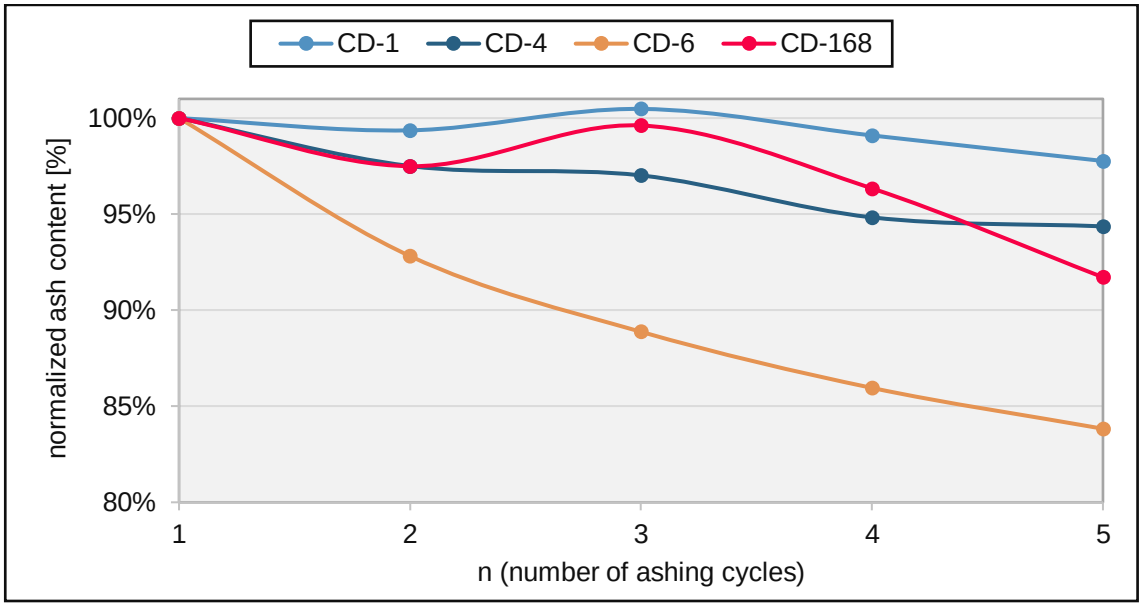


*Figure 48_Comparison of different samples during ash content determination at 575°C, over 60 hours; an ashing cycle takes 12 hours at 575°C followed by a cooling and weighting step; single numbered samples are pulps while 168 is a bleached paper*

### 3.2.1. Summary -Ash Content

The NREL protocol NREL LAP 42622 - "Determination of Ash in Biomass" was selected to determine the ash content. The biomass sample was incinerated at 575 °C in a muffle furnace for n times 12 hours until the ash content reaches a weight constant. This method was recommended and tested for biomass samples, while the TAPPI method applies exclusively to wood and wood-based materials. For these wood-based materials (paper and pulp), the type and concentration of fillers must be known to select the incineration temperature for TAPPI. With TAPPI, the high temperature of 900 °C converts carbonates into oxides, carbon dioxide and others (e.g., calcium carbonate is converted into calcium oxide). This changes the original content of inorganic substances, while temperatures below 575 °C leave the carbonates intact. For these reasons, the NREL protocol with two to three ashing cycles was selected for further determination of the ash content.

## 3.3. Sample Preparation for Determination

The following Figure 49 shows the overall process of acid hydrolysis. First, a ground sample with moisture content is weighed in (Figure 49**a**). Then sulfuric acid was added and incubated for 60 minutes with stirring. In the first few minutes after adding the acid, the sample powder turns into a highly viscous sample swamp and, depending on the lignin content, has a creamy white to black color (>3 m%) (Figure 49**b**). Over time, the sample swamp becomes increasingly liquid. After one hour, the swamp was diluted with deionized water to produce an opaque white to deep brown solution with varying amounts of solid particles (Klason lignin) (Figure 49**c**). The sample solution was now autoclaved at 121 °C for 60 minutes. During this time, the solution becomes transparent and mostly yellowish in color, and the solid particles settle to the bottom of the tube (Figure 49**d**). After this treatment, carbohydrates and acid-soluble lignin were determined from the filtrate, while the Klason lignin is determined from the solid particles.

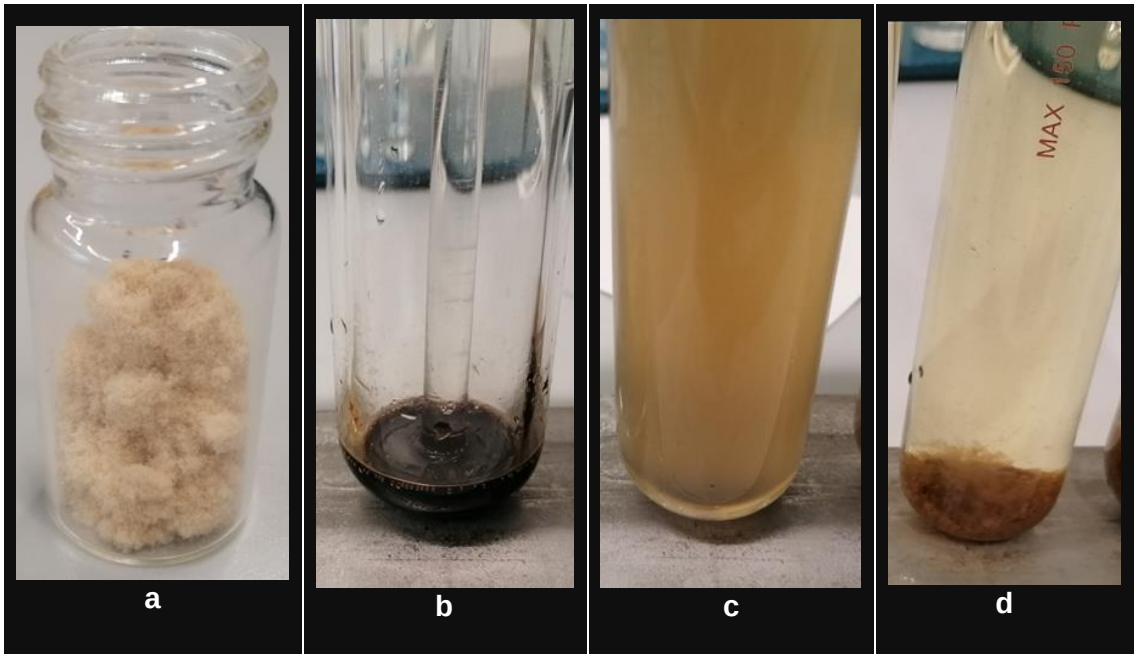


*Figure 49_Chronic development of pulp sample during sample preparation for determination steps; from left (**a**) to right (**d**), first a pre-treated biomass sample (here a pulp), secondly the sample during sulfuric acid treatment (black liquor), then the addition of deionized water and finally the biomass sample after autoclaving at 121°C for 60 minutes*

In this step, several parameters were crucial for correct sample preparation. Most importantly, the concentration of sulfuric acid, then the dilution with deionized water and finally the water bath temperature for incubation.

NREL LAP 42618 recommends a water bath temperature of 30 ± 3 °C, while ISO/FDIS 21436 recommends water bath temperatures of 20 °C and 30 °C. As the specifications in the literature range between 0 °C and 40 °C, the water bath temperature was ultimately set to room temperature to save energy. To ensure a constant dilution of the acid-treated sample, the required amount of water was weighed into beakers instead of volumetric vessels (measuring cylinders or graduated pipettes). The most important parameter for correct sample preparation was the concentration of sulfuric acid. The following Figure 50 and Table 6 shows a hydrolysis test with three different acid concentrations (hydrolysis time of 60 minutes). Two gradations of 2 molar each (64% (10 molar) and 55% (8 molar)) are made from the recommended concentration of 72% sulfuric acid (corresponds to 12 molar).

The influence of the acid concentration was visible in the following Figure 50, as the color was different for each Klason determination. A closer examination of the filter layers proves the incomplete hydrolysis in the 55% sulfuric acid, as the sample pieces were similar in color and shape to the original wood sample. The different fractions of the spruce sample (early wood, late wood, and bark) could be distinguished with the naked eye. At an acid concentration of 64 %, the color differs from the original sample (redder) and the shape was also smaller. But here too, it was possible to visually distinguish between wood and bark, albeit more difficult.

At the acid concentration of 72% recommended in the literature, the color changed back to a redder brown tone. A distinction between the wood fractions was no longer possible, indicating a more complete hydrolysis compared to the other two concentrations.

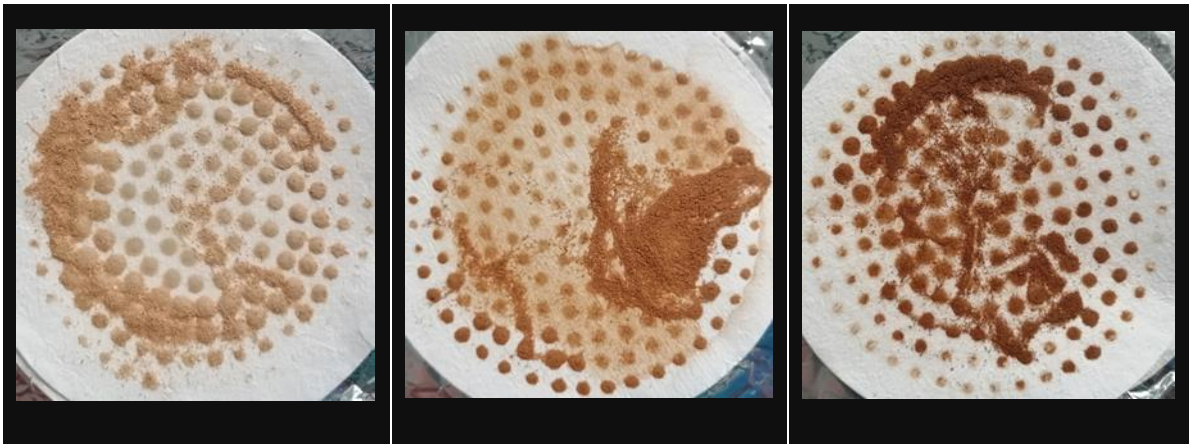

*Figure 50_Comparison of sample preparation of a spruce sample using different sulfuric acid concentrations (from left to right; 55% (8 Molar), 64% (10 M), 72% (12 M) sulfuric acid)*

The following Table 6 shows the influence of incomplete hydrolysis on the lignin determination. Since Klason lignin is defined as an insoluble substance that is determined by weighing, any substance that is not dissolved at the time of gravimetric determination is classified as part of the Klason lignin. Due to this behavior, extractives and ash content must be determined beforehand to correct the actual lignin content Table 6 shows the total lignin content, which varies between 28 and 74 m% of the initial dry mass. Looking first at the acid-soluble lignin, whose values were in the same range, no significant difference can be recognized. However, a large difference can be observed for Klason lignin. At the lowest acid concentration, a mass fraction of 73.26 m% of the original sample mass was determined as total lignin, which means that about three quarters of the sample was on the filter layer. At the next highest acid concentration of 10 molar, 44.80 m% was on the filter layer, which corresponds to about 50% of the total mass. As Table 1 shows, the lignin content of softwood was between 27 and 32 m%. In this range, the value of 27.63 m% total lignin for a spruce sample produced with a sulfuric acid concentration of 12 molar was perfect.

*Table 6_ Comparison of lignin content by preparing a spruce sample with different sulfuric acid concentrations; Klason lignin is determined gravimetrical, while acid soluble lignin was determined by UV/Vis spectroscopy at 205 nm*

| Acid Conc. [%/M] | Klason Lignin [m%] | Acid Soluble [m%] | Sum Lignin [m%] |
|---|---|---|---|
| **55/8** | 72.04 ± 0.23 | 1.02 | 73.06 ± 0.23 |
| **64/10** | 43.73 ± 1.40 | 1.07 | 44.80 ± 1.40 |
| **72/12** | 27.00 ± 1.18 | 0.63 | 27.63 ± 1.18 |

These results showed that acid hydrolysis requires a certain time and a certain acid concentration in order to achieve complete hydrolysis of the sample. Too high acid concentrations or too long hydrolysis times resulted in the formation of degradation products (furan derivatives).

### 3.3.1. Summary -Sample Preparation for Determination

Sample preparation for the determination of lignin and carbohydrates comprises several decisive parameters. The most important parameter was the acid concentration for hydrolysis. Like the grinding in the pre-treatment step, the acid concentration influenced the result in a similar way. Both factors, grinding and hydrolysis, influenced the lignin content of Klason. While the particle size of the sample was influenced by the grinding, the digestion of the sample was controlled by the acid concentration. For example, coarse sieving leads to large particle diameters that cannot be completely broken-down during hydrolysis. Similarly, an acid concentration that was too weak leads to incomplete digestion, even with very small particle diameters. As described in the previous Table 6, a reduction in the acid concentration from 72% to 64% leads to an increase in the Klason lignin content from 27.63 m% to 44.80 m%. This additional mass (undigested sample) of 17.17 m% was also weighed and incorrectly assigned to the lignin class. The other parameters in this step, the dilution with deionized water as well as the water bath temperature and the incubation time, were also important, but do not have as much potential for error in the final result.

## 3.4. Determination of Lignin

The entire lignin determination was divided into two parts. One part can be determined directly by weighing (Klason lignin), the other (acid-soluble lignin) indirectly by spectroscopy. The total lignin content is defined as the sum of the two lignin components. Several biomass samples with their specific color, the filter sheet pattern and the quantitative determination were presented in this section.

### 3.4.1. Klason Lignin

Klason lignin is defined as the content of acid-insoluble lignin and could be determined directly by weighing the filter layer. The following Figure 51 shows several Klason lignin determinations of different biomass samples. Here it was clear that each sample has its own filter pattern, color, and quantity.

Of these samples, the white crystalline sugar (WCS) (**c**) was particularly interesting as it produces a black pattern on the filter sheet, whereas starch and analytical sugars do not produce any visible pattern. The biomass samples **e** to **h** were again the samples used to demonstrate the ash content. These were three pulp samples and one bleached paper sample. The following Table 7 shows the Klason lignin content values. As expected, the Klason lignin content for starch and sugar was less than 1 m%, which was due to a weighing error as a starting mass of 300 mg is used. The black filter sheet pattern was interesting because the acid treatment of the white sugar sample **c** results in the organic carbon being converted to elemental carbon (caramelization process). Samples **e**, **f** and **g** shows a specific pattern with a specific brownish color. Depending on the lignin content and composition, a light to dark brown color can be seen. A comparison of samples **d** and **h** from Table 7 shows a similar Klason lignin content, although sample **d** was a standard sugar mixture and sample **h** was a fully bleached paper sample. As both samples showed a weak pattern, contain no lignin, and consist only of cellulose and hemicellulose, a chemical reaction of the sugars must take place in the presence of the acid. The result was an organic sugar residue, which was responsible for the weight.

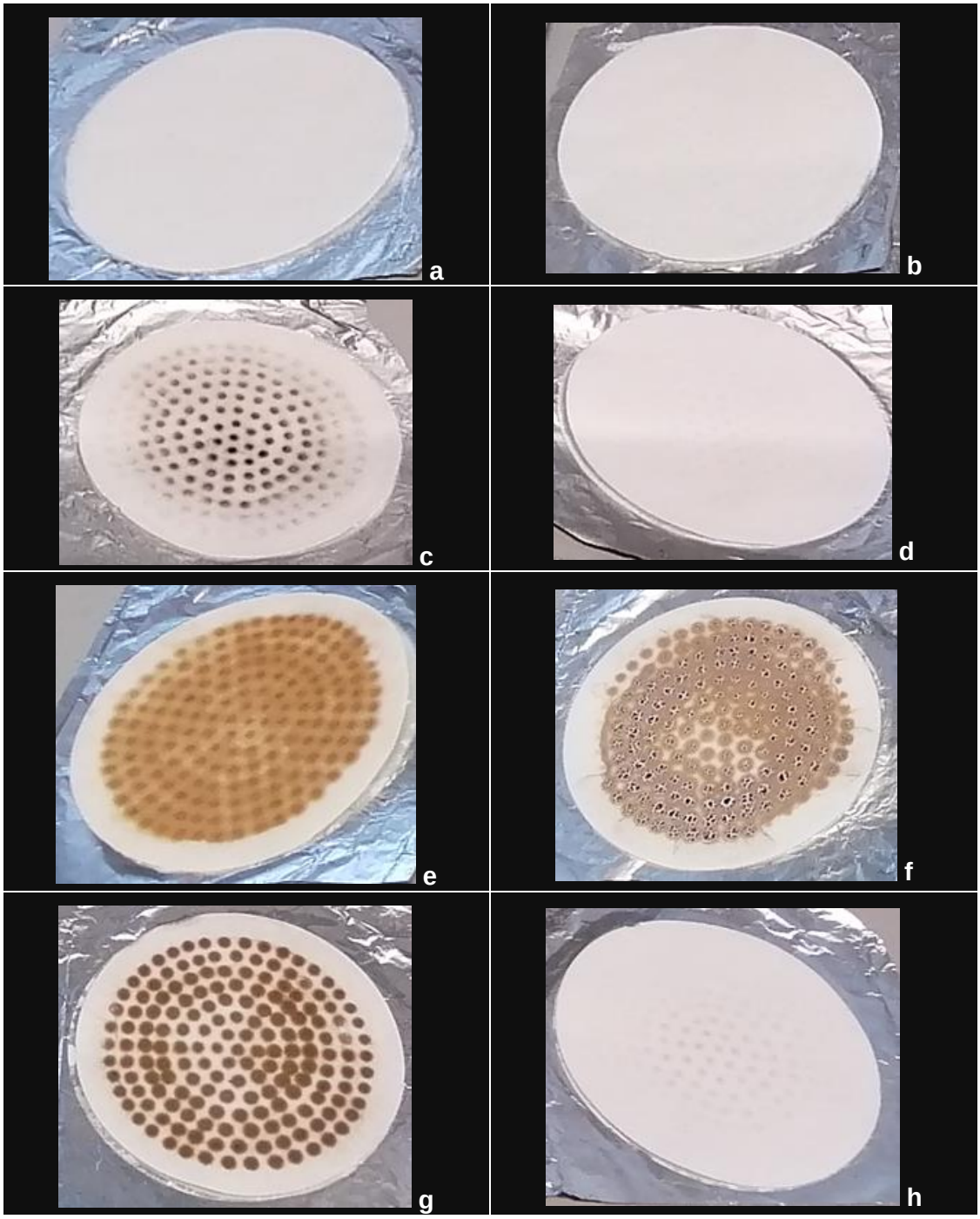


*Figure 51_Glass filter sheets of different biomass samples used for determination of Klason;* ***a****) was the blank measurement,* ***b****) was an analytical grade starch sample,* ***c****) was a commercial white refined sugar (WCS),* ***d****) was a sugar mixture of the five sugars used for LC measurements (ZMix),* ***e****) to* ***h****) were the samples CD-1 (Kraft paper), CD-4 (Kraft paper), CD-6 (recycled paper) and CD-168 (full bleached paper)*

*Table 7_Weighted values for Klason lignin determination of different samples; m% based on initial dry matter; $\overline{X}$ was mean value and SD means standard deviation of a double determination; WCS…white crystalline sugar; ZMix…mixture of five monosaccharide standards used in NREL*

| Sample | Klason Lignin Content [m%] | |
|---|---|---|
| | $\overline{X} \pm \mathrm{SD}$ | |
| **Starch (b)** | -0.49 ± 0.23 | |
| **WCS (c)** | 0.00 ± 0.92 | |
| **ZMix (d)** | 1.15 ± 0.47 | |
| | *Without* | *With Pretreatment* |
| **CD-1 (e)** | 5.17 ± 0.92 | 3.98 ± 0.92 |
| **CD-4 (f)** | 11.89 ± 0.92 | 10.93 ± 0.69 |
| **CD-6 (g)** | 12.81 ± 0.47 | 13.40 ± 0.86 |
| **CD-168 (h)** | 0.99 ± 0.93 | 0.74 ± 1.17 |

### 3.4.2. Acid Soluble Lignin

Compared to Klason lignin, this lignin content is lower, but it is acid-soluble (AS) and can only be determined indirectly by UV/Vis spectroscopy. For this purpose, a spectrum from 190 nm to 400 nm was recorded. The acid-soluble lignin was determined at 205 nm according to ISO/FDIS 21436 or at 240 nm according to NREL LAP 42618. The Beer-Lambert law Eq. (1) must be applied for quantitative concentration determination using UV/Vis spectroscopy. The absorbance $A$ of a sample result from the recorded spectrum at a specific wavelength. The path length $l$ (cm) is determined from the cuvettes used for spectroscopy and the concentration $c$ is sought. An absorption constant ($\varepsilon$) must be used to calculate c. In the NREL LAP, the value of ε at 240 nm is 25 l/(g*cm) (determined using the NIST standards for bagasse and Populus deltiodes), while the value of $\varepsilon$ in ISO/FDIS is 110 l/(g*cm) at 205 nm (average constant for wood samples). In the NREL LAP, the wavelengths 197 nm, 198 nm and 320 nm are also recommended for use,

depending on the type of biomass. To be physically valid with Lambert-Beer's law, the absorption values must be less than 1.

In order to check the background and possible interferences of the monosaccharides used and the internal standard, spectra of the untreated sugars were created and shown in the following Figure 52. This shows that xylitol (internal standard; red curve) had the lowest interference at 205 nm with an Abs value of <0.1. The monosaccharides had a measured Abs value of around 0.2, with the exception of mannose (purple curve), which has an Abs value of 0.66. After 223 nm, all sugars have a constant Abs value of < 0.1 and were without interference for the measurement at 240 nm.

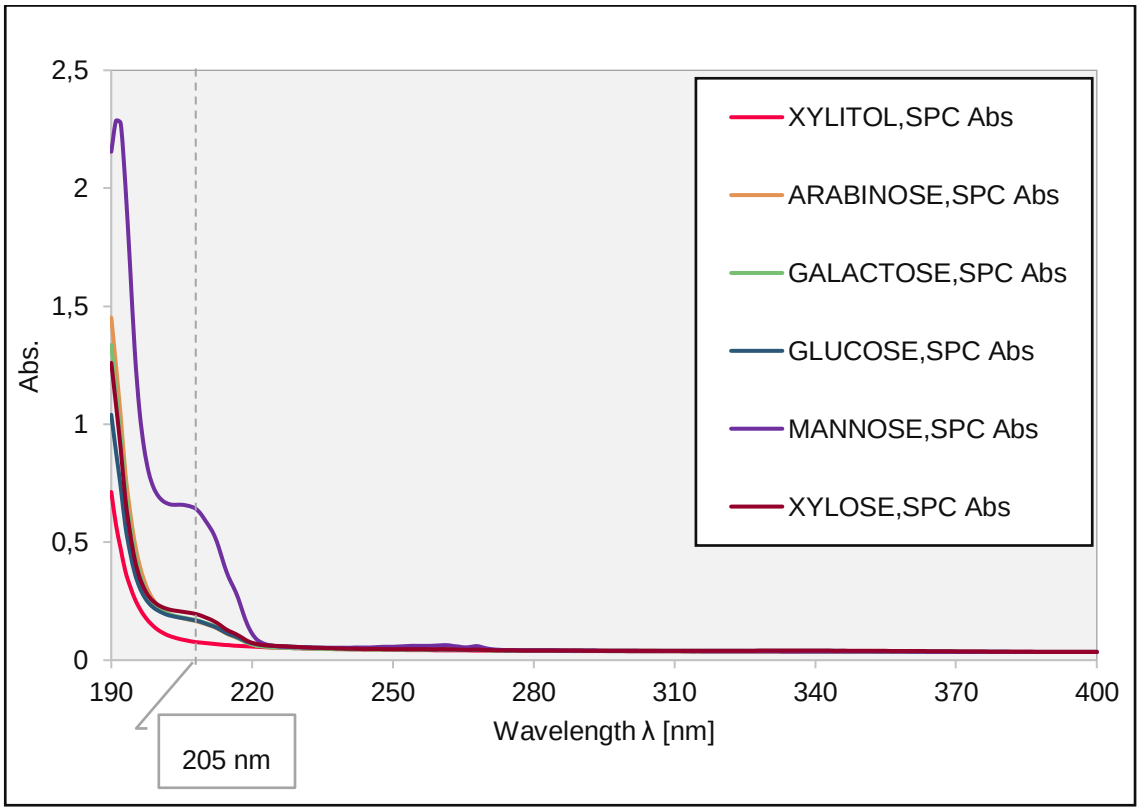


*Figure 52_UV/Vis spectra of monosaccharides and internal standard used in the determination step of carbohydrates; 205 nm indicated by vertical dashed line*

Figure 53 shows the UV/Vis spectrum of the MonoX pulp sample, the wavelengths for the determination of acid-soluble (AS) lignin were highlighted. The corresponding data and values were listed in Table 8 below. Various literature values for the absorption capacity at certain wavelengths were summarized here and the corresponding contents of acid-soluble lignin were listed. The color code indicates the corresponding literature, as two wavelengths were available for some determinations. The following Figure 53 shows six wavelengths with an absorbance value for quantitative determination. The

blank measurement provides a combined spectrum containing only water and sulfuric acid. The first two wavelengths (197 & 198 nm) lie exactly in this range and superimpose possible sample signals. The other three wavelengths (205, 240 and 320 nm) do not overlap the blank sample. In Table 8, NREL specifies two wavelengths for each of the four different biomass sources for AS lignin determination, while ISO/FDIS works with an average value at one wavelength.

For Populus deltoides (orange) (eastern poplar; Kanadische Schwarz-Pappel (ger.)), 197 nm and 240 nm are analyzed. The quantitative calculation results in values of 1.94 m% ± 3.64% (197 nm) and 2.92 m% ± 1.8% (240 nm) for the pulp sample MonoX, which gives a difference of about 1 m%. For Pinus radiata (green) (Monterey pine; Monterey-Kiefer (ger.)) and bagasse (grey) (crushed sugar cane fibers; Faserreste von Zuckerrohr (ger.)), 198 nm and 240 nm were determined. For the green/grey determination, the AS lignin content at 198 nm is 4.50 m% ± 3.8% / 2.81 m% ± 3.8% and at 240 nm 6.08 m% ± 1.8% / 2.92 m% ± 1.8%. This calculation results in a difference of 1.57 m% for green and 0.10 m% for grey. The last option listed in the NREL LAP for quantitative determination is based on corn stover (blue) (maize straw; Maisstroh (ger.)) at the wavelengths 198 nm and 320 nm. It yields 2.05 m% ± 3.8 % (198 nm) and 0.69 m% ± 5.4 % (320 nm) with a difference of 1.56 m%, which is similar to that of green.

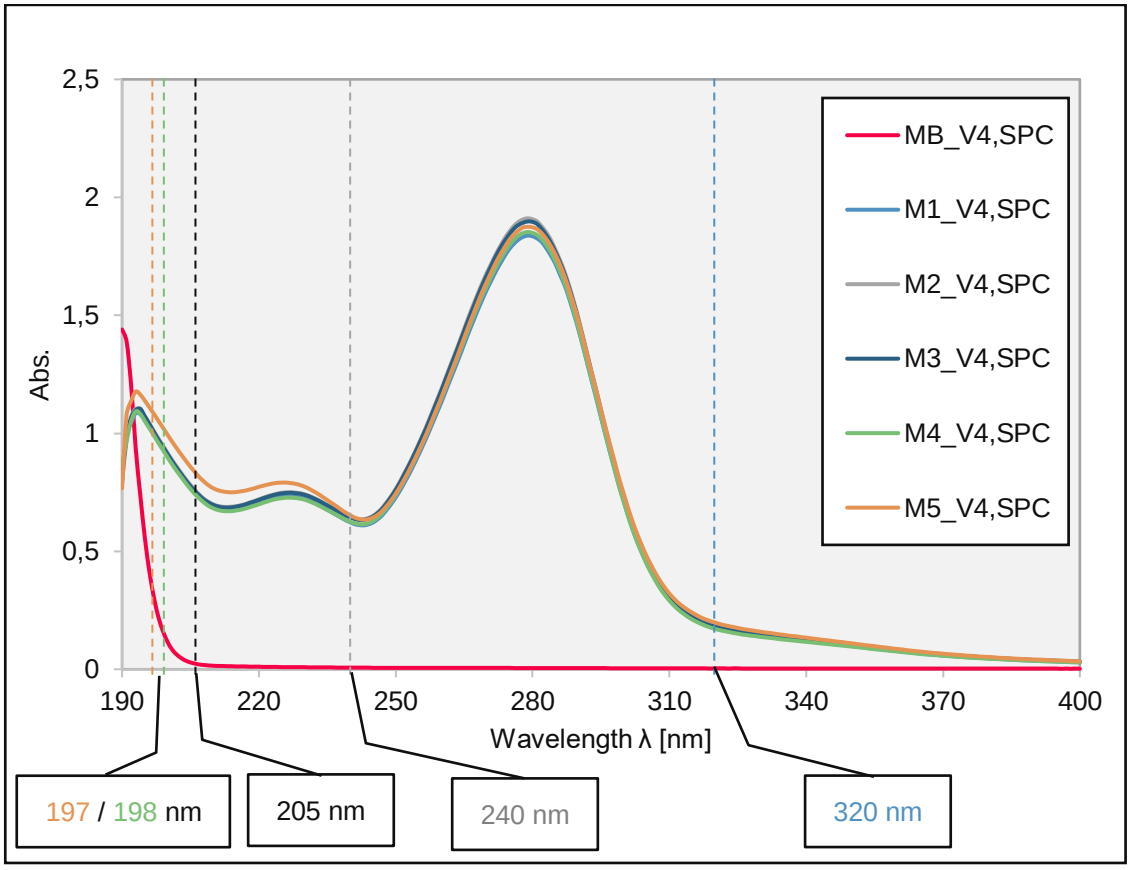


*Figure 53_UV/Vis spectra of the pulp sample MonoX in a five-fold determination in the range from 190 nm to 400 nm; highlighted the wavelength positions usable for acid soluble (AS) lignin determination*

As already mentioned, the first two possible usable wavelengths (197 & 198 nm) were in the blank range and can interfere, which leads to noise and makes decisions impossible. The wavelength of 320 nm had the highest relative standard deviation of 5.4 %, compared to 4.8 % (ISO) and 3.8 % / 1.8 % (198 nm / 240 nm). This also mades this wavelength unusable for precise determination. This leaves only two wavelengths (205 nm % 240 nm). Another selection criterion was a possible universal application, as the composition of a pulp or other lignocellulosic biomass was not always known. Due to these facts, the qualitative determination according to ISO/FDIS was carried out at 205 nm and 240 nm was used as the second wavelength with a coefficient of 25 l/(g cm).

*Table 8_UV/Vis data and values for acid soluble (AS) lignin determination at several wavelengths recommended in NREL and ISO/FDIS 21436; the values determined were given as the mean ($\bar{X}$), standard deviation (SD) and relative standard deviation (Rel. SD) of a five-fold determination; m% was defined as mass percent based on initial sample mass in dry state*

| Wavelength [nm] | Absorptivity [l/ (g cm)] | $\bar{X}$ [m%] | SD [m%] | Rel. SD | Literature |
|---|---|---|---|---|---|
| **197** | 60 | 1.94 | 0.07 | 3.6% | Populus deltoides (NIST SRM 8492) |
| **198** | 25 | 4.50 | 0.17 | 3.8% | Pinus Radiata (NIST SRM 8493) |
| **198** | 40 | 2.81 | 0.11 | 3.8% | Bagasse (NIST SRM 8491) |
| **198** | 55 | 2.05 | 0.08 | 3.8% | Corn Stover (NREL supplied feedstock) |
| **240** | 12 | 6.08 | 0.11 | 1.8% | Pinus Radiata (NIST SRM 8493 |
| **240** | 25 | 2.92 | 0.05 | 1.8% | Bagasse (NIST SRM 8491 |
| **240** | 25 | 2.92 | 0.05 | 1.8% | Populus deltoides (NIST SRM 8492) |
| **320** | 30 | 0.69 | 0.04 | 5.4% | Corn Stover (NREL supplied feedstock) |
| **205** | 110 | 0.82 | 0.04 | 4.8% | ISO/FDIS 21436 |

The following Figure 54 shows four spectra of different samples with different dilution factors to achieve an absorbance value below 1 at a wavelength of 205 nm and 240 nm. What was interesting about these spectra was the fact that the WCS sample was only refined sucrose but has an absorbance value (Abs) of >4. As the signal reaches noise at these high Abs values, this indicates that the detector was overloaded. Even a dilution of 1:10 is not sufficient to achieve Abs values < 1. Starch, on the other hand, is too diluted at a dilution of 1:4, as a range between 0.2 and 1.0 Abs was recommended for quantification and between 0.7 and 1.0 Abs was considered ideal according to NREL and ISO/FDIS. In addition, ZMix, a standard sugar blend, also had a high Abs value, but both ZMix and WCS contain no lignin at all. The pulp-based material samples (CDs), on the other hand, had similar Abs values and are ideal for determination with a 1:4 dilution.

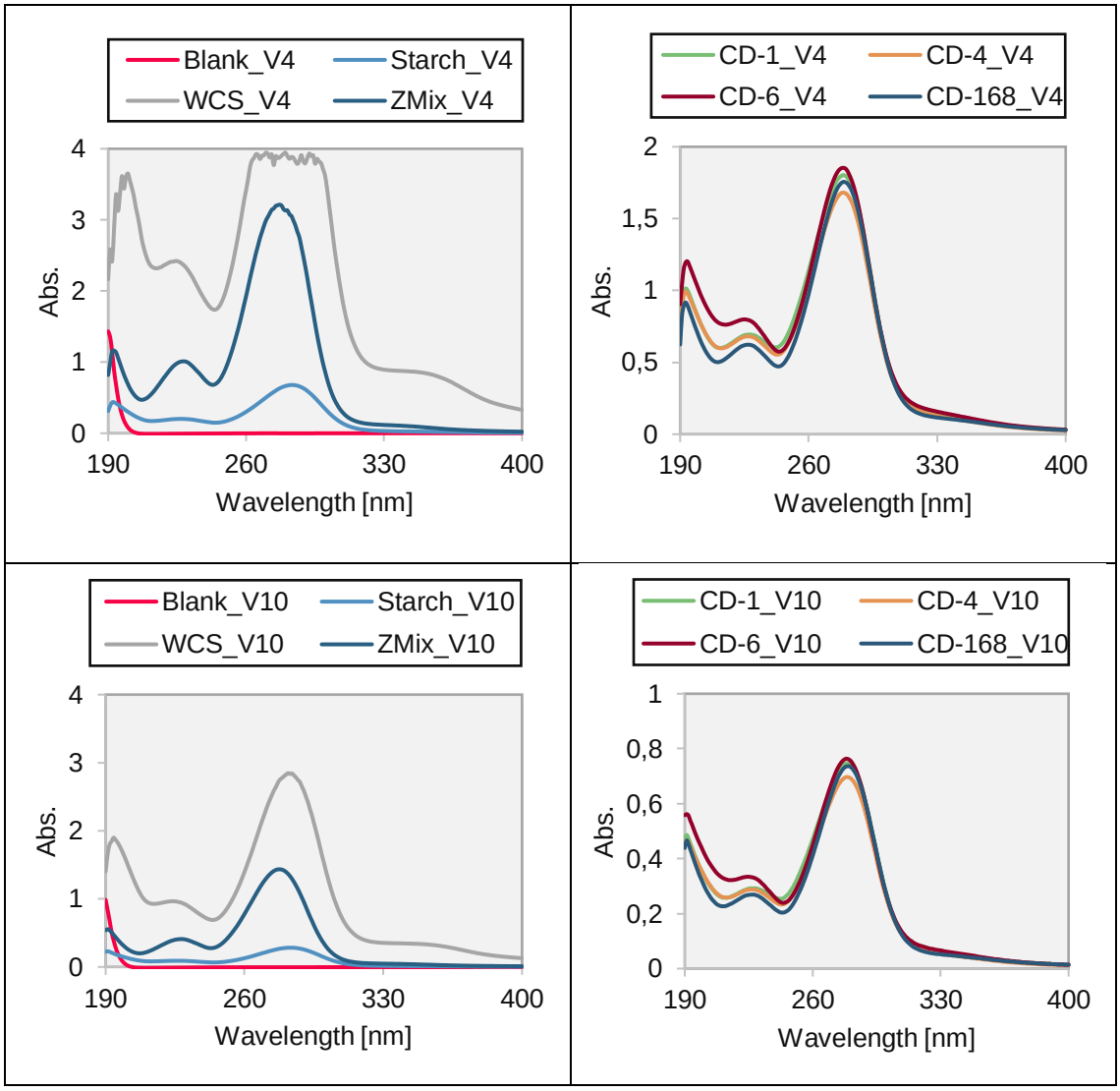


*Figure 54_UV/Vis spectrum of several biomass samples at different dilutions; dilution factor is 4 indicated by V4 (1:4) or 10 indicated by V10 (1:10) in the legend*

The reason for the detector overload was shown in the next Figure 55 from the work by Beisl et al. (2018). Here, a spectrum of furfural (FA), hydroxymethylfurfural (HMF), acetic acid and lignin is shown. These furfural derivatives were generated in situ by the dehydration reaction of mono- and disaccharides initiated by the presence of sulfuric acid and heat in the autoclave step. Pentoses (xylose and arabinose) are favored for a dehydration reaction in an acidic environment. The basic structure of FA and HMF is the furan ring, a heterocyclic organic substance with a five-membered aromatic ring containing an oxygen atom. This dehydration pathway for monosaccharides converts pentoses into furfurals and hexoses into HMFs. The blue lignin curve was generated by measuring a purified lignin from an organosolv pretreatment process for wheat straw. In the work by Beisl et al., 2018, this lignin curve has maxima at 203 nm and 274 nm. Acetic

acid has a maximum at 206 nm, but has a low absorption compared to other acids. FA and HMF each have two maxima. FA at 227 nm and 275 nm and HMF at 228 nm and 284 nm. The minima for FA are at 206 nm and 241 nm and for HMF at 211 nm and 244 nm. [6, 11, 30]

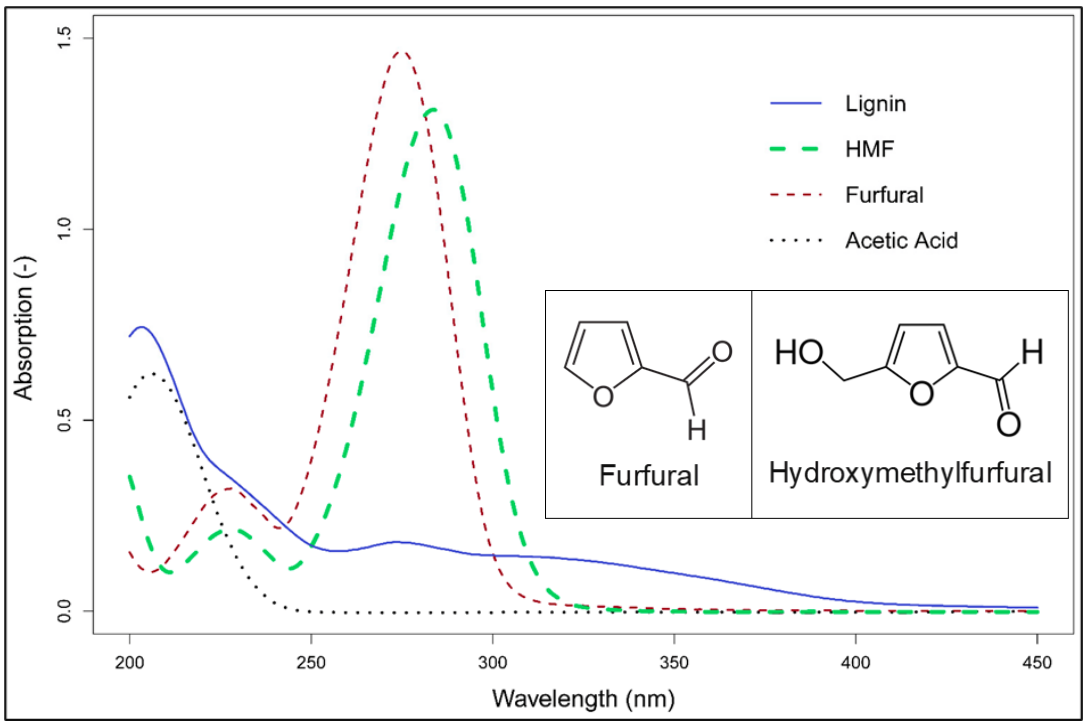


*Figure 55_UV/Vis spectra of the pure components measured in 60 wt % aqueous ethanol; pure lignin, HMF, and furfural were measured at concentrations of 10 mg/L and acetic acid at 1 g/L [11]*

This means that when determining acid-soluble lignin, the signals of these in-situ generated furan derivatives interfere with the lignin signals in the range from 200 nm to 330 nm. This can lead to an incorrect lignin content, as was shown for the CWS sample as well as for starch and ZMix. The following Figure 56 and Table 9 are used to illustrate the determination of acid-soluble lignin with values.

The Figure 56 shows six samples that were diluted so that they have an absorbance value < 1. Here it is clear that WCS was diluted 1:20 to achieve a correct Abs value, while the wood samples were diluted 1:4 and the starch 1:2. This high dilution for WCS indicates a high HMF concentration as the spectral curve shows maxima at 224 nm and 282 nm (HMF maxima at 228 nm and 284 nm). Since starch also shows maxima at these wavelengths, but at a much lower dilution (10-fold), the error in lignin content was not as large as with WCS. In addition, the three pulp samples had a similar spectrum with a similar acid-soluble lignin content, while the paper sample CD-168 had a weaker signal.

What all four samples had in common was that their peak maxima are at 225 nm and 279 nm, indicating the presence of FAs.

This false lignin content of CWS was shown in Table 9, where 3.27 m% acid-soluble lignin was determined at 205 nm and 8.6 m% at 240 nm. A lower content of acid-soluble lignin was determined for starch and ZMix, whereby the difference between the two wavelengths for ZMix is 5-fold. Here, a content of 0.5 m% was determined at 205 nm and 3.3 m% at 240 nm. Starch had a content of 0.3 m% (205 nm) and 0.9 m% (240 nm), which differ by 0.6 m% between these wavelengths. ZMix differs by 2.8 m% and CWS by 5.3 m%. The CD samples differ consistently between the wavelengths by about 2 m% with different tendencies. At 205 nm, the soluble lignin content increases for both sample types in the order of 0.7 m% (CD-1) to 0.9/1.0 m% (CD-6). At 240 nm, the untreated CD samples had a value of about 2.8 m%, with CD-4 having the lowest value of 2.7 m%. With pretreatment, they followed the concentration trend visible at 205 nm. CD-168 had the lowest lignin content of 0.5/0.6 m% (205 nm) and 2.2 m% (240 nm), which corresponds to that of ZMix (0.5 m% at 205 nm), albeit with a smaller difference of 1.6 m% compared to 2.8 m% (ZMix). Due to these interferences in the lignin spectrum, the total lignin content was calculated using the values for acid-soluble lignin determined at 205 nm.

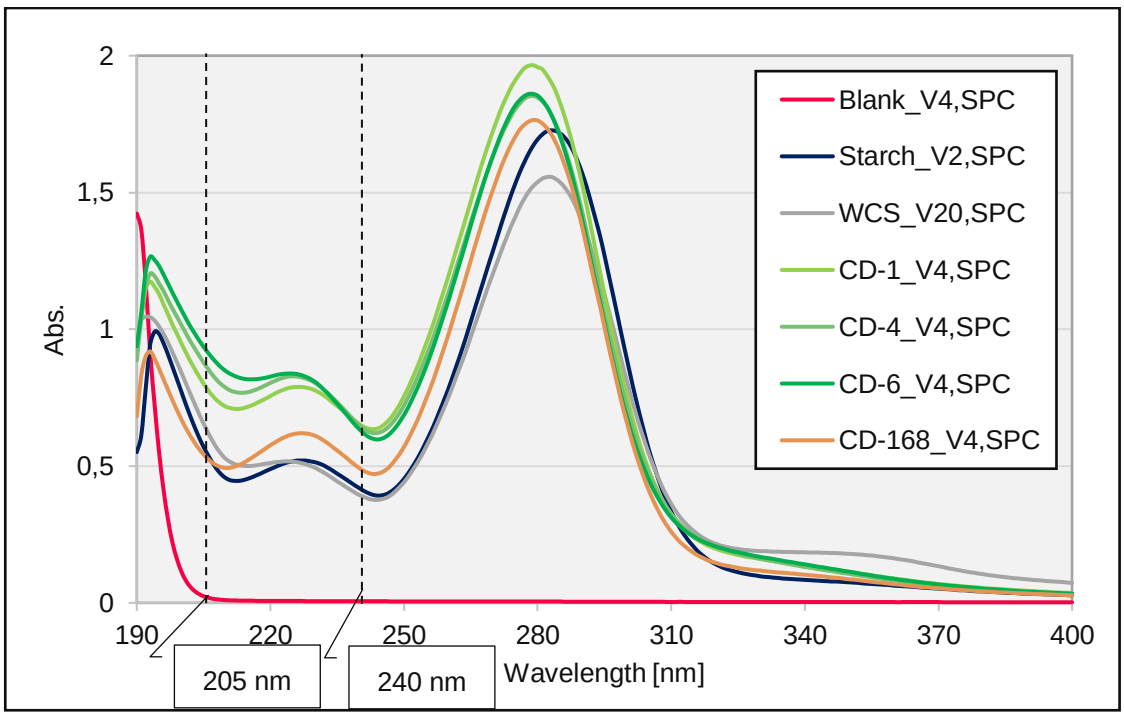


*Figure 56_UV/Vis spectra of six samples used for acid soluble lignin content determination at wavelength 205 nm and 240 nm which Abs < 1; blank sample (red curve) limits spectral range for determination in UV regime*

*Table 9_Values for acid soluble lignin determination of different samples at two wavelengths (λ = 205 nm (ISO/FDIS 21436); λ = 240 nm (NREL LAP 42618)); qualitative determination was achieved using Beer-Lambert law; m% based on initial dry matter; $\overline{X}$ is mean value and SD means standard deviation of a double measurements; LC Sugar Mix (ZMix) was measured only once (no deviation possible); in CD sample section, first value is raw sample, second is from pre-treated samples (raw / pre-treated)*

| Sample | Acid Soluble Lignin Content [m%] | | Delta [m%] |
|---|---|---|---|
| | $\lambda$ = 205 nm | $\lambda$ = 240 nm | |
| **Starch (b)** | 0.27 ± 0.04 | 0.85 ± 0.14 | 0.59 |
| **White Sugar (c)** | 3.27 ± 0.14 | 8.59 ± 0.44 | 5.33 |
| **LC Sugar Mix (d)** | 0.51 | 3.32 | 2.81 |
| **CD-1 (e)** | 0.73 ± 0.12 / 0.70 ± 0.06 | 2.79 ± 0.18 / 2.58 ± 0.10 | 2.07 / 1.88 |
| **CD-4 (f)** | 0.76 ± 0.20 / 0.81 ± 0.09 | 2.67 ± 0.37 / 2.73 ± 0.10 | 1.91 / 1.91 |
| **CD-6 (g)** | 0.89 ± 0.11 / 1.00 ± 0.16 | 2.75 ± 0.21 / 2.98 ± 0.30 | 1.86 / 1.98 |
| **CD-168 (h)** | 0.55 ± 0.02 / 0.55 ± 0.02 | 2.19 ± 0.07 / 2.19 ± 0.06 | 1.65 / 1.64 |

### 3.4.3. Total Lignin & Reproducibility

As already mentioned, the total lignin content is defined as the sum of acid-insoluble lignin (Klason) and acid-soluble lignin (at 205 nm). The following Table 10 summarizes the results of the total lignin determination. Except for starch, a lignin content could be determined for the first three sugar samples. In the case of WCS, the lignin content was due to the UV absorption of the FAs and HMFs formed. In the case of ZMix, the weighing error of 1 m% is responsible for this incorrect lignin content.

*Table 10 Calculated values for total lignin content from measured Klason lignin and acid-soluble lignin; total lignin was achieved as sum of Klason and acid soluble lignin determined at 205 nm; for ZMix only a single determination was performed; in CD sample section, first value was raw sample, second is from pre-treated samples (raw / pre-treated)*

| Sample | Klason Lignin Content [m%] | Acid Soluble Lignin Content [m%] | Total Lignin [m%] |
|---|---|---|---|
| | $\bar{X}$ ± SD | $\lambda$ = 205 nm | Klason + 205nm |
| **Starch (b)** | -0.49 ± 0.23 | 0.27 ± 0.04 | -0.23 ± 0.27 |
| **WCS (c)** | 0.00 ± 0.92 | 3.27 ± 0.14 | 3.27 ± 1.06 |
| **ZMix (d)** | 1.15 ± 0.47 | 0.51 | 1.66 ± 0.51 |
| **CD-1 (e)** | 5.17 ± 0.92 / 3.98 ± 0.92 | 0.73 ± 0.12 / 0.70 ± 0.06 | 5.89 ± 1.04 / 4.69 ± 0.99 |
| **CD-4 (f)** | 11.89 ± 0.92 / 10.93 ± 0.69 | 0.76 ± 0.20 / 0.81 ± 0.09 | 12.65 ± 1.12 / 11.74 ± 0.77 |
| **CD-6 (g)** | 12.81 ± 0.47 / 13.40 ± 0.86 | 0.89 ± 0.11 / 1.00 ± 0.16 | 13.70 ± 0.58 / 14.40 ± 1.01 |
| **CD-168 (h)** | 0.99 ± 0.93 / 0.74 ± 1.28 | 0.55 ± 0.02 / 0.55 ± 0.02 | 1.53 ± 0.95 / 1.30 ± 1.30 |

To test the reproducibility of this lignin determination with this device, a different pulp sample (MonoX) was used. Two reproducibility tests were performed. Firstly, a fivefold preparation and determination in a row on a single day (dependent determination) and secondly, a single preparation and determination on five different days (independent determination). The results of these tests were shown in the next Figure 57 and Table 11 as mean value and confidence interval (α=0.05; n=5). It can be seen here that the dependent test had a lower total lignin content of 0.6 % compared to the independent test, but this was in the same range due to the confidence interval. For the dependent test, a constant relative confidence interval of 5.9 % was determined for all lignin fractions. In the independent test, the AS lignin fraction had a relative confidence interval of 8.4 %, while the others had an interval of 17.6 % for AI lignin and 16.3 % for the total lignin content. This indicates a three times higher error potential for independent tests. This was particularly true for Klason lignin determination compared to spectroscopic analysis. A comparison of the results of the spectrometric lignin determination shows a

difference of 0.03 m% (3.4 %), which indicates a low error potential compared to Klason lignin, where a difference of 0.6 m% (11.0 %) could be achieved. As a result of this reproducibility test, the determination on a single day provides closer determination results than the determination over a longer period of time.

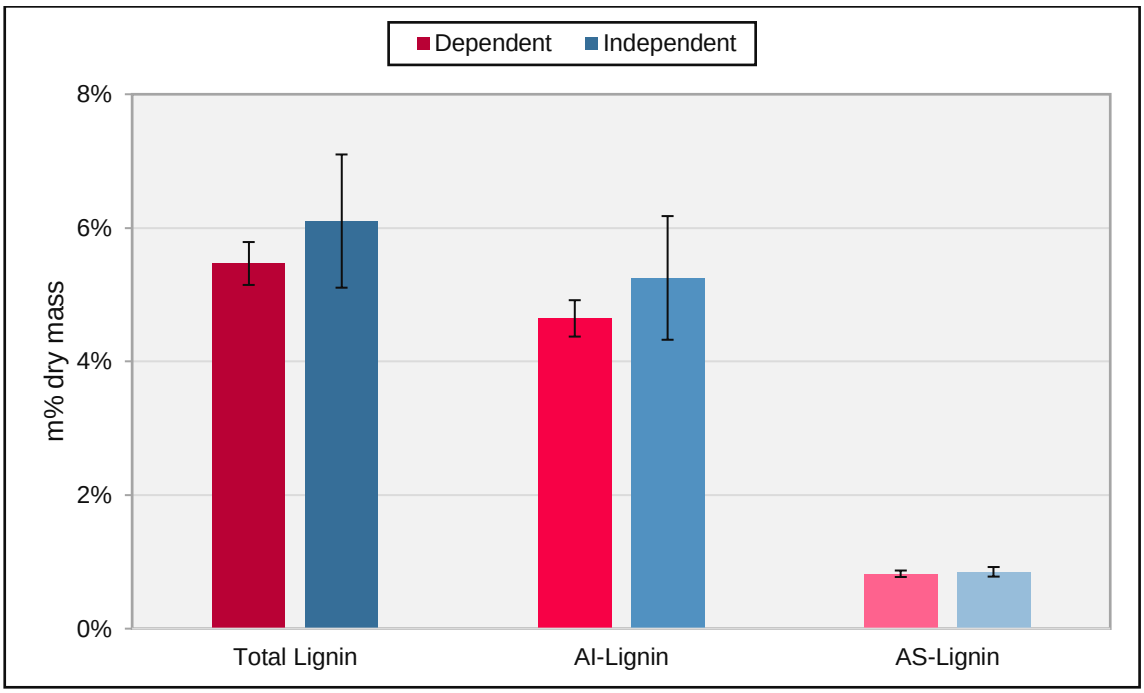


*Figure 57_Reproducibility test for a pre-treated pulp sample (MonoX); dependent test in which five preparations and determinations were carried out sequentially on one day (reddish bar) and independent test in which preparation and determination were carried out on five different days (bluish bar); values were shown as means with their confidence interval (α=0.05; n=5) as error bars; total lignin was given as the sum of AI (acid-insoluble) and AS (acid-soluble) lignin*

*Table 11_Values for reproducibility testing of a pre-treated pulp (MonoX) sample; dependent test was a determination process that was carried out five times in a row on a single day and independent test was a single process that was carried out on five different days; the values were presented as means with their confidence interval (α=0.05; n=5); total lignin was given as the sum of AI (acid-insoluble) and AS (acid-soluble) lignin*

| **Dependent [m%]** | | | **Independent [m%]** | | |
|---|---|---|---|---|---|
| *Total Lignin* | AI-Lignin | AS-Lignin | *Total Lignin* | AI-Lignin | AS-Lignin |
| *5.47 ± 0.32* | 4.64 ± 0.27 | 0.82 ± 0.05 | *6.10 ± 1.00* | 5.25 ± 0.93 | 0.85 ± 0.07 |

### 3.4.3. Summary -Determination of Lignin

Total lignin content is defined as the sum of acid-insoluble lignin (Klason) and acid-soluble lignin. While the Klason lignin was determined by gravimetric analysis of filter layers, acid-soluble lignin was only determined by UV/Vis spectroscopy. For spectroscopic analysis, several wavelengths (197, 198, 205, 240 and 320 nm) with their specific absorption constant (ε) are recommended for quantitative determination. As shown in Table 10, the lignin determination for Klason lignin showed a maximum mean weighing error of about ±1 m%, which was determined for samples **b** to **d** in which no lignin is present.

A certain amount of spectral interference was present and possible with acid-soluble lignin, which limits the number of wavelengths that can be used for determination. As the preparatory step for the determination requires high acid concentration and temperature, a certain proportion of the sugar was converted into furan derivatives. Due to their electronic structure, these furan compounds are strongly UV-active compounds, resulting in specific peak maxima at 227 nm and 275 nm for furfurals (FAs) and hydroxymethylfurfural (HMF) at 228 nm and 284 nm. In contrast, lignin exhibits weak maxima at 203 nm and 274 nm. Since dominant peak maxima of the furan compounds are at 275 nm and 284 nm, it was impossible to determine lignin in this range. This means that the wavelength of 320 nm was also excluded from the determination. The near UV wavelengths of 197 nm and 198 nm interfere with the blank sample due to the additional sulfuric acid signals. This leads to noise in highly concentrated sample measurements and requires precise use of the blank sample to minimize determination errors. Therefore, the wavelengths 205 nm and 240 nm were best suited for the determination. As can be seen in Table 9, the determination at 240 nm provides consistently higher concentrations (approx. 2 m%) compared to 205 nm with higher fluctuations in all measurements. This fact leads to the conclusion that 205 nm was primarily used for the determination of acid-soluble lignin and for the calculation of the total lignin content. The wavelength 240 nm with a coefficient of 25 l/(g*cm) was used as a backup.

Finally, a reproducibility test was carried out to determine deviations within a measurement series and from measurement series to measurement series. Also, because biological materials are not homogeneous by nature and to rule out process errors. A fivefold determination of a pulp sample (MonoX) showed that the determination of Klason lignin has a major influence on the total lignin and the source of error. It was also shown that a determination on a single day provides more coherent determination results than a determination on different days.

## 3.5. Determination of Carbohydrates

The carbohydrate concentrations were determined using two different HPLC systems with different detectors that require different preparation. The first system used a refractive index detector (RID), while the second system used a pulsed Amperometric detector (PAD). For the RID system, the sample liquid had to be neutralized with calcium carbonate, but was used concentrated. For the PAD system, the sample had to be diluted twice, 1:100 and 1:1000, to avoid overloading the detector.

Calibration curves were validated using ValiData 4.0.6, a excel macro for method validation developed by Rohrer, Wegscheider, Neuböck & Koeck.

### 3.5.1. HPLC-RID

The following Figure 58 shows a chromatogram of the 1 g/l calibration point with 3 g/l xylitol as internal standard (ISX). The positions of the sugar peaks had to be recognized in this example chromatogram. Glucose, xylose, and arabinose had the same peak shape, intensity, and height. Galactose, on the other hand, had a lower but similar shape, while the mannose peak had a broader peak shape. The peak of the internal standard eluted towards the end and had a similar peak shape to mannose, but with higher intensity as the concentration is three times higher.

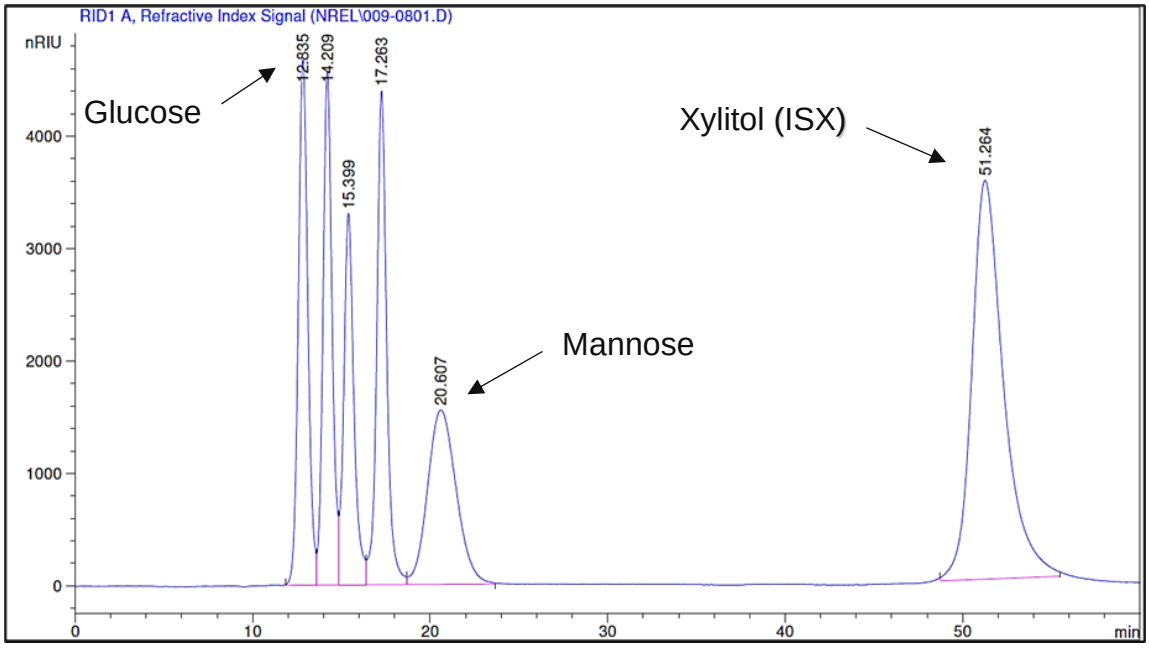


*Figure 58_LC sugar calibration chromatogram of 1 g/l with 3 g/l internal standard (ISX) concentration; peaks from left to right glucose, xylose, galactose, arabinose, mannose and xylitol (ISX)*

The chromatography and calibration data for the HPLC-RID system were listed in Table 12. The specific retention time for chromatography data is available here. For the calibration data, the linear range, limit of detection (LOD), limit of quantification (LOQ) and their linear equation with coefficient of quantification ($R^2$) were shown for the concentration calculation. Due to the LOQ of 0.24 g/l, the linear range for galactose is set from 0.2 g/l. The $R^2$ value shows a value >0.9998 for all five sugars, which indicates a good correlation of the calibration points with their linear equation.

*Table 12_Chromatography and calibration data for the HPLC-RID system; for the internal standard xylitol only chromatography data are available since no calibration is important as an internal standard*

| Compound | Ret. Time [min] | LOD [mg/l] | LOQ [mg/l] | Linear Range [g/l] | Equation (y= kx + d) | $R^2$ |
|---|---|---|---|---|---|---|
| **Arabinose** | 17.26 | 26.8 | 96.0 | 0.1 - 4.0 | Y= 168611x + 2385 | 0.9998 |
| **Galactose** | 15.40 | 67.9 | 241.8 | 0.2 - 4.0 | Y= 137704x + 899.1 | 0.9999 |
| **Glucose** | 12.84 | 25.9 | 92.8 | 0.1 - 4.0 | Y= 169961x + 2713 | 0.9998 |
| **Mannose** | 20.61 | 32.4 | 115.6 | 0.1 - 4.0 | Y= 169961x + 1696 | 0.9998 |
| **Xylose** | 14.21 | 29.9 | 106.8 | 0.1 - 4.0 | Y= 162404x + 1313 | 0.9999 |
| **Xylitol (ISX)** | 51.26 | -- | -- | -- | -- | -- |

### 3.5.2. HPAE-PAD

The following Figure 59 shows a calibration point chromatogram for the HPAE-PAD system with a uniform concentration of 3 mg/l for all substances. This chromatogram shows that the internal standards had the same peak shape and intensity. The first peak of xylitol is located in the dirt elution area due to the very short retention time of 1.73 minutes, which led to overlaps and thus to falsely higher ISX concentrations. For this reason, the internal standard in this system was replaced by fucose (4.74 minutes). In this system, the separation time was the first 25 minutes. Thereafter, the KOH concentration was increased to initiate the regeneration step of the detector, as seen at the large group of peaks around minute 30. The five sugars were well separated, apart from xylose and mannose, which can interact with each other at higher concentrations.

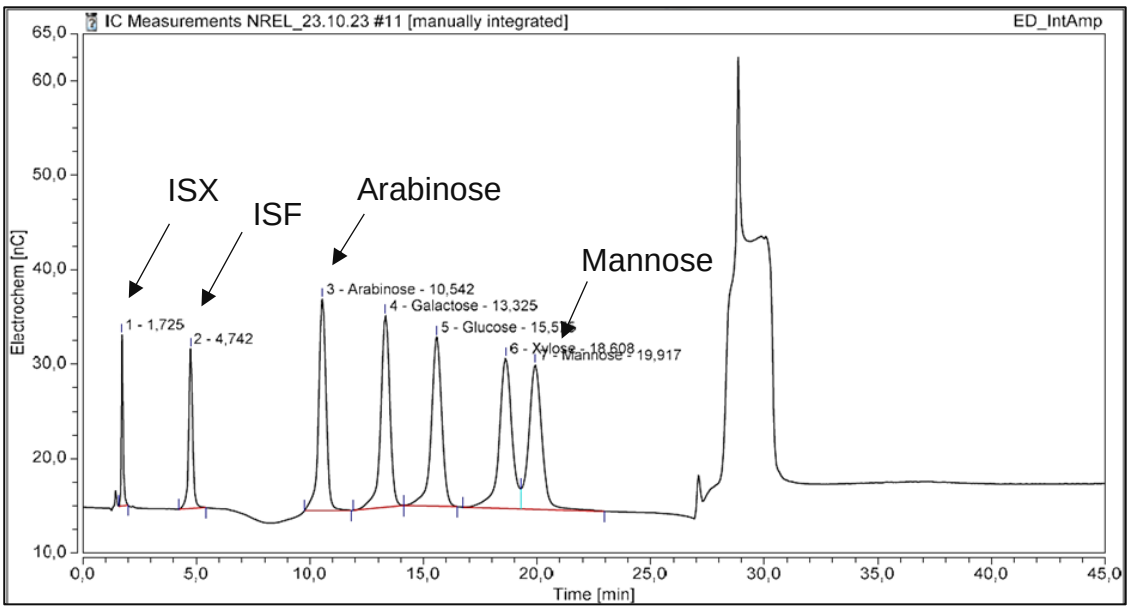


*Figure 59_AE sugar calibration chromatogram of 3 mg/l for all substances; peaks from left to right xylitol (ISX), fucose (ISF), arabinose, galactose, glucose, xylose and mannose*

Since the HPAE PAD system is not listed in the NREL LAPs, the calibration range and the linear range must be validated. The following Figure 60 shows the behavior of the area concentration of ISF. The saturation event of the detector can be seen here, as the curve flattens out from 5.0 mg/l. As the behavior of the sugars was very similar, the calibration range of 0.1 to 4.0 mg/l was selected for all substances. In addition, the ISF concentration is set at 3 g/l. The chromatography and calibration data for the HPAE-PAD system were listed in the following Table 13. Due to the LOQ of galactose and mannose, the linear range was defined from 0.2 mg/l upwards. The values for $R^2$ are >0.9955, which also indicates a good correlation of the calibration points with their linear equation.

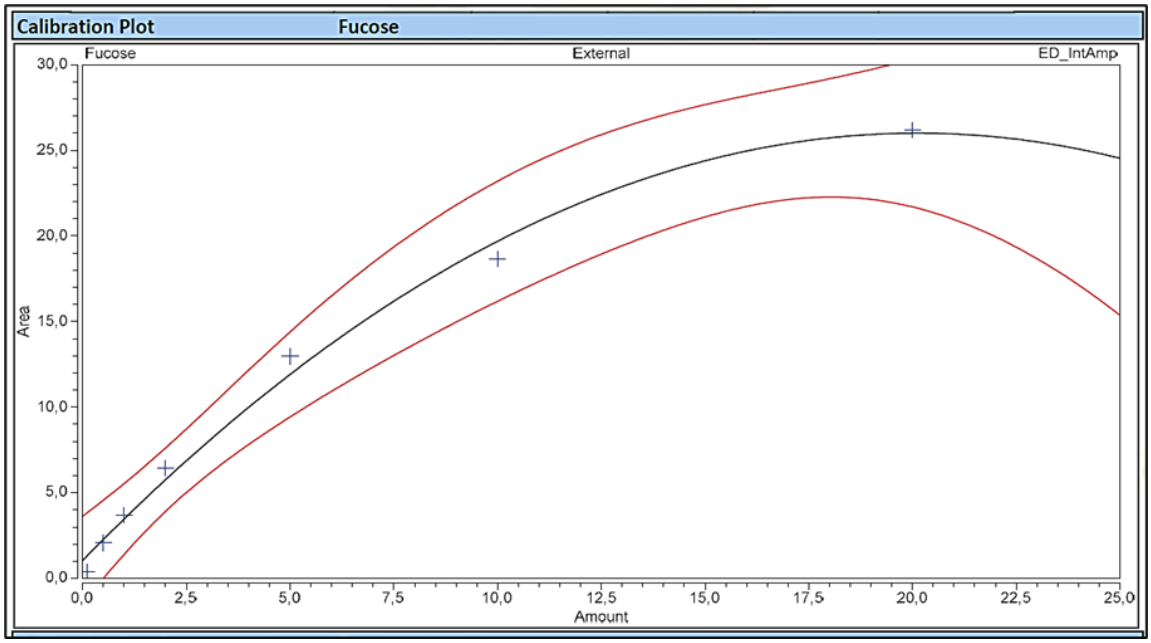


*Figure 60_Chromatogram of linearity validation of fucose in the concentration range between 0.1 and 20.0 mg/l; linearity is given from 0.1 up to 5.0 mg/l, otherwise saturation event starts*

*Table 13_Chromatography and calibration data for the HPAE-PAD system; only chromatography data is available for the internal standards xylitol and fucose, as calibration is not important here*

| Compound | Ret. Time [min] | LOD [µg/l] | LOQ [µg/l] | Linear Range [mg/l] | Equation (y= kx + d) | $R^2$ |
|---|---|---|---|---|---|---|
| **Arabinose** | 10.54 | 30.2 | 108.2 | 0.1 - 4.0 | Y= 2.616x + 0.270 | 0.9955 |
| **Galactose** | 13.33 | 44.7 | 159.9 | 0.2 - 4.0 | Y= 2.879x + 0.322 | 0.9967 |
| **Glucose** | 15.58 | 39.9 | 142.8 | 0.1 – 4.0 | Y= 2.867x + 0.257 | 0.9965 |
| **Mannose** | 19.92 | 55.9 | 199.6 | 0.2 – 4.0 | Y= 2.988x + 0.204 | 0.9983 |
| **Xylose** | 18.61 | 26.7 | 95.9 | 0.1 – 4.0 | Y= 3.105x + 0.288 | 0.9972 |
| **Fucose (ISF)** | 4.74 | -- | -- | -- | -- | -- |
| **Xylitol (ISX)** | 1.73 | -- | -- | -- | -- | -- |

### 3.5.3. LC Comparison

The comparison of the chromatography data shows that in the RID system the internal standard elutes last, whereas in the PAD system the internal standards elute first. A comparison of the monosaccharide peaks was shown in the following Table 14. The retention times for the five monosaccharides and their time difference to the first monosaccharide peak were shown here. In the RID system, the peaks were relatively close together, apart from mannose (see Figure 58), as all five sugar peaks interact with each other at a concentration of more than 1 g/l. In the PAD system, the peaks were better separated from each other; only xylose and mannose interact with each other when they exceed a concentration of 3 mg/l.

*Table 14_Comparison of the chromatography data of the monosaccharides for the two used LC systems; value in brackets was time difference to the first peak detected in the chromatogram*

| Compound | Ret. Time [min] (Δt to first peak [min]) | |
|---|---|---|
| | RID | PAD |
| **Arabinose** | 17.26 (+4.42) | 10.54 (±0) |
| **Galactose** | 15.40 (+2.56) | 13.33 (+2.79) |
| **Glucose** | 12.84 (±0) | 15.58 (+5.04) |
| **Mannose** | 20.611 (+7.77) | 19.92 (+9.38) |
| **Xylose** | 14.21 (+1.37) | 18.61 (+8.07) |

A comparison of the calibration data obtained for the two LC systems shows that $R^2$ was better for the system connected to the RID ($R^2$ >0.9998) than for the system connected to the PAD ($R^2$ >0.9955). The linear working range was also better for the RID, if the 1000 times more sensitive detection for the PAD was ignored. Here the linear range was always between 0.1 and 4.0, except for galactose, while for PAD galactose and mannose was set at 0.2 upwards. This fact for the linearity was a result of the LOQ values.

The following Figure 61 & Figure 62 shows a comparison of these two LC systems on real samples. The first real sample comparison were two reproducibility experiments (same as for lignin determination). The well-known MonoX pulp sample was used for this. In the first experiment, the reproducibility within a series is tested. This means that

a fivefold determination was measured on a single day (dependent). In the second experiment, the reproducibility was tested for five series, i.e., a single determination was carried out on five different days (independent). The results of these tests were shown in the next Figure 61.

Firstly, the reproducibility test shows that glucose was the dominant sugar in the sample, as cellulose is a polymer of glucose building blocks. Secondly, the confidence interval (CI) for the independent test was always wider. Furthermore, the CI determined for the HPAE-PAD was wider for both glucose determinations than for the HPLC-RID determination. In addition, the PAD often yields higher concentrations. For smaller fractions (like xylose and mannose), the PAD provided better results than the RID setup, which can handle medium to high concentrations better, due to the detector sensitivity.

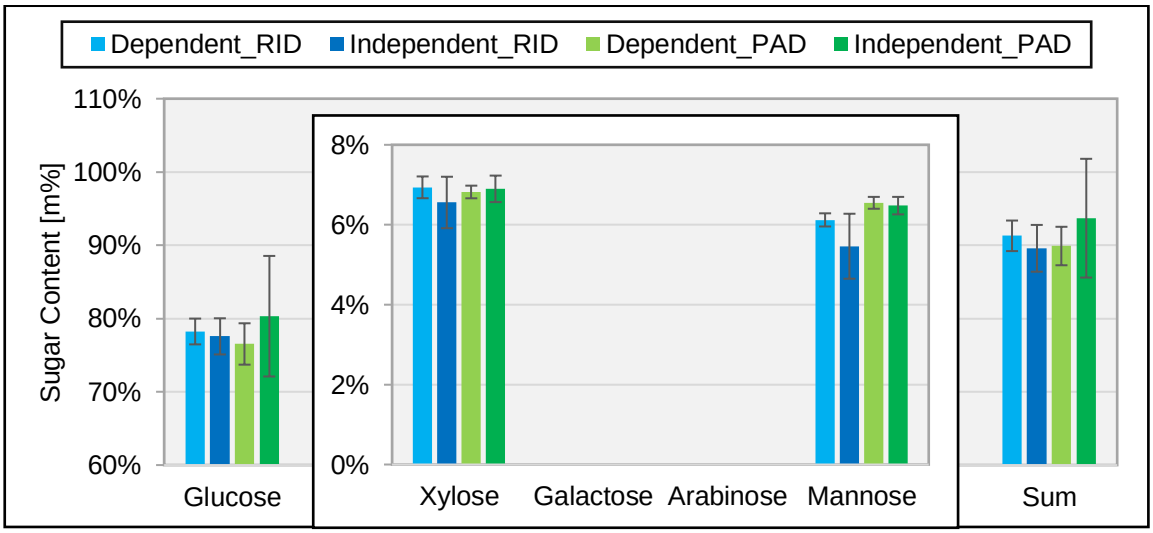


*Figure 61_Reproducibility experiments for the two LC systems; dependent means a five-fold determination on a single day, and independent means a single determination on five different days; confidence interval (α=0.05; n=5) as error bars*

The following Table 15 shows the previously discussed results with values. It could be observed here that the relative errors were similar for the dependent test, except for glucose and xylose, where there was a CI difference of 1.5 %. This trend was more clearly visible for the independent test. Here the CI difference was 7.0 % for glucose, 11.5 % for mannose and 5.0 % for xylose. As discussed, the RID had advantages in the determination of medium to high concentrations, while the PAD was favorable at very low concentrations. In addition, as already mentioned, the dependent test led to more similar values than the independent test.

*Table 15_Values of the reproducibility experiments for the two LC systems; dependent means a five-fold determination on a single day, and independent means a single determination on five different days; confidence interval (α=0.05; n=5) as relative error; LOD…limit of detection*

| Substance | Dependent [m%] | | Independent [m%] | |
|---|---|---|---|---|
| | ***PAD*** | ***RID*** | ***PAD*** | ***RID*** |
| **Arabinose** | <LOD | <LOD | <LOD | <LOD |
| **Galactose** | <LOD | <LOD | <LOD | <LOD |
| **Glucose** | 76.5 ± 3.7% | 78.2 ± 2.2% | 80.3 ± 10.2% | 77.6 ± 3.2% |
| **Mannose** | 6.5 ± 2.3% | 6.1 ± 2.7% | 6.5 ± 3.4% | 5.5 ± 14.9% |
| **Xylose** | 6.8 ± 2.3% | 6.9 ± 3.9% | 6.9 ± 4.8% | 6.6 ± 9.8% |
| **Sum** | 89.9 ± 2.9% | 91.3 ± 2.3% | 93.7 ± 8.7% | 89.6 ± 3.6% |

As a result of these experiments and since the error of glucose had a greater influence on the final error of the sugar sum, the HPLC-RID system was favored for carbohydrate determination. To verify this conclusion, five lignocellulosic samples were analyzed for their carbohydrate content in extracted (Sox) and non-extracted form (10 samples). For more realistic circumstances, these samples were prepared in duplicate and their sample filtrate solutions were used. These 20 solutions (5x2 extracted (Sox); 5x2 non-extracted) were measured with both systems. The results were shown in the next Figure 62. In comparison to the fivefold determination of cellulose (MonoX), the previously made observations for the doublet determination only apply to four out of 10. Conversely, 5 out of 10 measurements and one sample (CD-6_Sox) do not differ in error.

The following Table 16 also shows that the relative SDs for the RID system only exceed a 5% SD limit twice, while four exceedances were recorded for the PAD system. This led to a lower scatter of results for the RID system in these measurements. To summarize, it had to be said that the LC system with RI detector was preferable for sugar analysis and determination.

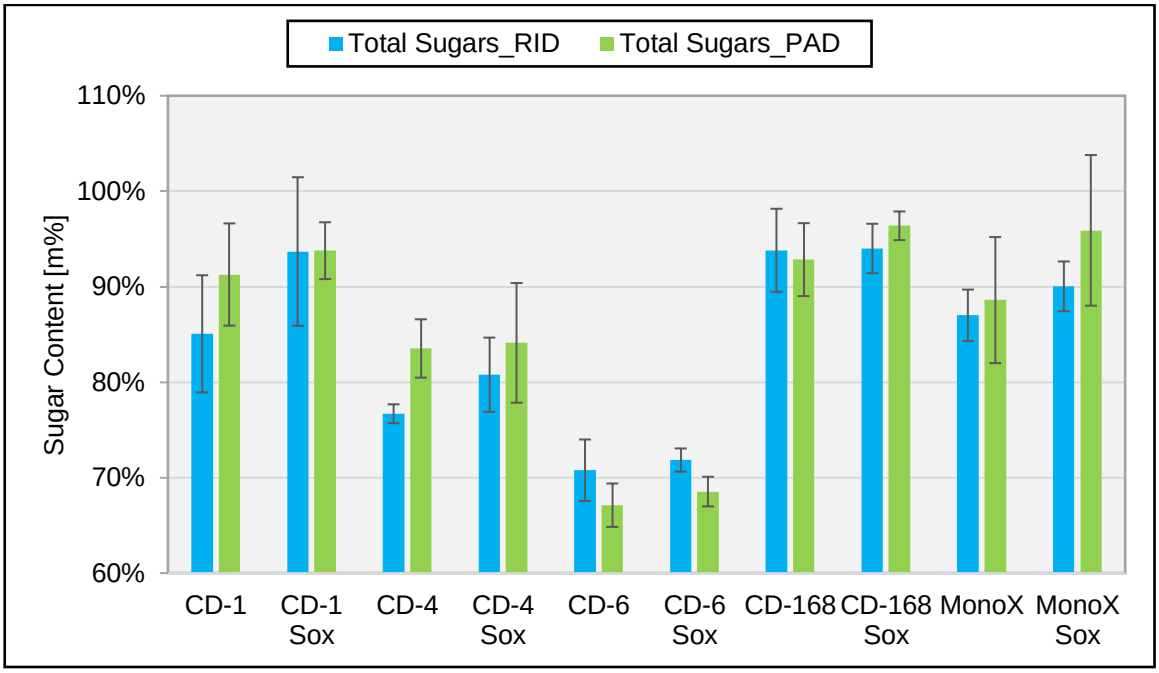


*Figure 62_Carbohydrate determination on five different lignocellulose samples; determination is performed in doublet (independent) and their standard deviation as error bars; Sox indicates the extracted form*

*Table 16_Values for carbohydrate determination on five different lignocellulose samples; determination is performed in doublet (independent); values are given as mean with absolute standard deviation (SD) and relative SD (in separate column)*

| Sample | Σ (Sugar RID) [m%] | Rel. SD | Σ (Sugar PAD) [m%] | Rel. SD |
|---|---|---|---|---|
| **CD-1** | 85.1 ± 6.1 | 7.2% | 91.3 ± 5.4 | 5.9% |
| **CD-1 Sox** | 93.7 ± 7.8 | 8.3% | 93.8 ± 3.0 | 3.2% |
| **CD-4** | 76.7 ± 1.0 | 1.3% | 83.5 ± 3.1 | 3.7% |
| **CD-4 Sox** | 80.8 ± 3.9 | 4.8% | 84.1 ± 6.3 | 7.5% |
| **CD-6** | 70.8 ± 3.2 | 4.6% | 67.1 ± 2.3 | 3.4% |
| **CD-6 Sox** | 71.6 ± 1.6 | 2.3% | 68.5 ± 1.6 | 2.3% |
| **CD-168** | 93.8 ± 4.3 | 4.6% | 92.8 ± 3.8 | 4.1% |
| **CD-168 Sox** | 94.0 ± 2.6 | 2.8% | 96.4 ± 1.5 | 1.6% |
| **MonoX** | 87.0 ± 2.7 | 3.1% | 88.6 ± 6.6 | 7.5% |
| **MonoX Sox** | 90.0 ± 2.6 | 2.9% | 95.9 ± 7.9 | 8.2% |

### 3.5.4. Summary -Determination of Carbohydrates

The carbohydrate concentrations were determined using two different HPLC systems with different detectors (refractive index detector (RID) and pulsed Amperometric detector (PAD)), which required different preparations. A calibration curve was created for an initial comparison of these two systems (see Table 12 & Table 13). This showed that the RI detector had $R^2$ values >0.9998 and a linear range between 0.1 and 4.0 g/l for all sugars except galactose (0.2 to 4.0 g/l). PAD, on the other hand, had $R^2$ values >0.9955 with a linear range between 0.1 and 4.0 mg/l, but here apart from galactose and mannose (for both 0.2 to 4.0 mg/l). A comparison of the retention time shows that the PAD system achieved a better separation of the sugar peaks, but always works with low concentrations. RID achieved a weaker separation but measures the sample liquids directly (undiluted). These detector specifications could also be checked in the reproducibility test (Figure 61 & Table 15). Here it had to be seen that the deviations were smaller at high concentrations in the RID system and at low concentrations in the PAD system. This led to large error bars in the calculation of the total sugar content for the PAD (Figure 62 & Table 16). To summarize, the LC system with RI detector was preferable for sugar analysis and determination due to less sample preparation for analysis, linearity between 0.1 and 4.0 g/l for 4 out of 5 sugars and lower errors under real conditions (duplicate determinations & 2 out of 10 samples exceeding a relative standard deviation limit of 5 %).

## 3.6. Kappa Number

The kappa number was determined in accordance with ISO 302:2015 "Pulps - Determination of Kappa number" for ground extracted and non-extracted samples. To compare the determined kappa number (Kappa Exp) with the determined total lignin content, this total content was converted into Kappa Calc using a rule of thumb. The kappa number is approximately proportional to 6.57 times the lignin content in per cent. [28, 76, 77])

These three values related to the lignin content are plotted in the following Figure 63. Here it could be seen, that for 7 out of 10 samples the calculated kappa number was higher than the experimentally determined one. In Figure 63, blue cross (Kappa Exp) and red circle (Kappa Calc) only matched three times. For both CD-1 and MonoX in extracted form. Furthermore, it could be seen that the extracted samples showed a closer agreement of cross and circles, except for CD-6.

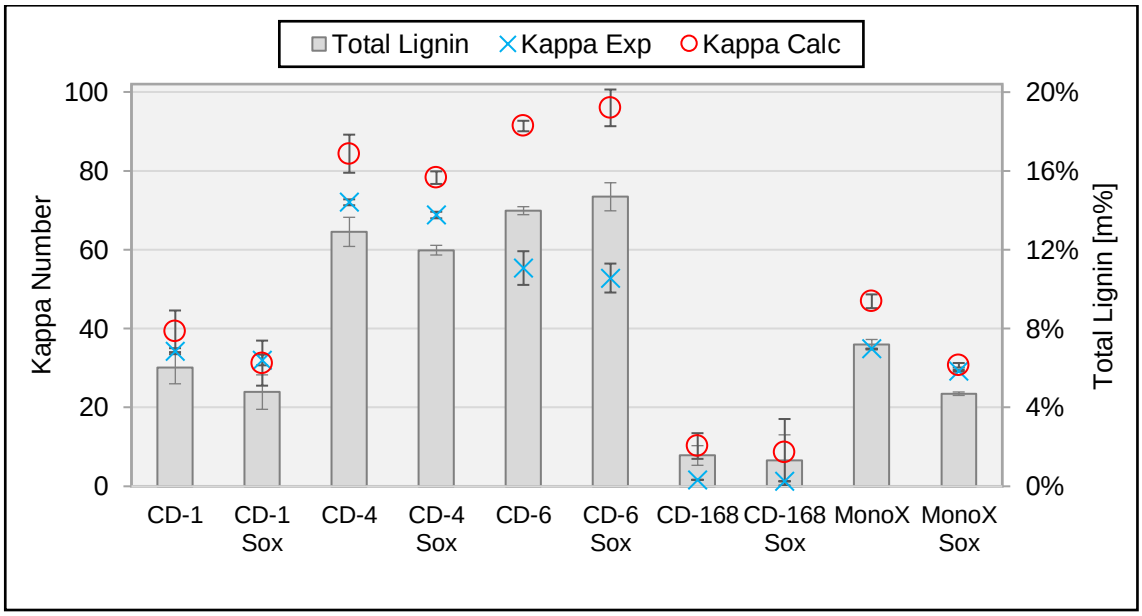


*Figure 63_Comparison plot of Kappa numbers and total lignin content; total lignin content is shown as bars with secondary axis; on primary axis Kappa numbers which are compared between ISO 302 determined Kappa number (Kappa Exp (blue crosses)) and calculated Kappa number (Kappa Calc (red circles)); error bars are given as result of a two-fold determination; Sox indicates extracted form*

The following Table 17 shows the numerical values of the previous Figure 63 with the difference values of the two kappa numbers. Table 17 shows that CD-6 Sox with a kappa number of 43 had the largest difference between the two kappa numbers determined. Followed by its non-extracted form. The other eight samples did not exceed a kappa difference of 13. The smallest differences in kappa numbers were found for CD-1 Sox

(0.8) and MonoX Sox (1.4). For MonoX in particular, solvent extraction led to a significant reduction in the kappa number difference. This indicates that extractable substances were also weighed as Klason lignin or that furan derivatives interfere in the spectroscopic determination.

It could also be shown that the experimentally determined kappa numbers were generally smaller than the calculated ones. This led to the conclusion that the determination of the kappa number was a very useful addition to the determination of the actual total lignin. The advantage of this can be seen for sample CD-168, a fully bleached paper that contains very little to no lignin. While NREL LAP provided a kappa number of around 9, ISO 302 yields a kappa of around 1. Furthermore, here the relative SD values for NREL were 32 % and 97 %, indicating a large deviation. As a result, a variation for CD-168_Sox in kappa number between 0 and 17 was possible (8.65 ± 8.39 m%).

*Table 17_Values for Kappa number and total lignin as mean value of a two-fold determination with relative standard deviation (rel. SD); in the last column are the difference values between Kappa Calc and Kappa Exp; Sox indicates extracted form*

| Sample | Total Lignin | | Kappa Calc | | Kappa Exp | | Δ(Calc-Exp) |
|---|---|---|---|---|---|---|---|
| | *Mean* | *Rel. SD* | *Mean* | *Rel. SD* | *Mean* | *Rel. SD* | |
| **CD-1** | 5.89 | 13% | 39.29 | 13% | 34.26 | 2% | 5.02 |
| **CD-1 Sox** | 4.69 | 18% | 31.24 | 18% | 32.04 | 4% | -0.80 |
| **CD-4** | 12.65 | 6% | 84.35 | 6% | 72.02 | 1% | 12.32 |
| **CD-4 Sox** | 11.74 | 2% | 78.28 | 2% | 68.79 | 1% | 9.48 |
| **CD-6** | 13.70 | 1% | 91.36 | 1% | 55.35 | 8% | 36.02 |
| **CD-6 Sox** | 14.40 | 5% | 95.97 | 5% | 52.81 | 7% | 43.16 |
| **CD-168** | 1.53 | 32% | 10.22 | 32% | 1.64 | -- | 8.58 |
| **CD-168 Sox** | 1.30 | 97% | 8.65 | 97% | 1.28 | -- | 7.37 |
| **MonoX** | 7.04 | 4% | 46.92 | 4% | 34.87 | 0% | 12.05 |
| **MonoX Sox** | 4.60 | 2% | 30.69 | 2% | 29.28 | 1% | 1.41 |

### 3.6.1. Summary -Kappa Number

The determination of the kappa number is a useful addition to the determination of total lignin, as some samples have a high error potential. This is especially true for recycled and fully bleached lignocellulosic samples. It can be shown that sample extraction leads to better agreement in lignin determination in 4 out of 5 samples.

## 3.7. Biomass Analysis Comparison

In this section, a comparison of the biomass analysis was discussed. This comparison was performed in the form of a Pseudo Robin Ring (PRR) test, where each sample was measured in duplicate and according to NREL. This PRR was performed between four laboratories: Graz University of Technology (TUG) (twice; RID and PAD), Vienna University of Technology (TUW) and Celignis Analytical (CA). For comparison, 5 lignocellulose samples were selected, ground with a centrifugal mill, and prepared for dispatch to TUW and Celignis Analytical. The selected samples were CD-1 and CD-4, both kraft paper, CD-6, a recycled paper, CD-168, a fully bleached paper, and MonoX, a pulp sample (see Figure 36). Due to resource constraints and particular interest, the focus of this comparison was on carbohydrate and lignin determination, especially for the last two biomass samples of CD-168 & MonoX. Therefore, TUW was instructed to analyze only these two fractions on these two samples. For the other biomass compounds (extracts & ash content), only comparisons between TUG and Celignis Analytical were carried out.

In the following illustrations, these four compound results were highlighted in color. Celignis Analytical was always shown in orange and TUW in blue. TUG was shown in red and in dark red if the sample is in its extracted form (Sox). In the carbohydrate section, TUG is divided into a red (RID system) and a green (PAD system) fraction.

### 3.7.1. Extractives

The first compound for comparison was the extractables between Celignis Analytical (CA) and TUG. Figure 64 shows these results. Since TUG uses Soxhlet extraction for extraction, only one extraction could be performed in a given time period. In contrast, Celignis Analytical uses an accelerated solvent extraction system (ASE). This system allowed the same efficient extraction within a few hours compared to classic Soxhlet extraction, which takes days.

Figure 64 shows that CA extracts more material compared to TUG. Except for MonoX, here a similar concentration of extractable substances could be achieved. For the first two kraft paper samples, the difference was 0.95 m% (CD-1) and 0.68 m% (CD-4). A difference of 2.04% was calculated for the recycled paper (CD-6) and a similar difference of 2.08 m% for the bleached paper (CD-168). As already mentioned, a small difference (0.02m%) was obtained for MonoX. This result showed that this extractable amount can lead to a falsely higher Klason lignin content. This was due to the fact that some of these extractables may be insoluble in water and therefore remained on the filter used for

Klason lignin determination. These results spoke in favor of the advantage of sample comminution and extraction.

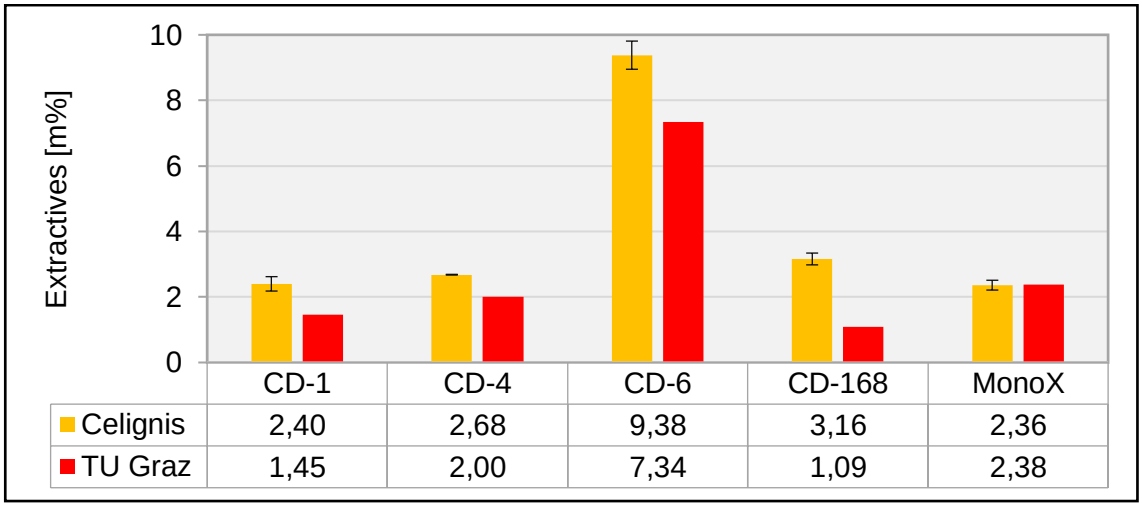


| | CD-1 | CD-4 | CD-6 | CD-168 | MonoX |
|---|---|---|---|---|---|
| Celignis | 2,40 | 2,68 | 9,38 | 3,16 | 2,36 |
| TU Graz | 1,45 | 2,00 | 7,34 | 1,09 | 2,38 |

*Figure 64_Analysis comparison of extractives; since Soxhlet extraction takes his time only a single extraction could be performed in a given time*

### 3.7.2. Ash Content

Second compound for comparison was the ash content. Here too, only between TUG and CA. This determination was carried out according to NREL LAP 42622 at a temperature of 575°C. These results were shown in the following Figure 65 & Figure 66 and Table 18. As mentioned at the beginning of the chapter, the results of the non-extractable form for TUG were shown in red and the extractable form (Sox) in dark red. Like the extractables, CA achieved the highest ash content for all five samples.

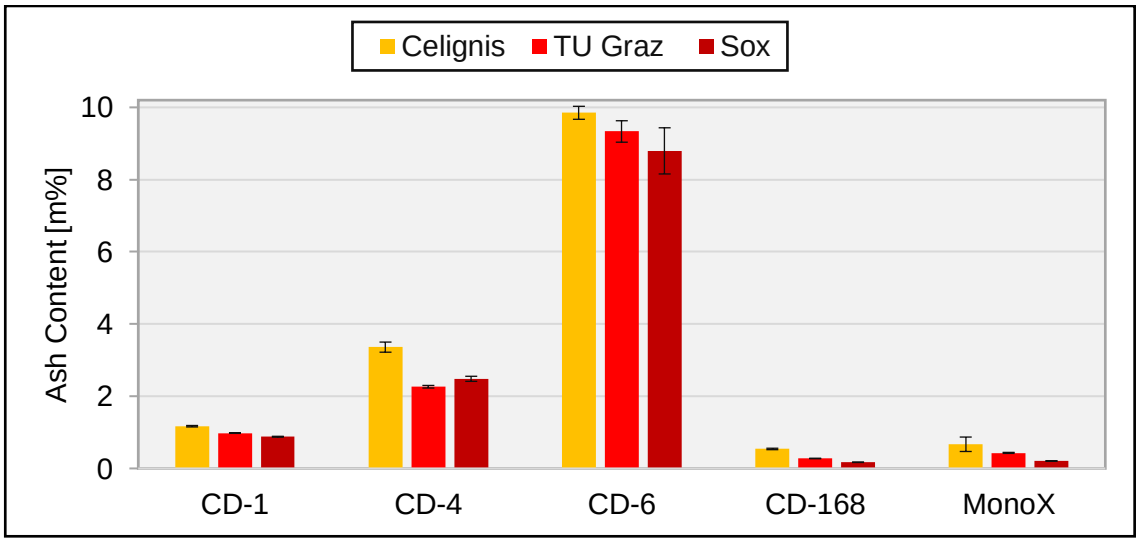


*Figure 65_Analysis comparison of ash content; Sox indicates extracted form*

*Table 18_ Analysis comparison of ash content; Sox indicates extracted form; values in table are given as mean ($\bar{X}$) in m% with relative standard deviation (rel. SD)*

| Sample Name | Celignis Analytical | | TU Graz | | TU Gras_Sox | |
|---|---|---|---|---|---|---|
| | $\bar{X}$ [m%] | Rel. SD | $\bar{X}$ [m%] | Rel. SD | $\bar{X}$ [m%] | Rel. SD |
| **CD-1** | 1,17 | 2% | 0,98 | 1% | 0,88 | 1% |
| **CD-4** | 3,36 | 4% | 2,26 | 2% | 2,48 | 3% |
| **CD-6** | 9,85 | 2% | 9,33 | 3% | 8,80 | 7% |
| **CD-168** | 0,54 | 4% | 0,28 | 2% | 0,17 | 3% |
| **MonoX** | 0,67 | 30% | 0,43 | 3% | 0,21 | 4% |

A comparison between extracted and non-extracted sample form led to different results. A decreasing trend of the ash content in the extracted form can be observed for all samples. An exception was the paper sample CD-4, where a reverse trend could be observed. In addition, samples CD-4 and CD-6 showed a higher ash content than the extractable content. The next Figure 66 shows a closer look where it could be observed that CA achieved for MonoX a relative standard deviation of 30 %. This range can led to similar results as for the non-extracted MonoX sample and showed so similar trends as for the extractables.

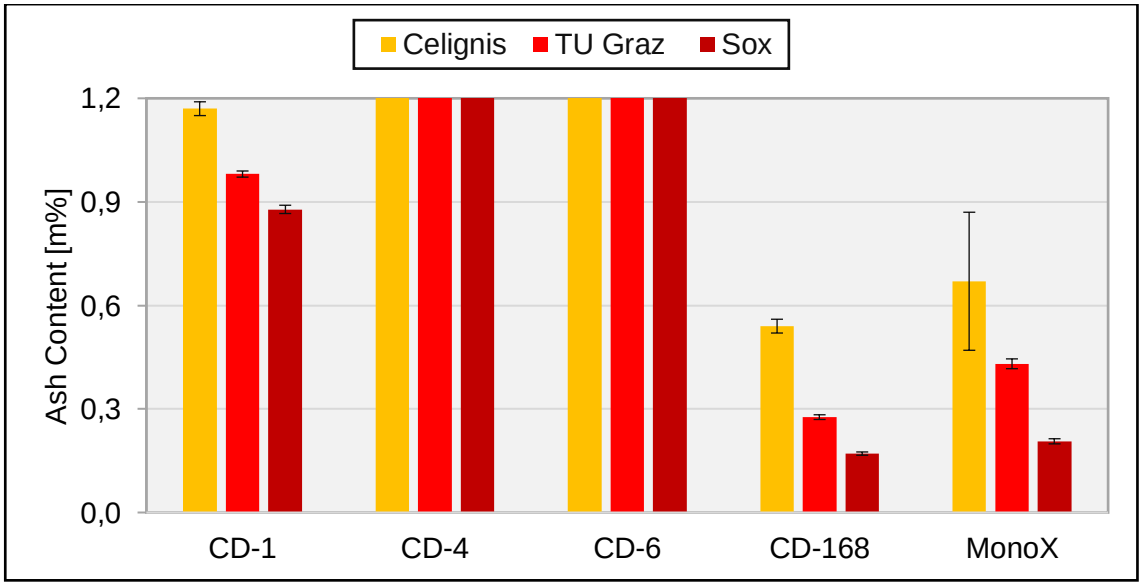


*Figure 66_A closer look to analysis comparison of ash content; Sox indicates extracted form*

### 3.7.3. Lignin

The first component of interest was the lignin content in the lignocellulosic biomass. As mentioned at the beginning, the TUW (blue) was included in the following two sections of lignin and carbohydrate comparison for the samples CD-168 and MonoX. The total lignin content was divided into two components (soluble and insoluble), which were first discussed separately and then as the sum of the total lignin.

Starting with the acid insoluble (Klason) lignin, which was shown in Figure 67. As a reminder, this fraction was made up of acid-insoluble substances that are determined by weighing. Other insoluble substances such as resins and metals had to be included. A first look at Figure 67 shows that sample CD-168, a fully bleached paper, exhibits a large variation in values. From a Klason lignin content of 0.74 m% to 11.08 m%. CA determined a value of 2.76 m% with a relative standard deviation (SD) of 12%. TUG provides values between 0.99 m% and 0.74 m% (Sox) with a relative SD of 94% and 173% for both sample configurations. As mentioned in other sections, this discrepancy was due to weighing errors and non-lignin substances, as this sample contains little to no lignin, which could not be accurately captured with this coarse configuration. TUW, on the other hand, provided a lignin content of 11.08 m%. The numerical values were summarized in Table 19.

The next interesting example was MonoX. Based on previous results, the lignin content of Klason should be between 4 and 6 m%. Only the TUG Sox sample and the non-extracted sample using SD lie within this interval. CA and TUW yield 10.09 m% and 8.24 m%, which is about twice as much as the smallest expected value. The samples CD-1 and CD-4 had almost similar values around 4.5 m% and 11.5 m%. The values differ for CD-6, as CA determined the lowest value of 10.79 m%. TUG, on the other hand, delivered values of around 13 m%. Here, too, it could be shown that extraction led to more promising values, except for sample CD-6, the recycled paper. The generally low deviations in the values determined by CA should also be mentioned.

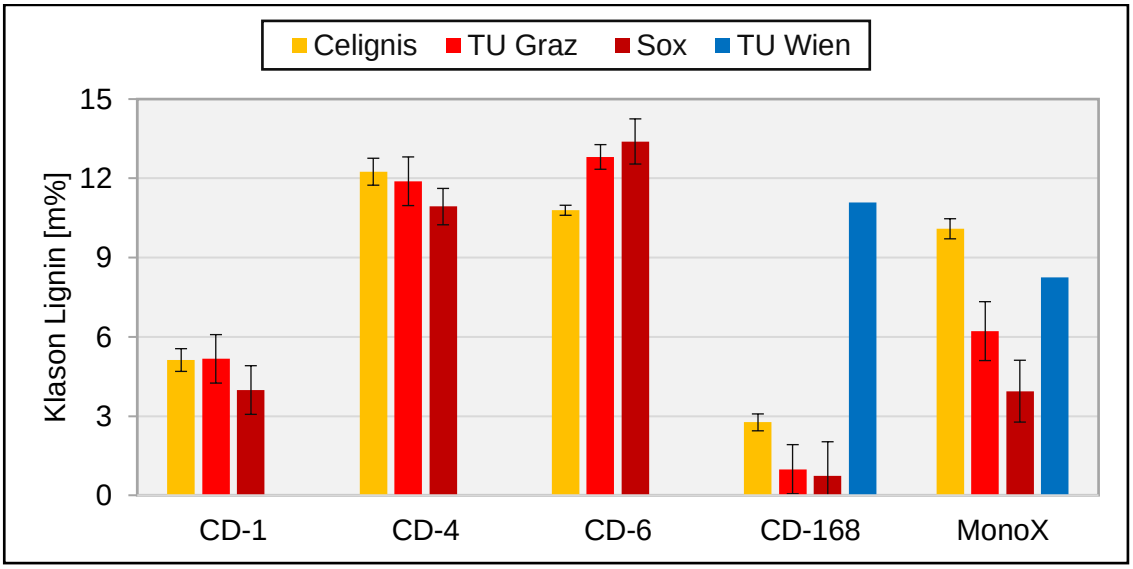


*Figure 67_Analysis comparison of Klason (Acid-Insoluble) lignin content; Sox indicates extracted form; TUW only provides a single determination*

In contrast to the Klason lignin fraction, the acid-soluble lignin was determined by UV/Vis spectroscopy of the resulting sample supernatant. Figure 68 shows the results of these spectroscopic measurements. The first observation was the lower range of the y-axis, which was in the range <1.5 m%. In addition, the results for most samples were between 0.6 and 1.2 m%, except for CD-168. Compared to Klason lignin, the SDs were more evenly distributed here (see Table 19).

Starting with TUG, the relative SDs for non-extracted samples were >10% for the paper samples, except for bleached paper. The extracted samples show similar variations to the non-extracted samples. The bleached paper and pulp samples showed evenly distributed SDs. As already observed for Klason lignin, the smallest deviations were also obtained for CA for all samples. A similar mean value was obtained for CD-1 in all laboratories. The following two samples of CD-4 and CD-6 showed an increasing mean value of CD to Sox with an increase of 0.13 m% for both. For CD-168, the reverse case was observed here, with the difference that the TUG modifications match. For MonoX, CA and TUG Sox match, while the other two laboratory values were larger. In addition, the results of CA are always between 0.67 and 0.76 m% for all samples, while the other laboratories show a greater scattering of results.

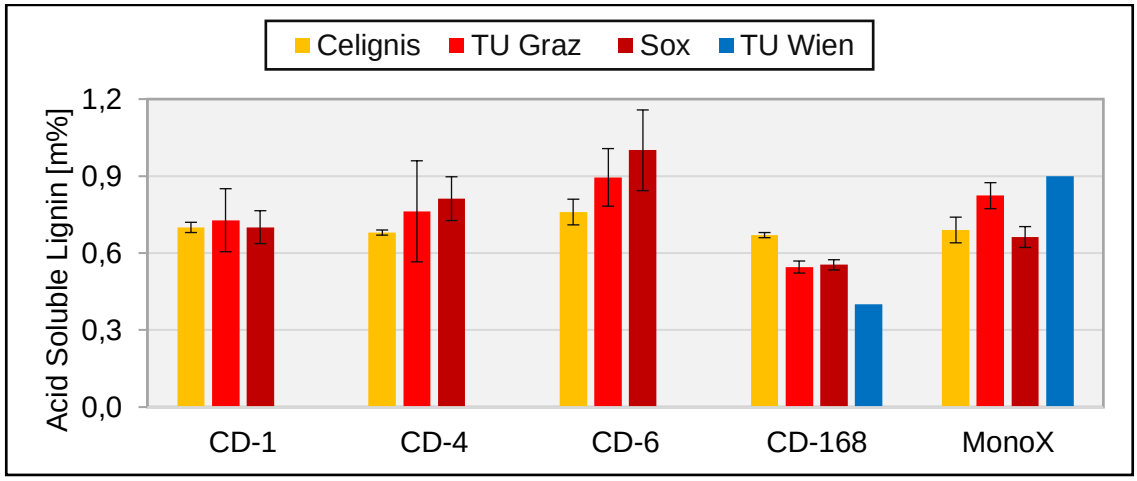


*Figure 68_Analysis comparison of Acid-Soluble lignin content; Sox indicates extracted form; TUW only provides a single determination*

By calculating the sum of these two fractions, the acid-insoluble (AI) and the acid-soluble (AS) lignin, the total lignin could be determined. These sums were plotted in the Figure 69 and listed in Table 19. According to the error calculations, the errors were also calculated as the sum of the two fractions. As a result, the error was more strongly influenced by the Klason lignin error. Since the Klason lignin accounts for the greater proportion of the lignin content, the total lignin behaves similarly to it. As already described for Klason lignin, the first two samples decrease on average from CA to TUG Sox, while the opposite is the case for CD-6. Different results between 1.30 and 11.48 m% were obtained for CD-168. TUG achieved similar results for both forms (1.30 m% (Sox) & 1.53 m%), but with a deviation for both of almost 100 %. There was also a decreasing trend for MonoX, except for TUW. It should also be mentioned here that CA achieved the smallest SD values for all samples.

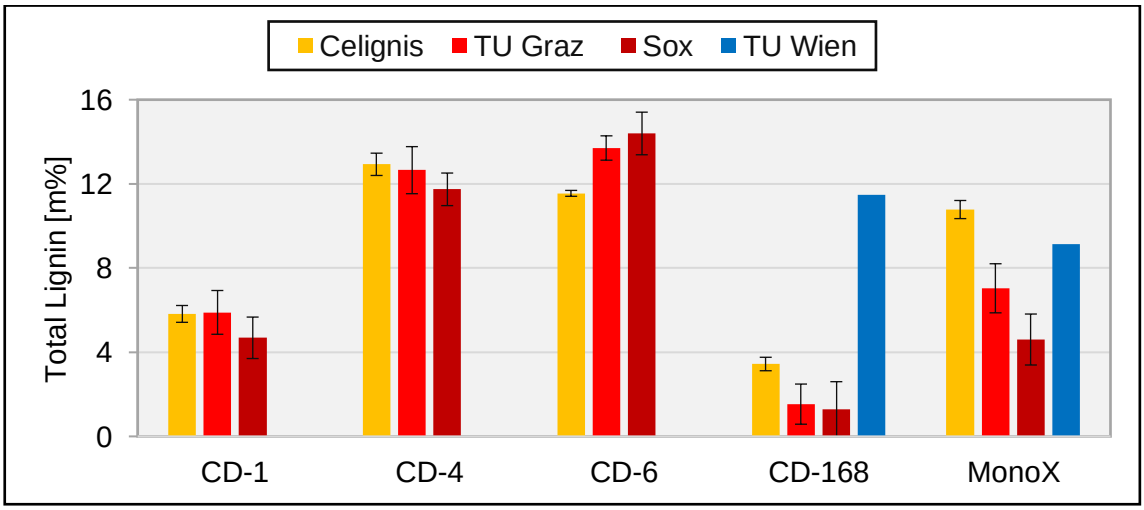


*Figure 69_Analysis comparison of total lignin content; Sox indicates extracted form; TUW only provides a single determination*

*Table 19_Summarized values for the different lignin fractions and total lignin content; the values are given as mean ($\bar{X}$) values in m% with relative standard deviations (rel. SD); TUW only provides a single determination*

| | Celignis | | TU Graz | | Sox | | TU Wien |
|---|---|---|---|---|---|---|---|
| **Klason-Lignin** | $\bar{X}$ [m%] | Rel. SD | $\bar{X}$ [m%] | Rel. SD | $\bar{X}$ [m%] | Rel. SD | |
| **CD-1** | 5.12 | 8% | 5.17 | 18% | 3.98 | 23% | |
| **CD-4** | 12.25 | 4% | 11.89 | 8% | 10.93 | 6% | |
| **CD-6** | 10.79 | 2% | 12.81 | 4% | 13.40 | 6% | |
| **CD-168** | 2.76 | 12% | 0.99 | 94% | 0.74 | 173% | 11.08 |
| **MonoX** | 10.09 | 4% | 6.21 | 18% | 3.94 | 30% | 8.24 |
| **AS-lignin** | | | | | | | |
| **CD-1** | 0.70 | 3% | 0.73 | 17% | 0.70 | 9% | |
| **CD-4** | 0.68 | 1% | 0.76 | 26% | 0.81 | 11% | |
| **CD-6** | 0.76 | 7% | 0.89 | 13% | 1.00 | 16% | |
| **CD-168** | 0.67 | 1% | 0.55 | 4% | 0.55 | 4% | 0.40 |
| **MonoX** | 0.69 | 7% | 0.82 | 6% | 0.66 | 6% | 0.90 |
| **Total Lignin** | | | | | | | |
| **CD-1** | 5.82 | 7% | 5.89 | 18% | 4.69 | 21% | |
| **CD-4** | 12.93 | 4% | 12.65 | 9% | 11.74 | 7% | |
| **CD-6** | 11.55 | 1% | 13.70 | 4% | 14.40 | 7% | |
| **CD-168** | 3.44 | 9% | 1.53 | 62% | 1.30 | 101% | 11.48 |
| **MonoX** | 10.78 | 4% | 7.04 | 17% | 4.60 | 26% | 9.14 |

In addition to the classic lignin determination according to NREL LAP, TUG determined a kappa number for all five samples in order to evaluate the total lignin content achieved. These results are shown in Figure 70, where the total lignin contents were shown as bars and their calculated kappa number as red circles. The kappa numbers achieved according to ISO 302 were shown as black crosses.

No match could be achieved between cross (Kappa Exp) and circle (Kappa Calc) for CD-4 and CD-6. For all CD-1s, Kappa Calc matched with Kappa Exp. A match was achieved for CD-168_Sox, but only because of the SD of 100%. For MonoX only a match at MonoX_Sox could be achieved. The samples of CD-6 showed the largest difference between the two kappa fractions with a kappa number of 36 and 43. Consequently, only 4 out of 15 kappa numbers could be matched. The determination of the total lignin according to NREL LAP 42618 resulted in a similar lignin content for 26 % of all samples. For the other 74 %, the NREL determination resulted in a higher lignin content.

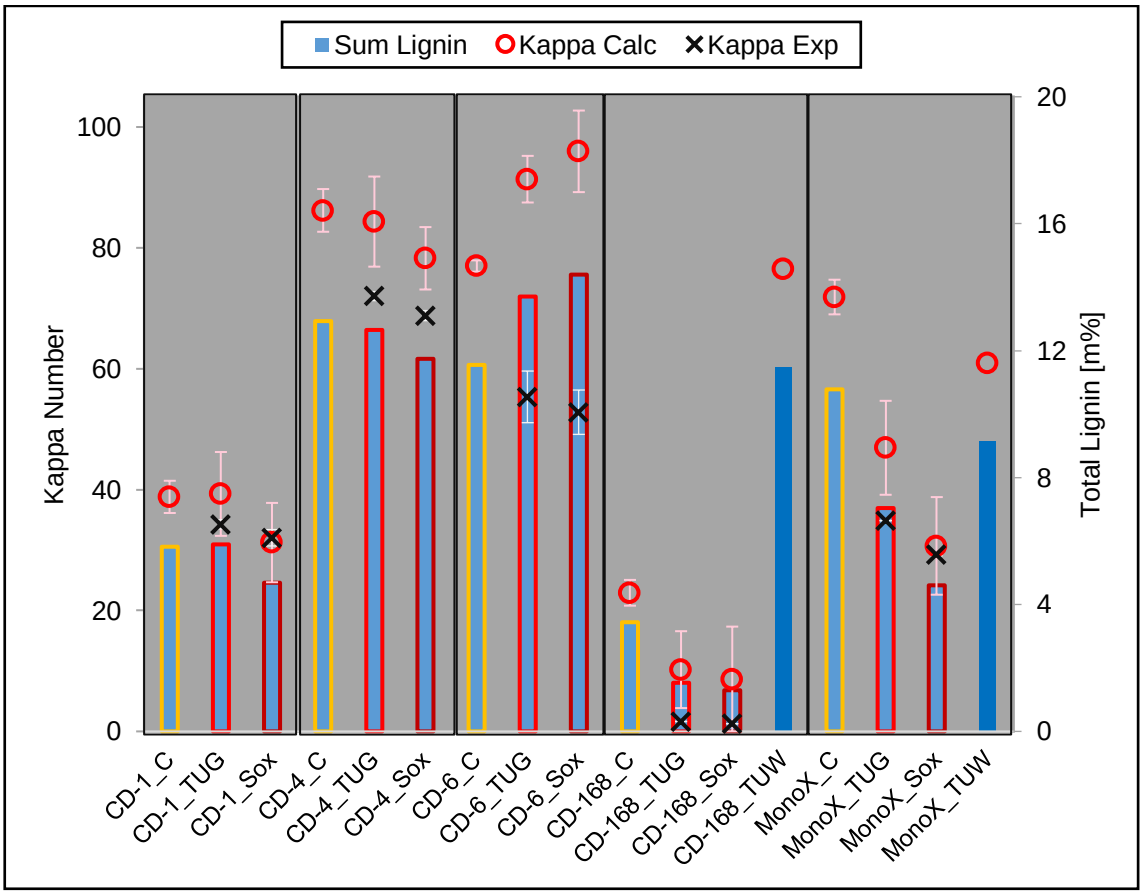


*Figure 70_Analysis comparison of Kappa Number and total lignin content; Celignis Analytical (CA) and TUW, other is TUG in extracted (Sox) or non-extracted form; Kappa Exp is only available for TUG samples, since only here a determination could be performed and this addition is just for checking for accuracy*

### 3.7.4. Carbohydrates

The other compound of interest was carbohydrates. According to the NREL LAP 42618, five different monosaccharides were common. These were arabinose, galactose, glucose, mannose, and xylose. The sum of these sugars gives the total carbohydrate content. As mentioned at the beginning of this chapter, the TUG carbohydrates were divided into two groups. The first group was represented by an HPAE-PAD system (green colors), while the second group used the standardized HPLC-RID system (red colors). For the determination of carbohydrates, the same sets of prepared samples were analyzed with both systems. The results obtained were first discussed for each individual monosaccharide and at the end as a sum of the total carbohydrates. For reasons of space, the numerical values of these determinations were summarized in two tables, with the first table containing glucose, xylose, and mannose (Table 20). The second table contains arabinose, galactose, and the sum of all sugars (Table 21).

The first monosaccharide for comparison was glucose, which is the building block of cellulose and therefore makes up the majority of carbohydrates. The results of the different laboratories were shown in Figure 71. As already mentioned in the section on lignin, CA also achieved the lowest SD in this section. A first look at Figure 71 shows that the extracted samples always had a higher sugar content compared to the non-extracted samples. Furthermore, the mean values of CA were often within the SDs of the non-extracted samples, while the Sox samples are usually above these values. This leads to the conclusion that CA had analyzed the non-extracted form or TUG overestimates the sugar content with both LC systems.

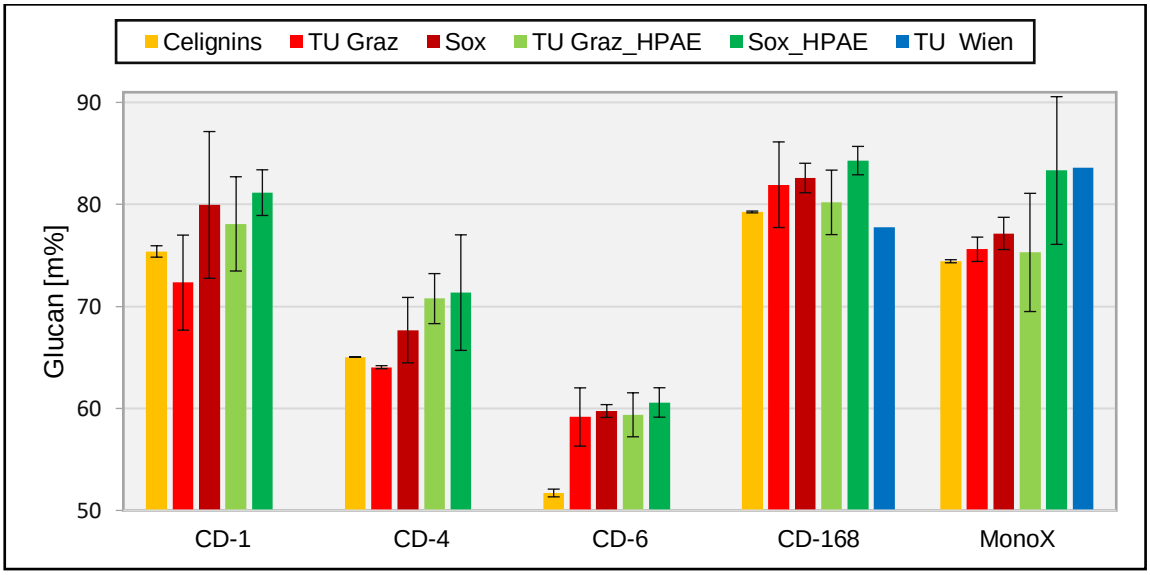


*Figure 71_Comparison of the monosaccharide glucose between different labs and sample configuration*

Compared to glucose, the next two sugars had a proportion of less than 10 m%. The second sugar for comparison was xylose. In Figure 72, the amount of xylose was plotted for all samples in the range between 5 and 9 m%. In this Figure 72, the PAD shows the lowest amounts (up to 1 m% less compared to RID). For the RID system, the results were always within the range of the CA results due to the large SD intervals. The detector specifications were also visible here, as the RID system delivers greater deviations at these low concentrations than the PAD system. The results from TUW were always greater (1 to 2 m%) than the results from the other laboratories.

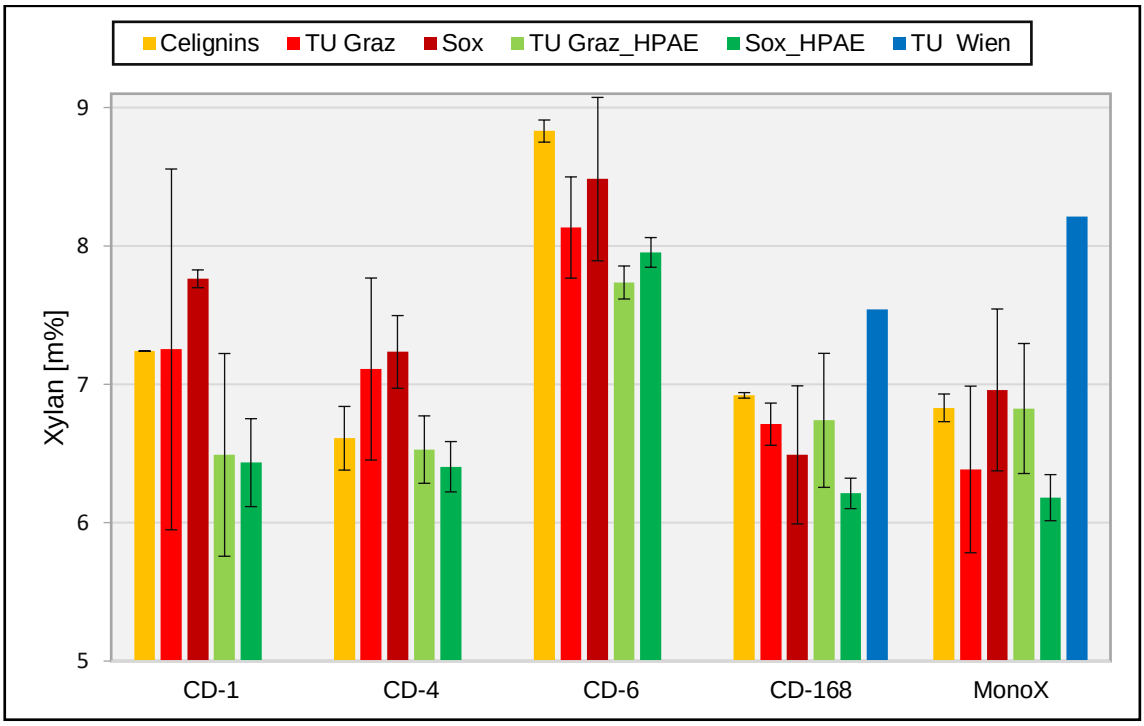


*Figure 72_Comparison of the monosaccharide xylose between different labs and sample configuration*

The next sugar was mannose, which was found between 3 m% and 7 m%. For TUG (PAD and RID) the limit of quantification (LOQ) is important as some results are below this limit. This could be seen in Figure 73, where some of the TU Graz results had no error bar or result. For RID the mannose LOQ is 3.3 m% and for PAD 5.8 m%. In the absence of an error bar, one of the two determinations gave a value <LOQ. For CD-6, the PAD system only achieved values <LOQ, so that a concentration could not be specified. Apart from CD-6, the PAD system always yields the highest concentrations for all samples. Followed by CA, TUW and TUG RID with the lowest results. It should also be mentioned here that CA achieved the smallest standard deviations.

The next Table 20 shows the previously recorded results in numbers.

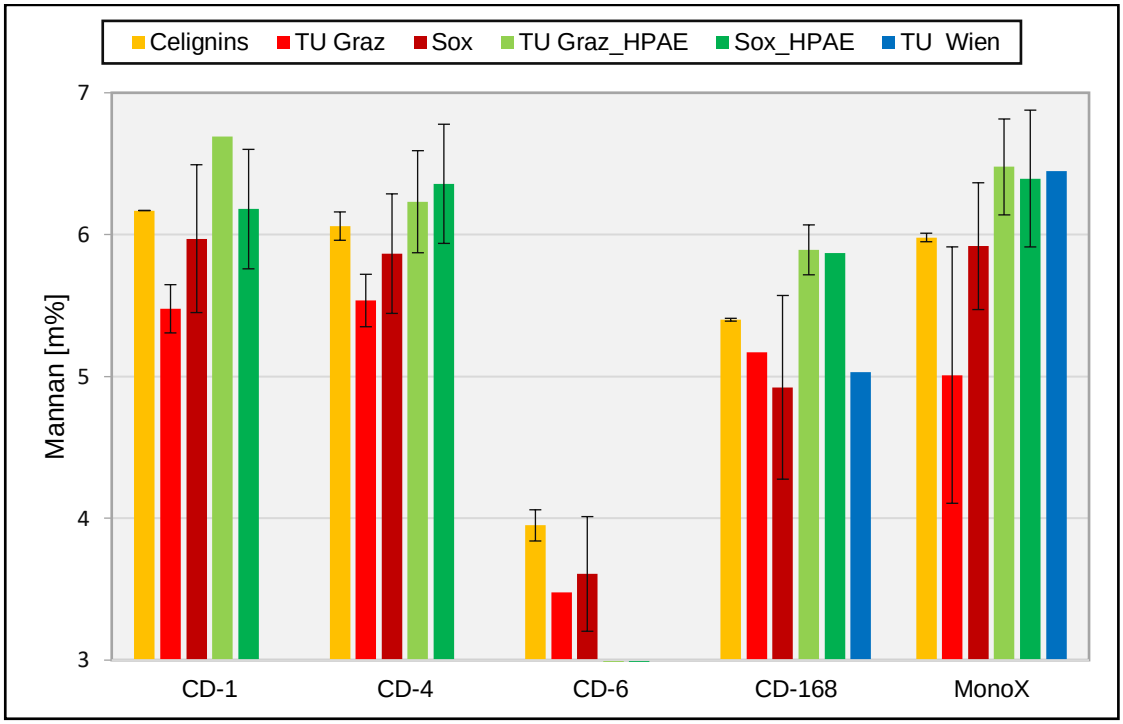


*Figure 73_Comparison of the monosaccharide mannose between different labs and sample configuration; lack of error bars and results for CD-6 because of results <LOQ*

*Table 20_Summarized values for the monosaccharide glucose, xylose and mannose; the values are given as mean value in m% with their relative standard deviation (rel. SD) in %; samples with a mark (*) at the end indicate a measurement in which a value reached a value <LOQ in duplicate determinations*

| | Celignis | TUG | Sox | TUG_HPAE | Sox_HPAE | TUW |
|---|---|---|---|---|---|---|
| **Glucan** | $\bar{X}$ [m%] ± rel.SD | $\bar{X}$ [m%] ± rel.SD | $\bar{X}$ [m%] ± rel.SD | $\bar{X}$ [m%] ± rel.SD | $\bar{X}$ [m%] ± rel.SD | $\bar{X}$ [m%] |
| **CD-1** | 75.4 ± 1% | 72.3 ± 6% | 80.0 ± 9% | 78.1 ± 6% | 81.2 ± 3% | -- |
| **CD-4** | 65.0 ± 0% | 64.0 ± 0% | 67.7 ± 5% | 70.8 ± 3% | 71.4 ± 8% | -- |
| **CD-6** | 51.7 ± 1% | 59.2 ± 5% | 59.7 ± 1% | 59.4 ± 4% | 60.6 ± 2% | -- |
| **CD-168** | 79.3 ± 0% | 81.9 ± 5% | 82.6 ± 2% | 80.2 ± 4% | 84.3 ± 2% | 77.8 |
| **MonoX** | 74.4 ± 0% | 75.6 ± 2% | 77.2 ± 2% | 75.3 ± 8% | 83.3 ± 9% | 83.6 |
| **Xylan** | | | | | | |
| **CD-1** | 7.24 ± 0% | 7.25 ± 18% | 7.76 ± 1% | 6.49 ± 11% | 6.43 ± 5% | -- |
| **CD-4** | 6.61 ± 3% | 7.11 ± 9% | 7.23 ± 4% | 6.53 ± 4% | 6.40 ± 3% | -- |
| **CD-6** | 8.83 ± 1% | 8.13 ± 4% | 8.48 ± 7% | 7.74 ± 2% | 7.95 ± 1% | -- |
| **CD-168** | 6.92 ± 0% | 6.71 ± 2% | 6.49 ± 8% | 6.74 ± 7% | 6.21 ± 2% | 7.54 |
| **MonoX** | 6.83 ± 1% | 6.38 ± 9% | 6.96 ± 8% | 6.83 ± 7% | 6.18 ± 3% | 8.21 |
| **Mannan** | | | | | | |
| **CD-1** | 6.17 ± 0% | 5.48 ± 3% | 5.97 ± 9% | 6.69 ± 0% * | 6.18 ± 7% | -- |
| **CD-4** | 6.06 ± 2% | 5.54 ± 3% | 5.87 ± 7% | 6.23 ± 6% | 6.36 ± 7% | -- |
| **CD-6** | 3.95 ± 3% | 3.48 ± 0% * | 3.61 ± 11% | <LOQ | <LOQ | -- |
| **CD-168** | 5.40 ± 0% | 5.17 ± 0% * | 4.92 ± 13% | 5.89 ± 3% | 5.87 ± 0% * | 5.03 |
| **MonoX** | 5.98 ± 1% | 5.01 ± 18% | 5.92 ± 8% | 6.48 ± 5% | 6.40 ± 8% | 6.45 |

Compared to the previously discussed sugars, the proportion of the last two sugars was less than 1 m%. These two sugars were also only available from CA and TUW and shown in Figure 74 for arabinose and in Figure 75 for galactose. For TUG, the results were below the limit of detection (<LOD), which means that the values obtained were statistically not usable for qualitative or quantitative statements. The LOD for the RID was 0.8 m% for arabinose and 2.0 m% for galactose. For the PAD system, these limits were 0.9 m% for arabinose and 1.3 m% for galactose. Therefore, these two sugars were not available for TUG in the following Figure 74 & Figure 75.

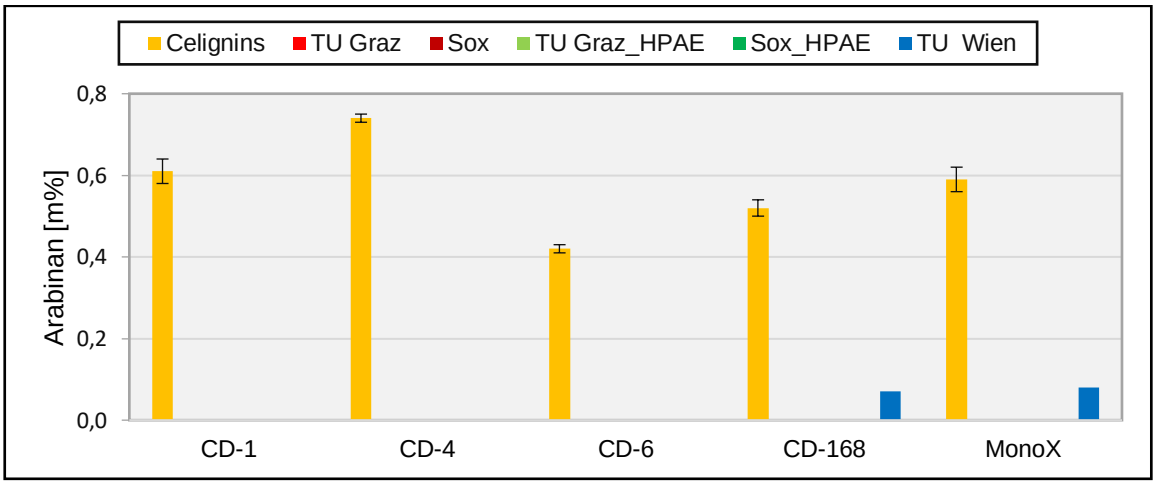


*Figure 74_Comparison of the monosaccharide arabinose between CA and TUW; results for TUG are for all samples <LOD*

The comparison of the last two monosaccharides shows that CA achieves the highest sugar concentrations with standard deviations. The results from TUW showed sugar concentrations below 0.1 m% for arabinose and 0.05 m% for galactose.

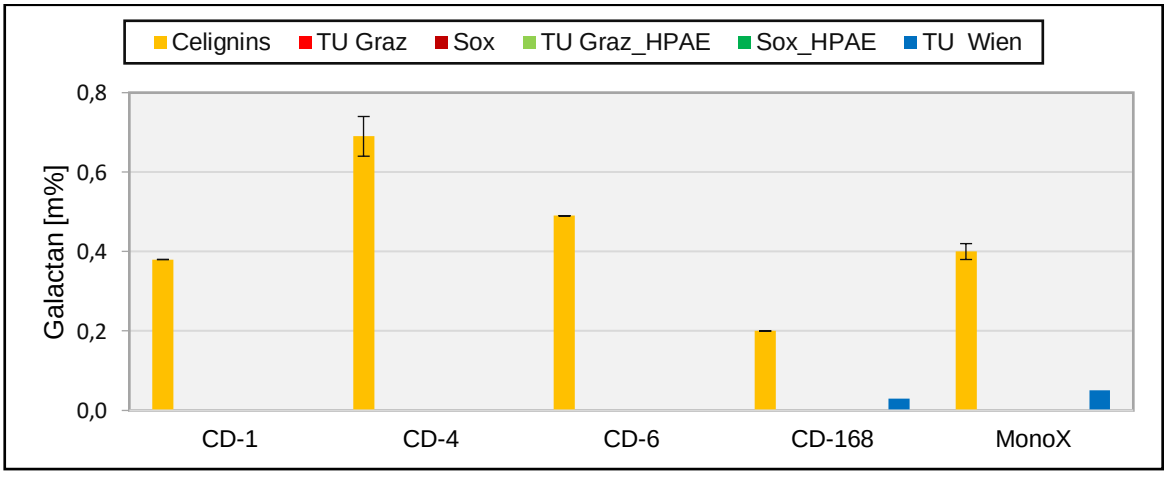


*Figure 75_Comparison of the monosaccharide galactose between CA and TUW; results for TUG are for all samples <LOD*

The determined concentrations of these five monosaccharides could be added together to determine the total sugar content. This sum was plotted for all laboratories in the next figure 75. Since cellulose is the main building block for plant-based structures, glucose made up the largest part of this sum. As a result, the sum behaved like that of glucose. The non-extracted form always leads to a lower average concentration. The PAD system, especially in extracted form, achieved the highest concentrations for all samples except CD-168. The results of CA were always in the middle between the results of the two sample forms (extracted and non-extracted). For TUW, the result of 90.5 m% for CD-168 are below the mean (94 m%) and for MonoX the biggest total sugar concentration of 98.4 m% was achieved. A sugar sum between 87 and 96 m% (Δ= 9 m%) was determined for MonoX. Values between 92 and 96 m% (Δ= 4 m%) were given for CD-168 and between 65 and 72 m% (Δ= 7 m%) for CD-6. Concentrations between 77 and 84 m% (Δ= 7 m%) were determined for CD-4 and between 85 and 94 m% (Δ= 9 m%) for CD-1.

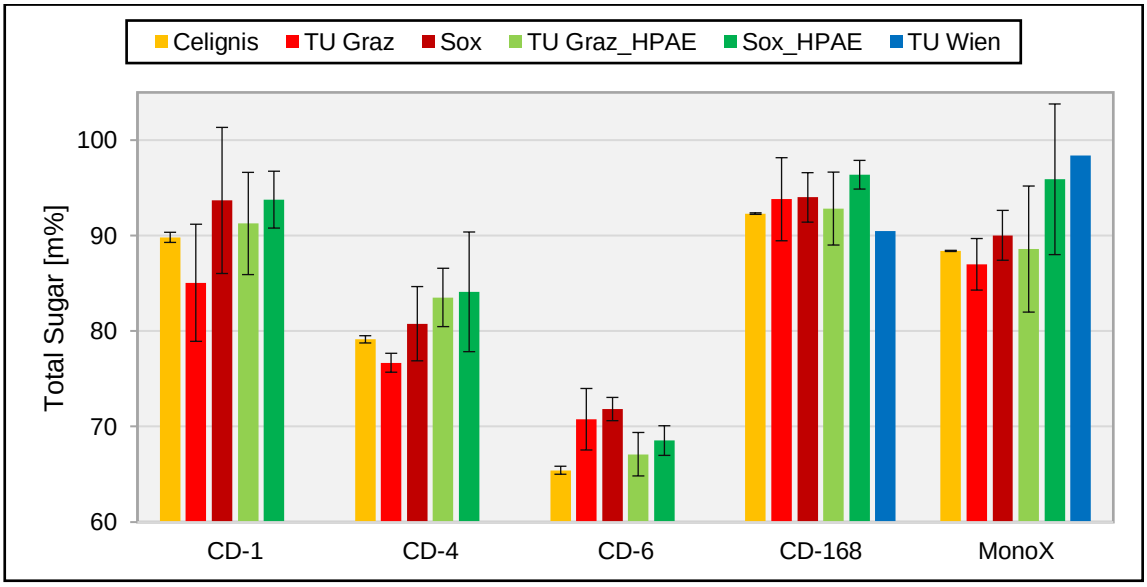


*Figure 76_Comparison of the sum of all monosaccharides between all participating laboratories and sample configurations*

Table 21 shows the previously recorded results in numbers.

A comparison of the fivefold determination carried out for MonoX (section 3.5.3) shows that the values determined for this pseudo-round robin lie within the carbohydrate range determined for the independent reproducibility test (89.6 m% ± 3.6% (RID) & 93.7 m% ± 8.7% (PAD)) and the dependent reproducibility test (89.9 m% ± 2.9% (RID) & 91.3 m% ± 2.3% (PAD)) (except of the result of TUW).

*Table 21_Summarized values for the monosaccharide arabinose, galactose and the sum of all sugars; the values are given as mean value in m% with their relative standard deviation (rel. SD) in %*

| | Celignis | TUG | Sox | TUG_HPAE | Sox_HPAE | TUW |
|---|---|---|---|---|---|---|
| **Arabinan** | $\bar{X}$ [m%] ± rel.SD | $\bar{X}$ [m%] ± rel.SD | $\bar{X}$ [m%] ± rel.SD | $\bar{X}$ [m%] ± rel.SD | $\bar{X}$ [m%] ± rel.SD | $\bar{X}$ [m%] |
| **CD-1** | 0.61 ± 5% | <LOD | <LOD | <LOD | <LOD | -- |
| **CD-4** | 0.74 ± 1% | <LOD | <LOD | <LOD | <LOD | -- |
| **CD-6** | 0.42 ± 2% | <LOD | <LOD | <LOD | <LOD | -- |
| **CD-168** | 0.52 ± 4% | <LOD | <LOD | <LOD | <LOD | 0.07 |
| **MonoX** | 0.59 ± 5% | <LOD | <LOD | <LOD | <LOD | 0.08 |
| **Galactan** | | | | | | |
| **CD-1** | 0.38 ± 0% | <LOD | <LOD | <LOD | <LOD | -- |
| **CD-4** | 0.69 ± 7% | <LOD | <LOD | <LOD | <LOD | -- |
| **CD-6** | 0.49 ± 0% | <LOD | <LOD | <LOD | <LOD | -- |
| **CD-168** | 0.20 ± 0% | <LOD | <LOD | <LOD | <LOD | 0.03 |
| **MonoX** | 0.40 ± 5% | <LOD | <LOD | <LOD | <LOD | 0.05 |
| **Sum Sugar** | | | | | | |
| **CD-1** | 89.8 ± 1% | 85.1 ± 7% | 93.7 ± 8% | 91.3 ± 6% | 93.8 ± 3% | -- |
| **CD-4** | 79.1 ± 0% | 76.7 ± 1% | 80.8 ± 5% | 83.5 ± 4% | 84.1 ± 7% | -- |
| **CD-6** | 65.4 ± 1% | 70.8 ± 5% | 71.8 ± 2% | 67.1 ± 3% | 68.5 ± 2% | -- |
| **CD-168** | 92.3 ± 0% | 93.8 ± 5% | 94.0 ± 3% | 92.8 ± 4% | 96.4 ± 2% | 90.5 |
| **MonoX** | 88.4 ± 0% | 87.0 ± 3% | 90.0 ± 3% | 88.6 ± 7% | 95.9 ± 8% | 98.4 |

### 3.7.5. Sum of Matter

The final sum of matter was defined as the sum of extractables, ash content, total lignin and total sugar. The error calculation was performed in the same way, resulting in a summation error.

The final results are shown in Figure 77 and Table 22. A first observation leads to the fact that the main compound glucose dominates the characteristics and trends of the final results. The mean values of the total mass were between 93 and 108 m% (without TUW between 93 and 102 m%). As already mentioned for the carbohydrates, extraction led to higher values than non-extraction. While a similar mean value could be calculated for CD-168 and MonoX. Since the error was calculated as the sum of the four compounds, the carbohydrates, especially glucose, had the greatest influence on the error. Since CA has the smallest relative SDs overall (<1.1 %), the smallest SDs were also achieved by CA in this section. This led to a total substance content for the MonoX sample of 102 m% with a deviation of 0.7% for CA. TUW achieved the maximum substance value for the same sample with 108 m%, followed by Sox_HPAE with 103 m%. The high values and deviations of the HPAE system result, as discussed, from the detector properties and additional sample preparations.

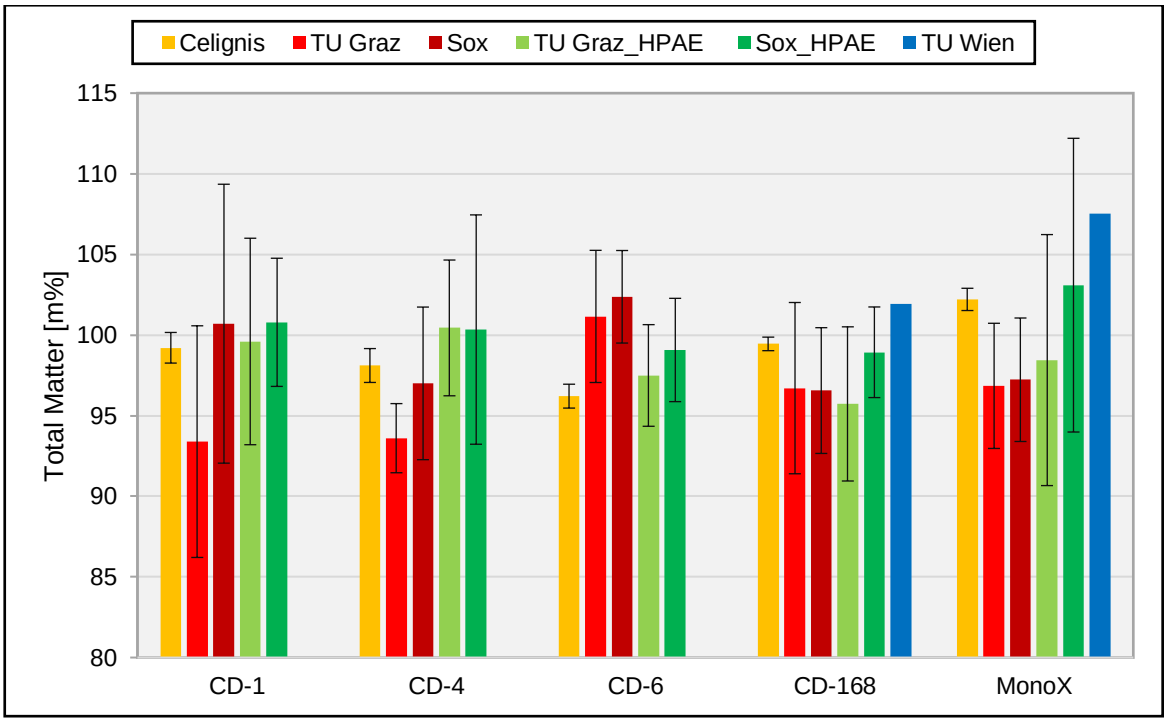


*Figure 77_Comparison of total matter content between different laboratories and sample forms; the mean values and errors are calculated as sum of the four different determined fraction mean and error values*

The mean values of the five results were 98.7 m% for CD-1, 97.9 m% for CD-4, 99.3 m% for CD-6, 97.5 m% for CD-168 and 99.6 m% for MonoX (excluding TUW), which was close to the 100 m% mark. The following Table 22 also shows that the PAD system exceeds the 5% deviation limit four times compared to the RID system (for both CD-1 forms and once for CD-168 non-extracted).

*Table 22_Summarized values for the calculated total matter; the values are given as mean value in m% with their relative standard deviation (rel. SD) in %*

| | Celignis | TUG | Sox | TUG_HPAE | Sox_HPAE | TUW |
|---|---|---|---|---|---|---|
| **Total Matter** | $\bar{X}$ [m%] ± rel.SD | $\bar{X}$ [m%] ± rel.SD | $\bar{X}$ [m%] ± rel.SD | $\bar{X}$ [m%] ± rel.SD | $\bar{X}$ [m%] ± rel.SD | $\bar{X}$ [m%] |
| **CD-1** | 99.2 ± 1.0% | 93.4 ± 7.7% | 101 ± 8.6% | 99.6 ± 6.4% | 101 ± 3.9% | -- |
| **CD-4** | 98.1 ± 1.1% | 93.6 ± 2.3% | 97.0 ± 4.9% | 100 ± 4.2% | 100 ± 7.1% | -- |
| **CD-6** | 96.2 ± 0.8% | 101 ± 4.1% | 102 ± 2.8% | 97.5 ± 3.2% | 99.1 ± 3.2% | -- |
| **CD-168** | 99.5 ± 0.4% | 96.7 ± 5.5% | 96.6 ± 4.0% | 95.7 ± 5.0% | 98.9 ± 2.8% | 102 |
| **MonoX** | 102 ± 0.7% | 96.8 ± 4.0% | 97.2 ± 3.9% | 98.4 ± 7.9% | 103 ± 8.8% | 108 |

All TUG measurements showed so far were measured independently of each other, i.e., they are measured on two different days (double determination). This measurement method makes it possible to recognize system errors in the determination system. In the following Figure 78 and Table 23, the lignin and carbohydrate determinations for the MonoX sample were carried out consecutively on one day (dependent & double determination). The results obtained were compared with CA. The values for extractives and ash content were unchanged. By performing the dependent determination, the values for sugar could be reduced from 90.0 m% ± 2.9% to 89.9 ± 2.4%. The total lignin content was changed from 7.0 m% ± 17% to 7.0 m% ± 5.2%. This results in a total substance value of 99.8 m% ± 2.5% (dependent) compared to 97.2 m% ± 3.9% (independent). As explained in sections 3.4.3 & 3.5.3, a dependent determination leads to results with a lower deviation but makes the measurement more susceptible to systematic errors.

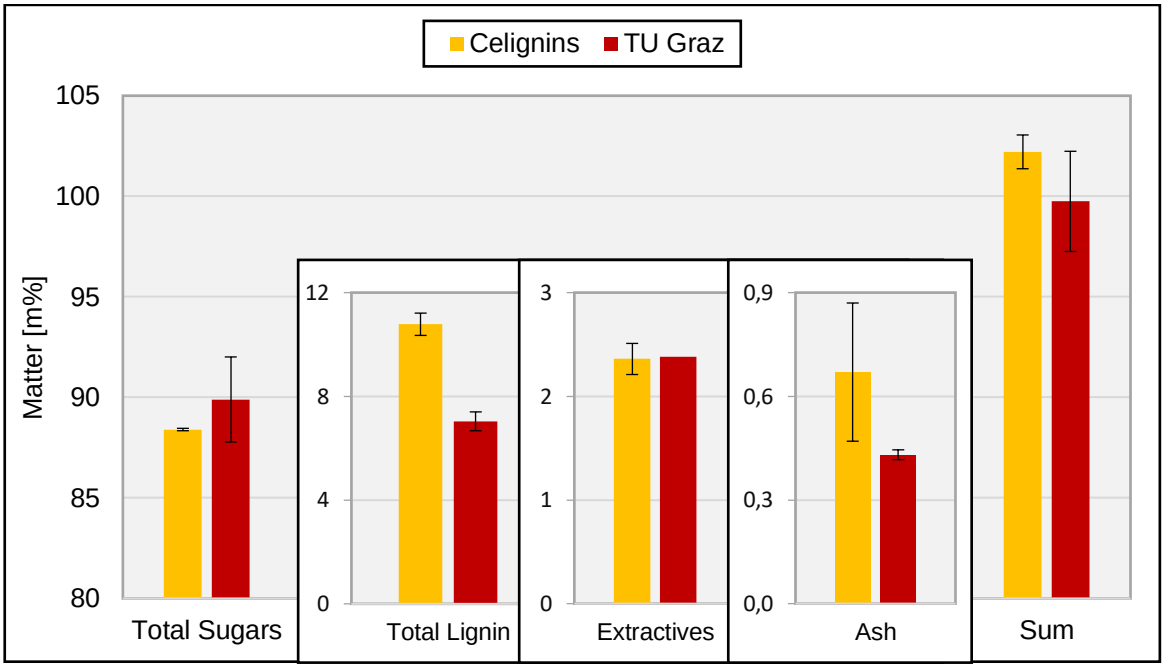


*Figure 78_Comparison between Celignis Analytical and a dependent TU Graz measurement using the HPLC-RID system*

*Table 23_ Comparison between Celignis Analytical and a dependent TU Graz measurement using the HPLC-RID system; mean and SD values are given in m%, while relative SDs are given in % in the brackets; extractables for TUG could only perform once due to time reasons*

| | Celignis Analytical [m%] | TU Graz (Sox & RID) [m%] |
|---|---|---|
| **Total Sugar** | 88.40 ± 0.06 (0.1%) | 89.90 ± 2.11 (2.4%) |
| **Total Lignin** | 10.78 ± 0.43 (4.0%) | 7.04 ± 0.36 (5.2%) |
| **Extractives** | 2.36 ± 0.15 (6.4%) | 2.38 |
| **Ash Content** | 0.67 ± 0.20 (29.9%) | 0.43 ± 0.01 (3.3%) |
| **Sum of Matter** | **102.21 ± 0.84 (0.8%)** | **99.75 ± 2.49 (2.5%)** |

### 3.7.6. Summary -Biomass Analysis Comparison

In this section, a comparison of biomass analysis was discussed (Pseudo Robin Ring (PRR) test), where each sample was measured in duplicate and according to NREL. This PRR was performed between four laboratories: Graz University of Technology (TUG) (twice; RID and PAD), Vienna University of Technology (TUW) and Celignis Analytical (CA). Five lignocellulose samples were selected for comparison. These were CD-1 and CD-4, both kraft paper, CD-6, a recycled paper, CD-168, a fully bleached paper, and MonoX, a pulp sample.

The comparison of the extractables between CA and TUG leads to the conclusion that an ASE system could achieve up to 2 m% more efficient extraction of the raw samples. This applies to recycled papers such as CD-6.

Similar behavior was observed for the ash content, with CA achieving the highest value of ash content (difference between 0.2 and 1.1 m%). It was also found that the ash content was always lower for the extracted samples than for the non-extracted samples.

Different results were obtained when determining the lignin content. Firstly, the acid-insoluble (Klason) lignin, whereby strongly fluctuating values were determined for CD-6, CD-168 and MonoX. Similar mean values with standard deviation were available for CD-1 and CD-4. The greatest fluctuations were found for sample CD-168, the fully bleached paper. Values between 0.74 and 11.08 m% were published. A uniformly lower concentration range was used for the acid-soluble lignin (<1.2 m%). Most published results were also between 0.6 and 1.2 m%, except for CD-168 (0.4 and 0.7 m%). The calculated sum of these two lignin fractions gives the total lignin content. Since the Klason lignin makes up the larger proportion, it had a greater influence on the total lignin result in mean value and standard deviation. As a result, the total lignin content behaves like the Klason lignin content. In addition to the NREL LAP 42618-compliant lignin determination, a kappa number determination was carried out. Using a rule of thumb, the total lignin content was converted into Kappa Calc. A comparison between Kappa Calc and Kappa Exp leads to the result that in 11 out of 15 cases the total lignin determination with NREL was overestimated. On the other hand, agreement between Kappa Exp and Kappa Calc could only be achieved 4 times. This result leads to the conclusion that, if possible, a kappa number determination was a useful addition to the lignin determination and for checking the accuracy of the results.

In accordance with NREL LAP 42618, five monosaccharides were determined for the five lignocellulose samples. Since cellulose was the main building block of these biomass samples and cellulose was a polymer of glucose monomers, the majority determined

was glucose (52 (CD-6) to 85 m% (CD-168)). The second most abundant monosaccharide was xylose (6 (CD-4) to 9 m% (CD-6)), followed by mannose (3 (CD-6) to 7 m% (CD-1)). Arabinose and galactose (<1 m%) could only be found quantitatively at CA and TUW. At TUG, these two sugars were below the LOD. In 3 out of 4 cases, the extracted sample showed a higher sugar content, between 0.2 m% and 8.6 m%. As with the lignin determination, the smallest deviations were also achieved with CA. Furthermore, in 4 out of 5 samples (except CD-6), CA yielded results that were between the results of the extracted and non-extracted determinations of the RID system. The PAD system always achieved higher results (except for CD-6) than the RID system. The TUW, on the other hand, was commissioned to analyze only CD-168 and MonoX. For total sugar content, the lowest sugar concentration (90 m%) was obtained for CD-168, while the highest sugar concentration (98 m%) was obtained for MonoX. A final comparison of MonoX with the reproducibility tests from section 3.4.3 shows that all results are within the independent (89.6 m% ± 3.6% (RID) & 93.7 m% ± 8.7% (PAD)) and dependent reproducibility test results (89.9 m% ± 2.9% (RID) & 91.3 m% ± 2.3% (PAD)) (except for the TUW result).

The final sum of matter was defined as the sum of the extractables, ash content, total lignin, and total sugar. The error calculation was performed in the same way, resulting in a summation error. Since cellulose is the main compound of these five samples, the main compound glucose dominates the characteristics and trends of the final results. The mean values of the total mass are between 93 and 108 m%, without TUW between 93 and 102 m%. The mean values of the five results were 98.7 m% for CD-1, 97.9 m% for CD-4, 99.3 m% for CD-6, 98.2 m% for CD-168 and 100.9 m% for MonoX, which was close to the 100 m% mark. Since the TUG duplicate determinations were carried out independently to recognize system errors, a dependent duplicate determination was also carried out. This resulted in lower deviations and a value closer to the 100 m% mark, which explained the low deviations of CA, but also their results for MonoX.

## 3.8. CASA Method

This L-cysteine-assisted sulfuric acid dissolution method (CASA) for lignocellulosic samples was first described by Lu et al. in 2021 and is a possible analytical method for lignin in solution. It uses a 0.1 g/ml L-cysteine stock solution in 72 % sulfuric acid (CASA reagent) to completely dissolve a lignocellulosic sample within several hours. The resulting liquid was then diluted 1:50 or 1:100 with deionized water and measured using UV/Vis spectroscopy (283 nm). This method contains several information that could facilitate the determination of biomass (according to NREL).

Firstly, this method provides information about the dissolution behavior of a sample over time and whether dissolution was possible. The second piece of information that this method provides concerns the carbohydrates. It had been observed that different carbohydrates give a different color. There were also two time points for qualitative sugar determination. The first time point was within 30 minutes, which indicates the easily accessible sugar, while the dominant sugar was observed after 60 minutes. The determination of carbohydrates (CHs) was limited by the lignin content of the samples. A lignin content of more than 6 m% only leads to a brownish color and only allows the estimation of the dominant sugar. This leads to the last available information of the qualitative lignin content. This was determined at 283 nm using UV/Vis spectroscopy.

### 3.8.1. Quick Test for CHs

The five monosaccharides used react with the L-cysteine/sulfuric acid solution in such a way that a specific color could be observed by eye. This observation could be used to qualitatively determine the easily accessible sugar (early phase) and the dominant sugar (late phase). The easily accessible sugar could only be determined within the first 30 minutes (early phase). After this time, the dominant sugar (sugar with the highest abundance in the sample) takes the upper hand in the solution and overlaps the colors of the easily accessible sugar. The dominant sugar was observed for >60 minutes (late phase). After 3 hours, the samples turned dark, and no further color change could be observed. Figure 79 below shows this color reaction for the five monosaccharides. As already mentioned, the determination could so far only be carried out with human eye and camera, as a dilution with deionized water only resulted in a colorless to yellow solution. This leads to the conclusion that the color was only stable in a strongly acidic environment in the presence of the amino acid L-cysteine. No color could be achieved using only 72% sulfuric acid solution.


*Figure 79_Time evolution of the monosaccharides in a CASA solution showing their specific color reaction; the first three figures (t= 0 to 30 min) are used for determination of the easily accessible, the last two figures (t= 120 min & 720 hours) are used to determine the dominant sugar*

Figure 79 shows that arabinose produces a yellow to orange color in the early phase and a pink color in the late phase. Galactose produced a violet color in the early phase and a dark pink color in the late phase. Glucose only produces blue colors, while mannose only produces violet colors. Xylose produces an orange color in the early stage and an

intense red color in the late stage. After 5 hours, the remaining colors overlap and form dark colors.

On the other hand, attention had to be paid to the lignin content. A total lignin content of >6 m% led to brownish colors. This behavior was shown in Figure 80, in which two spruce samples and a MonoX sample were subjected to a CASA run. The Klason lignin sample from spruce shows the typical brownish color. An extracted MonoX sample achieved a brownish color via a yellow path, while the extracted spruce sample became reddish brown via a xylene-like path.

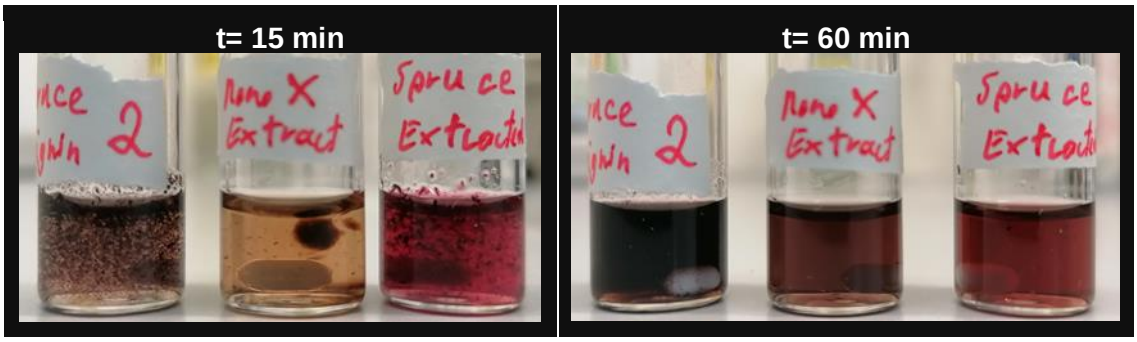


*Figure 80_Sample of how the total lignin interferes with the color reaction of the carbohydrates; shown from left to right, spruce Klason lignin fraction, MonoX (extracted) and a spruce sample (extracted)*

From these conclusions, a sample with a total lignin content of more than 6 m% shows a brownish color, while a sample with < 6 m% shows a carbohydrate color reaction. To demonstrate these results, several samples were prepared and used to prove these conclusions in Figure 81. The samples were from left to right: CD-168, CD-6, CD-4, CD-1, white granulated sugar (WZ) and analytical starch. The last sample was a blank sample (CASA solution only). A first qualitative observation could be made after 15 minutes. Samples CD-1 to CD-6 must had a total lignin content of >6 m%, while the others contain less to no lignin. After 30 minutes it became clear that WZ contains glucose (as WZ was sucrose, a disaccharide structure of glucose and fructose in a 1:1 ratio, the yellow color at minute 15 could be due to fructose). In the late stage of the determination (>60 minutes), the CD samples turned dark brown with bluish spots, with the exception of CD-168, which reaches a blue to violet color (glucose and xylose). WZ and starch turned blue, and the blank sample remains transparent. After 210 minutes reaction time, all samples turned dark with blue spots, as more than 50 m% consist only of glucose.

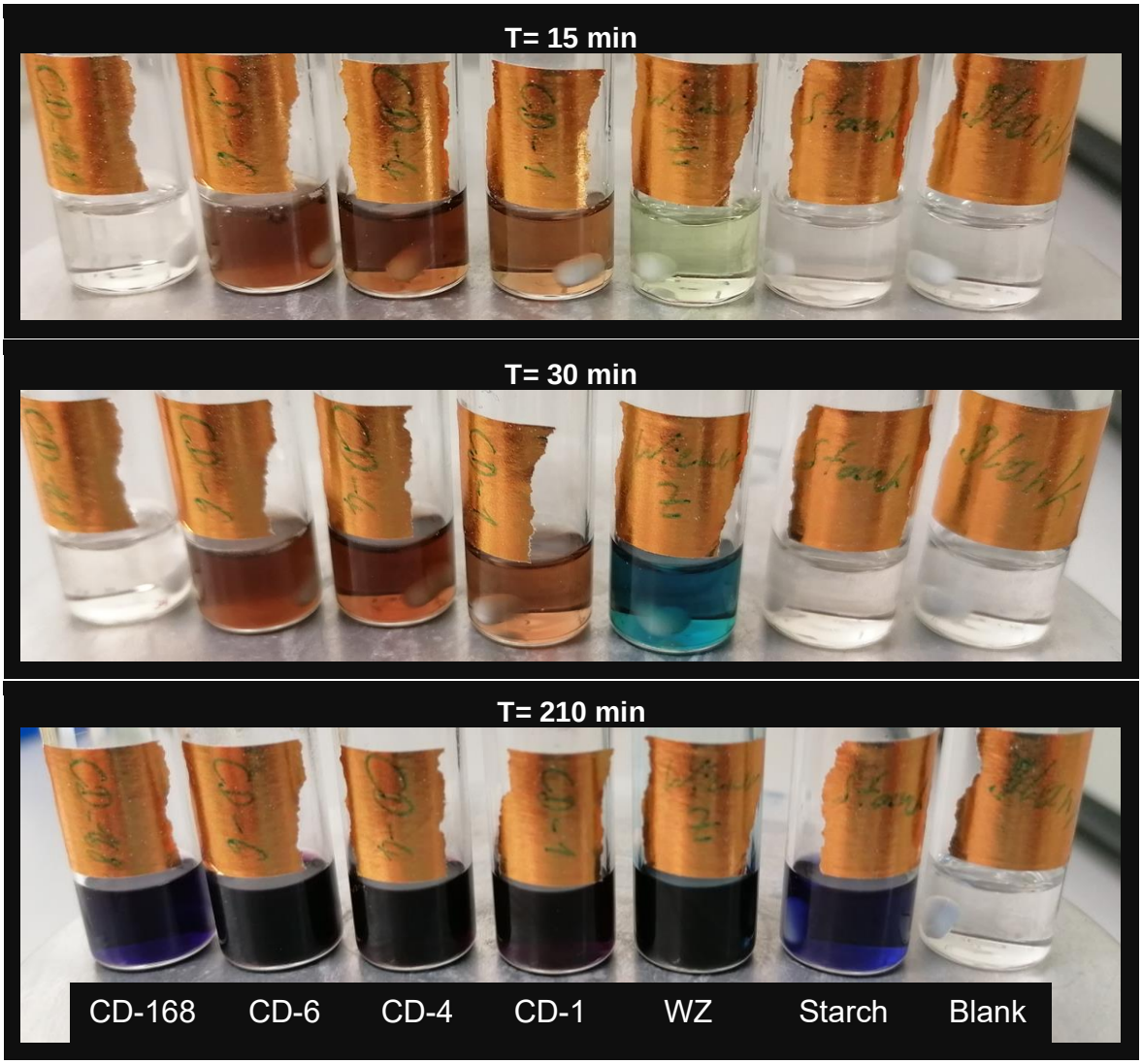


*Figure 81_Time evolution of six different samples; from left to right, CD-168, CD-6, CD-4, CD-1, white crystal sugar (WZ) and analytical grade starch*

In addition, color theory must be applied to some samples. Figure 82 shows two different maize stalk samples as an example of the application of color theory. At the beginning (<5 min) the sugars xylose and arabinose could be estimated. Over time, xylose dominates the early phase, as indicated by the intense red color at minute 15. In the late phase (210 minutes), the sample turned dark, with a different color being observed for the two samples. The young corn sample has developed a purple color, while the old corn sample has a red color. These two samples were analyzed for their carbohydrate content in accordance with NREL LAP 42618. The results showed a sugar composition of 36.4 m% glucose, 40.4 m% xylose and 4.0 m% arabinose for the young maize stalk. The composition of the old maize stalk sample was 36.9 m% glucose, 43.2 m% xylose and 4.3 m% arabinose. This ratio of glucose and xylose could be qualitatively predicted from the color development. The red color of the old maize sample indicates a higher

proportion of xylose than glucose. The purple color of the young maize sample is a color-theoretical result of a superposition of red and blue color.

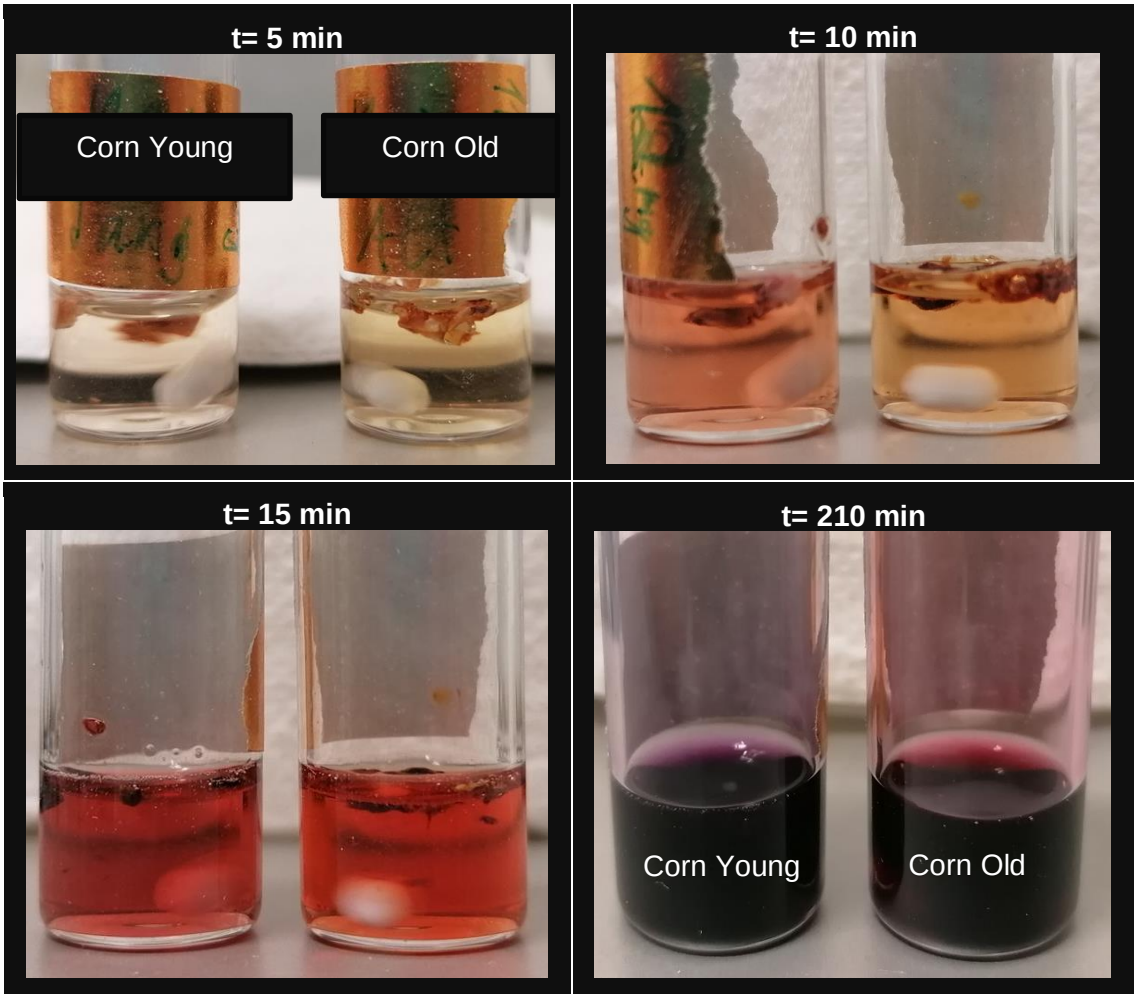


*Figure 82_Time evolution of two different corn stalk samples; left a sample of young corn stalk (Glucose: 36.4 ± 1.1 m%; Xylose: 40.4 ± 4.7 m%; Arabinose: 4.0 ± 0.0 m%) and on the right a sample of corn stalk after the harvest (Glucose: 36.9 ± 0.2 m%; Xylose 43.2 ± 0.4 m%; Arabinose: 4.3 ± 0.28 m%)*

Ultimately, this test method for qualitative carbohydrate determination was only an estimate, which depends primarily on the user's visual device (eye and/or camera) and the time of color observation. In addition, only five sugars were tested for their color reaction in this L-cysteine/sulfuric acid environment.

### 3.8.2. Estimation & Determination of Lignin

As this method was initially developed as an analytical method for lignin determination, this potential was also being examined. The CASA method for lignin determination was currently still a simple estimation test, as no absorption coefficients were available for quantitative determination. A simple check of the acid-soluble lignin content was carried out between NREL LAP and CASA using the previously used paper samples from the round robin test. Table 24 showed the results of the determination of the acid-soluble lignin according to NREL. As explained in section 3.4.2. Acid Soluble Lignin, some samples had a falsely higher acid-soluble lignin content due to furan derivative interactions. This applies especially to the refined white crystalline sugar (WZ), which had an measured acid-soluble lignin content between 3 and 9 m%, while no Klason lignin could be determined.

*Table 24_Results of the acid soluble lignin determination for the CD samples as well as analytical grade starch (ST) and commercial white crystalline sugar (WZ) according to NREL LAP*

| Sample | Acid Soluble Lignin Content [m%] | | Klason Lignin Content [m%] |
|---|---|---|---|
| | λ = 205 nm | λ = 240 nm | |
| **Starch (ST)** | 0.27 ± 0.04 | 0.85 ± 0.14 | -0.49 ± 0.23 |
| **CD-1** | 0.70 ± 0.06 | 2.58 ± 0.10 | 3.98 ± 0.92 |
| **CD-4** | 0.81 ± 0.09 | 2.73 ± 0.10 | 10.93 ± 0.69 |
| **CD-6** | 1.00 ± 0.16 | 2.98 ± 0.30 | 13.40 ± 0.86 |
| **CD-168** | 0.55 ± 0.02 | 2.19 ± 0.06 | 0.74 ± 1.17 |
| **White Sugar (WZ)** | 3.27 ± 0.14 | 8.59 ± 0.44 | 0.00 ± 0.92 |

Figure 83 shows the spectrum of the samples listed in Table 24. The wavelength for the determination was 283 nm (vertical red line) and the dilution for the samples is 1:50, except for WZ with 1:100. The peak for lignin was marked by an orange-colored line. The presents of lignin was proportional to the area enclosed by the orange line and the sample curve. A lignin content <1 m% was estimated for samples ST and CD-168. The samples were sorted according to decreasing lignin content, starting with CD-6 with the highest lignin content via CD-4 to CD-1 with the lowest lignin content. No lignin peak could be observed for WZ at a wavelength of 283 nm. The dilution factor of 1:100 was

also twice as strong as for all other samples. An unclassifiable peak could be observed at 314 nm for WZ.

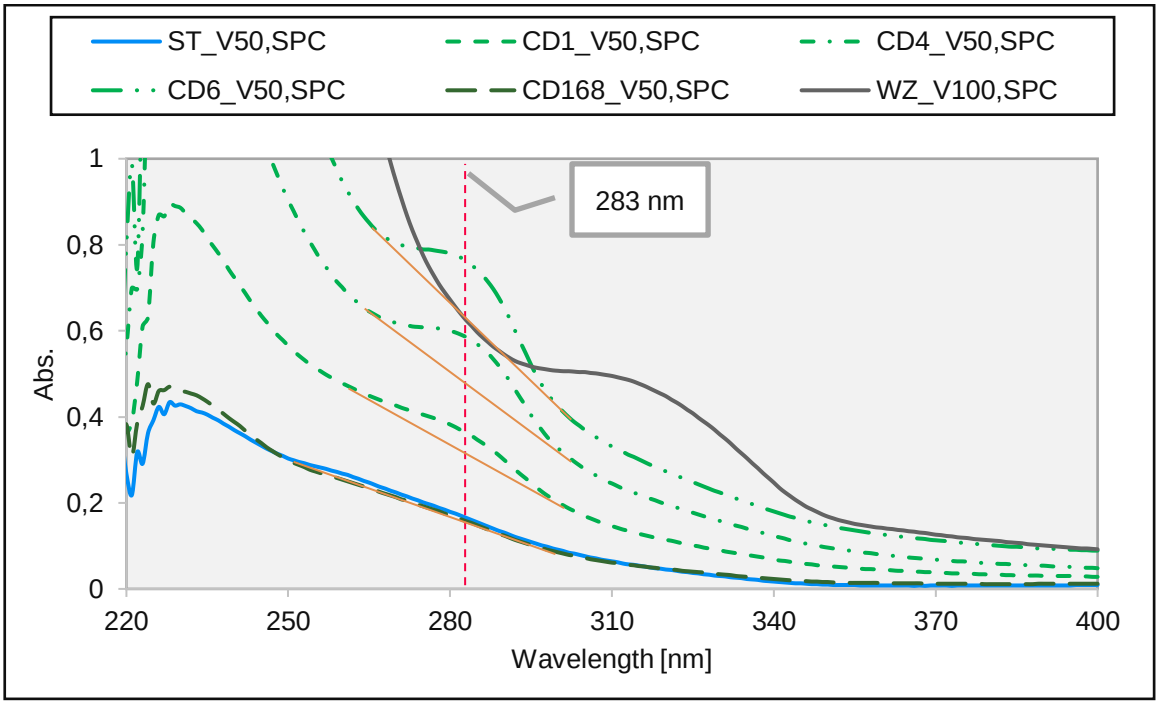


*Figure 83_UV/Vis spectrum of CD samples used in Round Robin test as well as analytical grade starch (ST) and commercial white crystalline sugar (WZ); dilution of all samples is 1:50 except of WZ witch is 1:100*

To summarize, it could be said that the CASA method for lignin determination was suitable for estimating and comparing samples. However, a quantitative determination of the total lignin content was not possible.

To carry out a possible quantitative determination of lignin, a simple spruce sample was analyzed according to the NREL LAPs. The Klason lignin obtained was used for this determination method experiment. A certain amount (10 mg per 1 ml CASA reagent) of spruce Klason lignin was weighed and dissolved with CASA reagent. After three days of stirring at room temperature, this lignin sample was completely dissolved. Using this solution, a dilution series (12-point) was prepared for calibration. The concentration for this calibration was between 1 mg/l and 100 mg/l. Figure 84 shows the calibration spectrum of a 12-point calibration. This spectrum clearly showed that the saturation effect sets in beginning at 100 mg/l solution. This was indicated by the non-linear increase in the absorbance value.

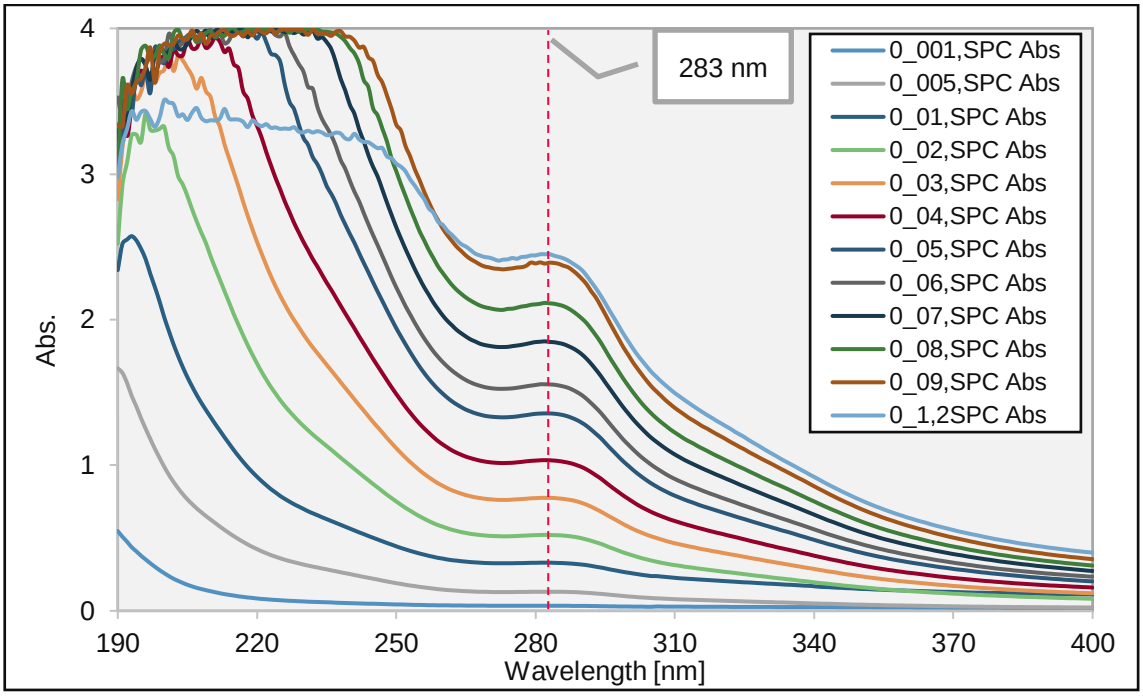


*Figure 84_Calibration spectrum of the dilution series between 1 and 100 mg/l of a spruce Klason lignin in CASA solution; for the 100 mg/l measurement the effects of saturation kicks in*

This linear increase was shown in Figure 85. In this Figure 85, the dilution series was plotted against the absorbance to obtain a linear relationship (linearity curve). The dilution point of 100 mg/l (0.1 g/l) had been removed from this graph as this point was affected by saturation effects and therefore cannot be used. By using Beer-Lambert law (Eq. (1)) on the linearity curve, an absorption coefficient $\varepsilon$ could be extracted from the slope for the spruce Klason lignin calibration line. With the absorption coefficient of 26.235 l/(g*cm) for spruce lignin, a quantitative lignin determination should be possible.

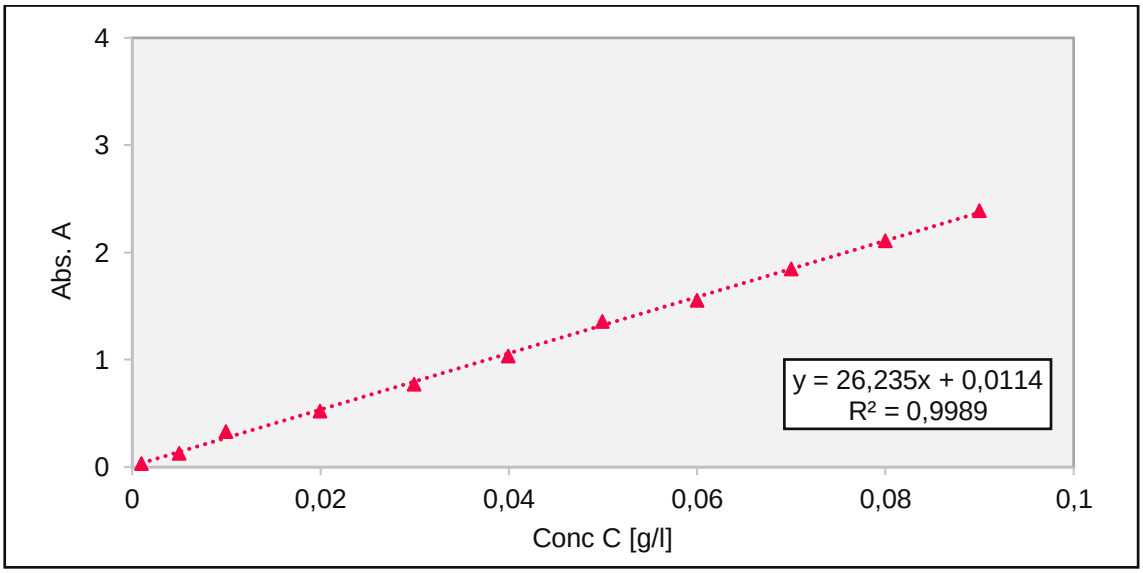


*Figure 85_Linearity plot of the spruce lignin calibration; the point of 100 mg/l (0.1 g/l) was removed*

To verify these results, a spruce sample was analyzed using the CASA method. Since the total lignin content was known by NREL LAP for this spruce sample, the total lignin content could be calculated. This calculated total lignin content (Conc Soll) was 3.6 mg for a 12 mg spruce sample containing 30 m% total lignin. In solution, this results in a lignin concentration of 3.6 g/l. Table 25 shows the result of this recovery test. The spruce solution was diluted 1:50 and 1:100 for UV/Vis spectroscopy. Using the Beer-Lambert law for quantification, an experimental concentration (Conc Ist) of 4.150 g/l was achieved for a 1:50 diluted measurement and 4.172 g/l for a 1:100 diluted solution. A recovery of 115.3 % (1:50) and 115.9 % (1:100) could be calculated for these two determinations.

*Table 25_Recovery test for total lignin content for a raw spruce sample using CASA method; the Soll concentration 3.6 g/l is achieved by 12 mg spruce (with 30 m% total lignin content) in 1 ml CASA reagent*

| Dilution | Abs | Conc [g/l] | | Recovery |
|---|---|---|---|---|
| | | Ist | Soll | |
| **LP50** | 2.178 | 4.150 | 3.6 | 115.3% |
| **LP100** | 1.095 | 4.172 | 3.6 | 115.9% |

The total lignin content determined was above 100 % for both measurements, which could be the acid-soluble lignin fraction that was not considered during dilution and calibration, as only the Klason lignin could be used for weighing. In addition, this test was carried out with a non-extracted spruce sample.

To summarize, it could be said that a quantitative determination using the CASA method was possible, but so far only represents a potential method that requires further research. This was mainly because the Beer-Lambert law is only valid under certain conditions. Examples of its limitations are a moderate analyte concentration (<0.01 M) and homogeneity in the solution as well as emission and absorption events of the analyte. Furthermore, this absorption coefficient was only applicable for the spruce wood sample used. As the lignin content varies from sample to sample, only an average coefficient could be determined for each sample.

### 3.8.3. Summary -CASA Method

This L-cysteine-assisted sulfuric acid dissolution method (CASA) for lignocellulosic samples was first described by Lu et al. in 2021 and is a potential analytical method for lignin in solution.

This method contains several information that could be useful for the determination of biomass (NREL). Firstly, this method provides information about the dissolution behavior of a sample over time and whether dissolution was possible. The second piece of information provided by this method concerns carbohydrates. It had been observed that different carbohydrates gave a different color. In addition, there were two time points for the qualitative sugar determination. The first time point was within 30 minutes (early phase), which indicates the easily accessible sugar, while the dominant sugar was observed after 60 minutes (late phase). This estimation of CHs was limited by the lignin content of the samples. A lignin content of >6 m% led to a brownish color and only allows the determination of the dominant sugar. This led to the last available information of the qualitative lignin content. This was determined using the dissolution method and at 283 nm using UV/Vis spectroscopy.

The carbohydrates were estimated optically by human eye and camera. In a first experiment, the five sugars used in NREL LAP42618 were treated with CASA reagent. The result of this experiment shows that a specific color could be observed for each monosaccharide. If several different sugars were present in similar quantities, the color theory must be applied (superimposition of red and blue to form violet).

Total lignin was estimated in a similar way, as visual interpretation by eye or camera allows an initial conclusion to be drawn as to whether the total lignin content was below or above 6 m%. A more precise distinction could be made using UV/Vis spectroscopy. As no absorption coefficients were currently available for this determination method, the CASA method for lignin determination was only suitable for estimation and relativization between samples. A quantitative determination of the total lignin content was not yet possible.

To attempt such a quantitative determination of total lignin, a spruce Klason lignin sample was weighed and dissolved within three days with stirring using CASA reagent. A dilution series of 12 points was prepared from this Klason lignin solution and used as a calibration to determine an absorption coefficient using Beer-Lambert law. The coefficient obtained was tested in a recovery experiment, in which a recovery of 115 to 116 % was achieved. The excess percentages could be acid soluble lignin as the calibration was based on

Klason lignin. To summarize, a quantitative determination with the CASA method was possible, but so far it was only a potential method that requires much more research. Furthermore, this absorption coefficient was only applicable to the spruce sample used here. As the lignin content varies from sample to sample, only an average coefficient could be determined, and that for each sample.

# 4. Summary & Conclusion

Results obtained by analyzing biomass were subject to natural variation due to its origin and inhomogeneous composition. The aim of this work was to test, optimize and expand current analysis methods. The basis for this work was NREL LAP 42618 - "Determination of structural carbohydrates and lignin". The sample pretreatments (NREL LAPs 42619 to 42622) were extended to include a centrifugal mill for greater sample homogeneity. The determination of lignin according to NREL LAP 42618 used for acid insoluble lignin a balancer and for acid soluble lignin UV/Vis spectroscopy. These two devices had an enormous potential for error due to their universal application. It was shown that the gravimetric determination of Klason lignin caused a falsely higher lignin content due to undissolved and insoluble sample components. Varying the digestion acid concentration from 72 % to 64 % led to a 17 m% increase in Klason lignin. The furan derivatives formed during hydrolysis complicate the UV/Vis spectroscopic determination of the acid-soluble lignin. The wavelengths 205 nm and 240 nm were the least affected. Carbohydrates were determined using two liquid chromatographs with different detectors (refractive index detector (RID) and pulsed Amperometric detector (PAD)). A comparison showed a better peak separation for the PAD system but requires dilutions. The RID system achieved weaker peak separation but better linearity and measures the sample liquids undiluted. As a result, the RID system was preferred for carbohydrate analysis.

A round robin test was carried out between Graz University of Technology (TUG), Vienna University of Technology (TUW) and Celignis Analytical (CA). The samples were CD-1 and CD-4, both kraft paper, CD-6, a recycled paper, CD-168, a fully bleached paper, and MonoX, a pulp sample. The comparison of the extractable substances showed that an accelerated solvent extraction system (CA) was able to extract up to 2 m% more compared to classic Soxhlet extraction (TUG). In terms of ash content, CA achieved the highest values for all samples.

Klason lignin was determined for CD-1 (3.98 to 5.17 m%), CD-4 (10.93 to 12.25 m%), CD-6 (10.79 to 13.40 m%), CD-168 (0.74 to 11.08 m%) and MonoX (3.94 to 10.09 m%). This shows, that Klason lignin determination was subject to large fluctuations and errors. Especially for low lignin samples such as CD-168. Acid-soluble lignin was determined between 0.6 and 1.2 m%, except for CD-168 (0.4 to 0.7 m%). A kappa number comparison led to the result that NREL showed a higher total lignin content of up to 6.47 m% in 11 out of 15 cases. The carbohydrate determination showed similar fluctuations and errors as for Klason lignin. Sugar content was found for CD-1 from 85.1 to 93.8 and CD-4 from 76.7 to 84.1 m%. For CD-6 from 65.4 to 71.8 m%, CD-168 from 90.5 to 96.4

m% and for MonoX from 87.0 to 98.4 m%. The monosaccharide arabinose and galactose (<1 m%) could only be quantitatively detected by CA and TUW. For TUG, these two sugars were below the detection limit. The averaged sum parameter was 98.7 m% for CD-1, 97.9 m% for CD-4, 99.3 m% for CD-6, 98.2 m% for CD-168 and 100.9 m% for MonoX, which was close to the 100 m% mark. Finally, the NREL LAB 42618 works for the lignocellulosic biomass samples used, but includes a reasonable error calculation with a standard deviation based on natural variations.

The L-cysteine-assisted sulfuric acid dissolution method (CASA), which was first described by Lu et al. 2021, was used as a possible lignin determination method. This method provided information about the presence of carbohydrates through different color reactions and dissolution behavior. A lignin content of >6 m% led to a brown color. A more precise distinction was made using UV/Vis spectroscopy. As no absorption coefficients were currently available, the CASA method was only suitable for estimation and relativization. To attempt a quantitative determination of total lignin, a spruce Klason lignin sample was dissolved and diluted. An absorption coefficient according to the Lambert-Beer law could be derived from a calibration curve. This achieved coefficient was tested in a recovery test. The results of this test showed satisfactory recovery rates of between 115 and 116%.

# Appendix

## a) List of Figures

## b) List of Tables

# References


[1] A. Sluiter, B. Hames, D. Hyman, C. Payne, R. Ruiz, C. Scarlata, J. Sluiter, D. Templeton, and and J. Wolfe: NREL. Determination of Total Solids in Biomass and Total Dissolved Solids in Liquid Process Samples: Laboratory Analytical Procedure (LAP).

[2] A. Sluiter, B. Hames, R. Ruiz, C. Scarlata, J. Sluiter, and and D. Templeton: NREL. Determination of Ash in Biomass: Laboratory Analytical Procedure (LAP); Issue Date: 7/17/2005.

[3] A. Sluiter, R. Ruiz, C. Scarlata, J. Sluiter, and and D. Templeton: NREL. Determination of Extractives in Biomass: Laboratory Analytical Procedure (LAP); Issue Date 7/17/2005.

[4] A. Sluiter, B. Hames, R. Ruiz, C. Scarlata, J. Sluiter, D. Templeton, and D. Crocker: NREL. Determination of Structural Carbohydrates and Lignin in Biomass: Laboratory Analytical Procedure (LAP) (Revised July 2011).

[5] H. R. Allcock, Frederick W. Lampe, and James E. Mark. 2003. *Contemporary polymer chemistry* (3rd ed.). Pearson Education/Prentice Hall, Upper Saddle River, N.J.

[6] Claudia Antonetti, Enrico Bonari, Domenico Licursi, Nicoletta Di Nassi O Nasso, and Anna M. Raspolli Galletti. 2015. Hydrothermal Conversion of Giant Reed to Furfural and Levulinic Acid: Optimization of the Process under Microwave Irradiation and Investigation of Distinctive Agronomic Parameters. *Molecules (Basel, Switzerland)* 20, 12, 21232–21253. DOI: https://doi.org/10.3390/molecules201219760.

[7] Michele Aresta, Ed. 2012. *Biorefinery*. *From biomass to chemicals and fuels*. De Gruyter textbook. de Gruyter, Berlin.

[8] B. Hames, R. Ruiz, C. Scarlata, A. Sluiter, J. Sluiter, and D. Templeton: NREL. Preparation of Samples for Compositional Analysis: Laboratory Analytical Procedure (LAP); Issue Date 08/08/2008.

[9] C. Barfoed. 1873. Ueber die Nachweisung des Traubenzuckers neben Dextrin und verwandten Krpern. *Fresenius, Zeitschrift f. anal. Chemie* 12, 1, 27–32. DOI: https://doi.org/10.1007/BF01462957.

[10] James A. Bassham, Andrew A. Benson, and Melvin Calvin. 1950. *The Path of Carbon in Photosynthesis VIII. The Role of MalicAcid. DOI: https://doi.org/*10.2172/910351.

[11] Stefan Beisl, Mathias Binder, Kurt Varmuza, Angela Miltner, and Anton Friedl. 2018. UV-Vis Spectroscopy and Chemometrics for the Monitoring of Organosolv

Pretreatments. *ChemEngineering* 2, 4, 45. DOI: https://doi.org/10.3390/chemengineering2040045.

[12] Nazmul H. Bhuiyan, Gopalan Selvaraj, Yangdou Wei, and John King. 2009. Role of lignification in plant defense. *Plant signaling & behavior* 4, 2, 158–159. DOI: https://doi.org/10.4161/psb.4.2.7688.

[13] M. Bial. 1903. Ueber die Diagnose der Pentosurie mit dem von mir angegebenen Reagens. *Dtsch med Wochenschr* 29, 27, 477–478. DOI: https://doi.org/10.1055/s-0028-1138555.

[14] Manfred Bial. 1902. Ueber den Werth des neuen (Bial'schen) Reagens für die Differentialdiagnose zwischen Diabetes und Pentosurie. *Dtsch med Wochenschr* 28, 37, 671–672. DOI: https://doi.org/10.1055/s-0028-1138936.

[15] Wout Boerjan, John Ralph, and Marie Baucher. 2003. Lignin biosynthesis. *Annual review of plant biology* 54, 519–546. DOI: https://doi.org/10.1146/annurev.arplant.54.031902.134938.

[16] Stu Borman. 1987. Eluent, Effluent, Eluate, and Eluite. *Anal. Chem.* 59, 2, 99A-99A. DOI: https://doi.org/10.1021/ac00129a735.

[17] Donald A. Bryant and Niels-Ulrik Frigaard. 2006. Prokaryotic photosynthesis and phototrophy illuminated. *Trends in microbiology* 14, 11, 488–496. DOI: https://doi.org/10.1016/j.tim.2006.09.001.

[18] H. F. Bunn and P. J. Higgins. 1981. Reaction of monosaccharides with proteins: possible evolutionary significance. *Science (New York, N.Y.)* 213, 4504, 222–224. DOI: https://doi.org/10.1126/science.12192669.

[19] Charles M. Cai, Taiying Zhang, Rajeev Kumar, and Charles E. Wyman. 2014. Integrated furfural production as a renewable fuel and chemical platform from lignocellulosic biomass. *J of Chemical Tech & Biotech* 89, 1, 2–10. DOI: https://doi.org/10.1002/jctb.4168.

[20] Karl Cammann. 2011. *Instrumentelle analytische Chemie*. *Verfahren, Anwendungen und Qualitätssicherung* (Nachdruck der 1. Aufl. 2001). Spektrum Lehrbuch. Spektrum Akademischer Verlag, Heidelberg.

[21] Carbohydrate analysis by high-performance anion-exchange chromatography with pulsed amperometric detection (HPAE-PAD).

[22] S. Chandrasekhar. 1953. Theoretical interpretation of the optical activity of quartz. *Proc. Indian Acad. Sci.* 37, 3, 468–484. DOI: https://doi.org/10.1007/BF03052667.

[23] Ke Chen and Phil S. Baran. 2009. Total synthesis of eudesmane terpenes by site-selective C-H oxidations. *Nature* 459, 7248, 824–828. DOI: https://doi.org/10.1038/nature08043.

[24] 2020. *Chlorzinkiod-Lösung, konz; Detail - Sanova GesmbH* (2020). Retrieved February 15, 2024 from https://www.morphisto.at/sanova-shop/detail/d/Chlorzinkiod-L%C3%B6sung_konz/.

[25] Gary D. ‡. a. Christian, Kevin ‡. a. Schug, and Purnendu K. Dasgupta. 2014. *Analytical chemistry* (Seventh edition). John Wiley and Sons, Incorporated, Hoboken, New Jersey.

[26] Jonathan Clayden, Nick Greeves, and Stuart G. Warren. 2012. *Organic chemistry* (Second edition). Oxford University Press, Oxford, New York.

[27] Beverly Cochran, Deborah Lunday, and Frank Miskevich. 2008. Kinetic Analysis of Amylase Using Quantitative Benedict's and Iodine Starch Reagents. *J. Chem. Educ.* 85, 3, 401. DOI: https://doi.org/10.1021/ed085p401.

[28] Peter M. Collins and Robert J. Ferrier. 1995. *Monosaccharides*. *Their chemistry and their roles in natural products*. Wiley, Chichester.

[29] M. M. Costa and J. L. Colodette. 2007. The impact of kappa number composition on eucalyptus kraft pulp bleachability. *Braz. J. Chem. Eng.* 24, 1, 61–71. DOI: https://doi.org/10.1590/S0104-66322007000100006.

[30] 2017. Determination of Furfural and Hydroxymethyl furfural by UV Spectroscopy in ethanol-water hydrolysate of Reed. *Journal of Bioresources and Bioproducts* 2, 4. DOI: https://doi.org/10.21967/jbb.v2i4.84.

[31] 2019. disaccharides. In *The IUPAC Compendium of Chemical Terminology*, Victor Gold, Ed. International Union of Pure and Applied Chemistry (IUPAC), Research Triangle Park, NC. DOI: https://doi.org/10.1351/goldbook.D01776.

[32] Fabian Ebner, Linda A. M. Gehre, and Claudia Tallian. 2017. *Naturstoffe und Biochemie*. Springer Fachmedien Wiesbaden, Wiesbaden.

[33] Anna Ebringerová, Zdenka Hromádková, and Thomas Heinze. 2005. Hemicellulose. In *Polysaccharides I*, Thomas Heinze, Ed. Advances in Polymer Science. Springer-Verlag, Berlin/Heidelberg, 1–67. DOI: https://doi.org/10.1007/b136816.

[34] Rachel Ehrenberg. 2018. What makes a tree a tree? *Knowable Mag. DOI: https://doi.org/*10.1146/knowable-033018-032602.

[35] Hans-Josef Endres and Andrea Siebert-Raths. 2009. *Technische Biopolymere*. *Rahmenbedingungen, Marktsituation, Herstellung, Aufbau und Eigenschaften*. Hanser, München.

[36] 1999. *Essentials of glycobiology*. Cold Spring Harbor Lab. Press, New York, NY.

[37] H. Fehling. 1849. Die quantitative Bestimmung von Zucker und Stärkmehl mittelst Kupfervitriol. *Ann. Chem. Pharm.* 72, 1, 106–113. DOI: https://doi.org/10.1002/jlac.18490720112.

[38] Dietrich Fengel and Gerd Wegener. 1989. *Wood*. *Chemistry, ultrastructure, reactions* (Pbk. ed.). Walter de Gruyter & Co, Berlin, New York.

[39] W. R. Fernell and H. K. King. 1953. The simultaneous determination of pentose and hexose in mixtures of sugars. *Analyst* 78, 923, 80. DOI: https://doi.org/10.1039/AN9537800080.

[40] Holger Fleischer. 2017. Fehlinterpretation der Fehling-Probe auf reduzierende Zucker – Von der Beobachtung im Chemieunterricht zur Evidenz gegen die Oxidation der Aldehydgruppe. *Chemkon* 24, 1, 27–30. DOI: https://doi.org/10.1002/ckon.201610283.

[41] Areski Flissi, Emma Ricart, Clémentine Campart, Mickael Chevalier, Yoann Dufresne, Juraj Michalik, Philippe Jacques, Christophe Flahaut, Frédérique Lisacek, Valérie Leclère, and Maude Pupin. 2020. Norine: update of the nonribosomal peptide resource. *Nucleic acids research* 48, D1, D465-D469. DOI: https://doi.org/10.1093/nar/gkz1000.

[42] Sabine L. Flitsch and Rein V. Ulijn. 2003. Sugars tied to the spot. *Nature* 421, 6920, 219–220. DOI: https://doi.org/10.1038/421219a.

[43] Francis A. Carey and Richard J. Sundberg. 2007. *Advanced Organic Chemistry; Part A: Structure and Mechanisms*. Springer US, Boston, MA.

[44] Jeanne W. George. 2001. The usefulness and limitations of hand-held refractometers in veterinary laboratory medicine: an historical and technical review. *Veterinary clinical pathology* 30, 4, 201–210. DOI: https://doi.org/10.1111/j.1939-165X.2001.tb00432.x.

[45] Lorna J. Gibson. 2012. The hierarchical structure and mechanics of plant materials. *Journal of the Royal Society, Interface* 9, 76, 2749–2766. DOI: https://doi.org/10.1098/rsif.2012.0341.

[46] Victor Gold, Ed. 2019. *The IUPAC Compendium of Chemical Terminology*. International Union of Pure and Applied Chemistry (IUPAC), Research Triangle Park, NC. DOI: https://doi.org/10.1351/goldbook.

[47] Bryan M. Ham and Aihui MaHam. 2016. *Analytical chemistry*. *A chemist and laboratory technician's toolkit*. Wiley, Hoboken, New Jersey.

[48] Henrik Hartmann and Susan Trumbore. 2016. Understanding the roles of nonstructural carbohydrates in forest trees - from what we can measure to what we want to know. *The New phytologist* 211, 2, 386–403. DOI: https://doi.org/10.1111/nph.13955.

[49] Karl Häusler and Heribert Rampf. 1982. *270 chemische Schulversuche mit Einführung in die Laborpraxis*. *10 Tabellen* (1. Aufl., [Nachdr.]). Oldenbourg, München.

[50] Thomas Heinze, Ed. 2005. *Polysaccharides I*. Advances in Polymer Science. Springer-Verlag, Berlin/Heidelberg. DOI: https://doi.org/10.1007/b136812.

[51] Gunnar Henriksson, Göran Gellerstedt, and Monica Ek, Eds. 2009. *Pulp and paper chemistry and technology*. de Gruyter, Berlin.

[52] Manfred Hesse, H. Meier, Bernd Zeeh, Stefan Bienz, Laurent Bigler, and Thomas Fox. 2012. *Spektroskopische Methoden in der organischen Chemie* (8. überarbeite und erweiterte Auflage). Georg Thieme Verlag, Stuttgart.

[53] Hans G. Hirschberg. 2014. *Handbuch Verfahrenstechnik und Anlagenbau*. *Chemie, Technik und Wirtschaftlichkeit* (Softcover reprint of the original 1st ed. 1999). Springer Berlin, Berlin.

[54] Thomas G. Hörner and Peter Klüfers. 2016. The Species of Fehling's Solution. *Eur J Inorg Chem* 2016, 12, 1798–1807. DOI: https://doi.org/10.1002/ejic.201600168.

[55] IMA. 2022. *The beer-lambert law - IMA* (2022). Retrieved February 15, 2024 from https://imamagnets.com/en/blog/the-beer-lambert-law/.

[56] Murray B. Isman. 2000. Plant essential oils for pest and disease management. *Crop Protection* 19, 8-10, 603–608. DOI: https://doi.org/10.1016/S0261-2194(00)00079-X.

[57] Jeffrey Rohrer. 2021. Carbohydrate analysis by high-performance anion-exchange chromatography with pulsed amperometric detection (HPAE-PAD). Technical Note.

[58] Antonia Johnston, Andrew T. Crombie, Myriam El Khawand, Leanne Sims, Gregg M. Whited, Terry J. McGenity, and J. Colin Murrell. 2017. Identification and characterisation of isoprene-degrading bacteria in an estuarine environment. *Environmental microbiology* 19, 9, 3526–3537. DOI: https://doi.org/10.1111/1462-2920.13842.

[59] Sven E. Jorgensen, Ed. 2008. *Encyclopedia of ecology* (1. ed.). Elsevier, Amsterdam.

[60] Rajan Katoch. 2011. *Analytical Techniques in Biochemistry and Molecular Biology*. Springer New York, New York, NY.

[61] P. R. B. Kozowyk, G. H. J. Langejans, and J. A. Poulis. 2016. Lap Shear and Impact Testing of Ochre and Beeswax in Experimental Middle Stone Age Compound Adhesives. *PloS one* 11, 3, e0150436. DOI: https://doi.org/10.1371/journal.pone.0150436.

[62] V. C. Kumari, Shashank M. Patil, Ramith Ramu, Prithvi S. Shirahatti, Naveen Kumar, B. P. Sowmya, Chukwuebuka Egbuna, Chukwuemelie Z. Uche, and Kingsley C. Patrick-Iwuanyanwu. 2022. Chromatographic techniques: types, principles, and applications. In *Analytical Techniques in Biosciences*. Elsevier, 73–101. DOI: https://doi.org/10.1016/B978-0-12-822654-4.00013-0.

[63] K. Kuroda, T. Ozawa, and T. Ueno. 2001. Characterization of sago palm (Metroxylon sagu) lignin by analytical pyrolysis. *Journal of agricultural and food chemistry* 49, 4, 1840–1847. DOI: https://doi.org/10.1021/jf001126i.

[64] Lab-Training.com. 2014. *Beer- Lambert Spectroscopic Absorbance Principle* (2014). Retrieved February 15, 2024 from.

[65] 2008. *Lebensmittelchemie*. Springer-Lehrbuch. Springer Berlin Heidelberg, Berlin, Heidelberg. DOI: https://doi.org/10.1007/978-3-540-73202-0.

[66] Stuart E. Lebo, Jerry D. Gargulak, and Timothy J. McNally. 2001. Lignin. In *Kirk-Othmer Encyclopedia of Chemical Technology*. Wiley. DOI: https://doi.org/10.1002/0471238961.12090714120914.a01.pub2.

[67] 2005. *Lehninger principles of biochemistry* (Fourth edition, first printing). W.H. Freeman and Company, New York.

[68] Dane R. Letourneau and Dietrich A. Volmer. 2023. Mass spectrometry-based methods for the advanced characterization and structural analysis of lignin: A review. *Mass spectrometry reviews* 42, 1, 144–188. DOI: https://doi.org/10.1002/mas.21716.

[69] Steven Y. Lin and Carlton W. Dence. 1992. *Methods in lignin chemistry*. Springer, Berlin, Barcelona.

[70] John C. Lindon, George E. Tranter, and David W. Koppenaal, Eds. 2017. *Encyclopedia of spectroscopy and spectrometry* (3rd edition). Academic Press is an imprint of Elsevier, Kidlington, Oxford, United Kingdom.

[71] Georg Löffler and Petro E. Petrides. 1997. *Biochemie und Pathobiochemie* (Fünfte, neu konzipierte und in allen Teilen komplett überarbeitete Auflage). Springer Lehrbuch. Springer Berlin Heidelberg, Berlin, Heidelberg, s.l.

[72] Fachuang Lu, Chen Wang, Mingjie Chen, Fengxia Yue, and John Ralph. 2021. A facile spectroscopic method for measuring lignin content in lignocellulosic biomass. *Green Chem.* 23, 14, 5106–5112. DOI: https://doi.org/10.1039/D1GC01507A.

[73] A. Ludwiczuk, K. Skalicka-Woźniak, and M. I. Georgiev. 2017. Terpenoids. In *Pharmacognosy*. Elsevier, 233–266. DOI: https://doi.org/10.1016/B978-0-12-802104-0.00011-1.

[74] Samy A. Madbouly and Chaoqun Zhang, Eds. 2021. *Biopolymers and composites*. *Processing and characterization*. De Gruyter STEM. Walter de Gruyter, Berlin, Boston.

[75] Sheri Madhu, Hayden A. Evans, Vicky V. T. Doan-Nguyen, John G. Labram, Guang Wu, Michael L. Chabinyc, Ram Seshadri, and Fred Wudl. 2016. Infinite Polyiodide Chains in the Pyrroloperylene-Iodine Complex: Insights into the Starch-Iodine and Perylene-Iodine Complexes. *Angewandte Chemie (International ed. in English)* 55, 28, 8032–8035. DOI: https://doi.org/10.1002/anie.201601585.

[76] Silvia Maitz and Marlene Kienberger. 2021. Investigation of acid hydrolysis for carbohydrate analysis in kraft black liquor. *Holzforschung* 76, 1, 49–59. DOI: https://doi.org/10.1515/hf-2021-0047.

[77] Alexandr A. Makarov, Andrea Rizzotto, Peter Meinke, and Eric C. Schirmer. 2016. Purification of Lamins and Soluble Fragments of NETs. *Methods in enzymology* 569, 79–100. DOI: https://doi.org/10.1016/bs.mie.2015.09.006.

[78] K. K. Mäkinen. 2000. The rocky road of xylitol to its clinical application. *Journal of dental research* 79, 6, 1352–1355. DOI: https://doi.org/10.1177/00220345000790060101.

[79] Edyta Małachowska, Marcin Dubowik, Piotr Boruszewski, Joanna Łojewska, and Piotr Przybysz. 2020. Influence of lignin content in cellulose pulp on paper durability. *Scientific reports* 10, 1, 19998. DOI: https://doi.org/10.1038/s41598-020-77101-2.

[80] Jasna Malešič, Ida Kraševec, and Irena Kralj Cigić. 2021. Determination of Cellulose Degree of Polymerization in Historical Papers with High Lignin Content. *Polymers* 13, 12. DOI: https://doi.org/10.3390/polym13121990.

[81] Constantin Mamat. 2016. *Organische Chemie*. Fernstudium Bachelor Chemie. Springer Spektrum, Berlin, Heidelberg.

[82] Patrick T. Martone, José M. Estevez, Fachuang Lu, Katia Ruel, Mark W. Denny, Chris Somerville, and John Ralph. 2009. Discovery of lignin in seaweed reveals convergent evolution of cell-wall architecture. *Current biology : CB* 19, 2, 169–175. DOI: https://doi.org/10.1016/j.cub.2008.12.031.

[83] Debra Mohnen. 2008. Pectin structure and biosynthesis. *Current opinion in plant biology* 11, 3, 266–277. DOI: https://doi.org/10.1016/j.pbi.2008.03.006.

[84] Hans Molisch. 1886. Zwei neue Zuckerreactionen. *Monatshefte fr Chemie* 7, 1, 198–209. DOI: https://doi.org/10.1007/BF01516570.

[85] Hervan M. Morgan, Wei Xie, Jianghui Liang, Hanping Mao, Hanwu Lei, Roger Ruan, and Quan Bu. 2018. A techno-economic evaluation of anaerobic biogas producing systems in developing countries. *Bioresource technology* 250, 910–921. DOI: https://doi.org/10.1016/j.biortech.2017.12.013.

[86] Immanuel Munk. 1886. Zur quantitativen Bestimmung des Zuckers und der sog. reducirenden Substanzen im Harn mittelst Fehling'scher Lösung. *Archiv f. pathol. Anat.* 105, 1, 63–82. DOI: https://doi.org/10.1007/BF01925199.

[87] Ayesha Naseer, Anum Jamshaid, Almas Hamid, Nawshad Muhammad, Moinuddin Ghauri, Jibran Iqbal, Sikander Rafiq, Shahzad khuram, and Noor S. Shah. 2019. Lignin and Lignin Based Materials for the Removal of Heavy Metals from Waste Water-An Overview. *Zeitschrift für Physikalische Chemie* 233, 3, 315–345. DOI: https://doi.org/10.1515/zpch-2018-1209.

[88] National Academy of Sciences. 1975. *Productivity of world ecosystems*. *Proceedings of a symposium, pres. August 31 - September 1, 1972 at the V general assembly of the Special Committee for the Intern. Biological Program, Seattle, Washington*. /Publication] / National Academy of Sciences, 2317. National Academy of Sciences, Washington, NY.

[89] 2024. *National Renewable Energy Laboratory (NREL) Home Page* (February 2024). Retrieved February 15, 2024 from https://www.nrel.gov/index.html.

[90] 2008. *Naturstoffchemie*. *Eine Einführung* (3., vollst. überarb. und erw. Aufl.). Springer-Lehrbuch. Springer, Berlin, Heidelberg.

[91] David L. Nelson and Michael M. Cox. 2017. *Lehninger principles of biochemistry* (Seventh edition, international edition). W.H. Freeman; Macmillan Higher Education, New York NY, Houndmills, Basingstoke.

[92] M. Ohta, M. Iwasaki, K. Kouno, and Y. O. UEDA. 1985. Mechanism of the Molisch reaction. *Chem. Pharm. Bull.* 33, 7, 2862–2865. DOI: https://doi.org/10.1248/cpb.33.2862.

[93] Kintaro Oshima and B. Tollens. 1901. Ueber Spectral-Reactionen des Methylfurfurols. *Ber. Dtsch. Chem. Ges.* 34, 2, 1425–1426. DOI: https://doi.org/10.1002/cber.19010340212.

[94] Donald L. Pavia, Gary M. Lampman, George S. Kriz, and James R. Vyvyan. 2015. *Introduction to spectroscopy* (Fifth edition). Cengage Learning, Australia.

[95] Mohammad Pessarakli. 2005. *Handbook of Photosynthesis, Second Edition* (2nd ed.). Books in Soils, Plants, and the Environment. CRC Press, Baton Rouge.

[96] Fredus N. Peters. 1936. The Furans: Fifteen Years of Progress. *Ind. Eng. Chem.* 28, 7, 755–759. DOI: https://doi.org/10.1021/ie50319a002.

[97] Rémy J. Petit and Arndt Hampe. 2006. Some Evolutionary Consequences of Being a Tree. *Annu. Rev. Ecol. Evol. Syst.* 37, 1, 187–214. DOI: https://doi.org/10.1146/annurev.ecolsys.37.091305.110215.

[98] Ward W. Pigman. 1972. *THE CARBOHYDRATES 2E V1A*. *Chemistry and Biochemistry* (2nd ed.). Elsevier Science, Oxford.

[99] Zoë A. Popper, Gurvan Michel, Cécile Hervé, David S. Domozych, William G. T. Willats, Maria G. Tuohy, Bernard Kloareg, and Dagmar B. Stengel. 2011. Evolution and diversity of plant cell walls: from algae to flowering plants. *Annual review of plant biology* 62, 567–590. DOI: https://doi.org/10.1146/annurev-arplant-042110-103809.

[100] Joachim Radkau and Ingrid Schäfer. 2007. *Holz*. *Wie ein Naturstoff Geschichte schreibt*. Stoffgeschichten, Bd. 3. Oekom Verl., München.

[101] Himadri Rajput, Eilhann E. Kwon, Sherif A. Younis, Seunghyun Weon, Tae H. Jeon, Wonyong Choi, and Ki-Hyun Kim. 2021. Photoelectrocatalysis as a high-efficiency platform for pulping wastewater treatment and energy production. *Chemical Engineering Journal* 412, 128612. DOI: https://doi.org/10.1016/j.cej.2021.128612.

[102] Hanne Rautenstrauch, Anne Rebenstorff, Steffen Gudenschwager, and Klaus Ruppersberg. 2023. Ein sicherer Kohlenhydratnachweis. *Chemie in nserer Zeit* 57, 3, 172–179. DOI: https://doi.org/10.1002/ciuz.202100036.

[103] Jane B. Reece and Neil A. Campbell. op. 2011. *Campbell biology* (9th ed.). Pearson, Boston.

[104] T. A. Richmond and C. R. Somerville. 2000. The cellulose synthase superfamily. *Plant physiology* 124, 2, 495–498. DOI: https://doi.org/10.1104/pp.124.2.495.

[105] Marcel B. Roberfroid. 2007. Inulin-type fructans: functional food ingredients. *The Journal of nutrition* 137, 11 Suppl, 2493S-2502S. DOI: https://doi.org/10.1093/jn/137.11.2493S.

[106] RSC Education. 2024. *App quantifies chemicals in thin-layer chromatography* (February 2024). Retrieved February 15, 2024 from https://edu.rsc.org/science-research/app-quantifies-chemicals-in-thin-layer-chromatography/3010338.article.

[107] Klaus Ruppersberg, Hanne Rautenstrauch, and Stefan Thomsen. 2022. Know Thy Carbs! Safer Carbohydrate Detection Methods for School Labs – Part 2. *ChemViews. DOI: https://doi.org/*10.1002/chemv.202200023.

[108] L. RUZICKA. 1953. The isoprene rule and the biogenesis of terpenic compounds. *Experientia* 9, 10, 357–367. DOI: https://doi.org/10.1007/BF02167631.

[109] David Sadava. 2011. *Life*. *The science of biology* (9th edition). W.H.Freeman, Sunderland, Mass.

[110] Thomas A. Sanders. 2016. Introduction. In *Functional Dietary Lipids*. Elsevier, 1–20. DOI: https://doi.org/10.1016/B978-1-78242-247-1.00001-6.

[111] Wantana Sangchoom and Robert Mokaya. 2015. Valorization of Lignin Waste: Carbons from Hydrothermal Carbonization of Renewable Lignin as Superior Sorbents for CO 2 and Hydrogen Storage. *ACS Sustainable Chem. Eng.* 3, 7, 1658–1667. DOI: https://doi.org/10.1021/acssuschemeng.5b00351.

[112] Henrik V. Scheller and Peter Ulvskov. 2010. Hemicelluloses. *Annual review of plant biology* 61, 263–289. DOI: https://doi.org/10.1146/annurev-arplant-042809-112315.

[113] Tina B. Schreier and Julian M. Hibberd. 2019. Variations in the Calvin-Benson cycle: selection pressures and optimization? *Journal of experimental botany* 70, 6, 1697–1701. DOI: https://doi.org/10.1093/jxb/erz078.

[114] Theodor Seliwanoff. 1887. Notiz über eine Fruchtzuckerreaction. *Ber. Dtsch. Chem. Ges.* 20, 1, 181–182. DOI: https://doi.org/10.1002/cber.18870200144.

[115] R. R. Selvendran and M. A. O'Neill. 1987. Isolation and analysis of cell walls from plant material. *Methods of biochemical analysis* 32, 25–153. DOI: https://doi.org/10.1002/9780470110539.ch2.

[116] T. D. Sharkey. 1996. Isoprene synthesis by plants and animals. *Endeavour* 20, 2, 74–78. DOI: https://doi.org/10.1016/0160-9327(96)10014-4.

[117] Alvin Silverstein, Virginia B. Silverstein, and Laura S. Nunn. 2008. *Photosynthesis* (Revised ed.). Science concepts, Second series. Twenty-First Century Books, Minneapolis, MN.

[118] Michael Simone-Finstrom and Marla Spivak. 2010. Propolis and bee health: the natural history and significance of resin use by honey bees. *Apidologie* 41, 3, 295–311. DOI: https://doi.org/10.1051/apido/2010016.

[119] Douglas A. Skoog, Donald M. West, and F. J. Holler. op. 2014. *Skoog and West's fundamentals of analytical chemistry* (9th edition). Cengage Learning, Belmont (Calif.).

[120] Peter J. Smith, Thomas M. Curry, Jeong-Yeh Yang, William J. Barnes, Samantha J. Ziegler, Ashutosh Mittal, Kelley W. Moremen, William S. York, Yannick J. Bomble, Maria J. Peña, and Breeanna R. Urbanowicz. 2022. Enzymatic Synthesis of Xylan Microparticles with Tunable Morphologies. *ACS materials Au* 2, 4, 440–452. DOI: https://doi.org/10.1021/acsmaterialsau.2c00006.

[121] H. S. Son, Y. S. Hong, W. M. Park, M. A. Yu, and C. H. Lee. 2009. A novel approach for estimating sugar and alcohol concentrations in wines using refractometer and hydrometer. *Journal of food science* 74, 2, C106-11. DOI: https://doi.org/10.1111/j.1750-3841.2008.01036.x.

[122] André M. Striegel. 2009. *Modern Size-Exclusion Chromatography*. *Practice of gel permeation and gel filtration chromatography* (2. ed.). Wiley, Hoboken, N.J.

[123] Tayyab Muhammad. 2018. Bioethanol production from lignocellulosic biomass by environment-friendly pretreatment methods: A review. *Appl. Ecol. Env. Res.* 16, 1, 225–249. DOI: https://doi.org/10.15666/aeer/1601_225249.

[124] Gianni Teo, Yasuo Suzuki, Sandie L. Uratsu, Bruce Lampinen, Nichole Ormonde, William K. Hu, Ted M. DeJong, and Abhaya M. Dandekar. 2006. Silencing leaf sorbitol synthesis alters long-distance partitioning and apple fruit quality. *Proceedings of the National Academy of Sciences of the United States of America* 103, 49, 18842–18847. DOI: https://doi.org/10.1073/pnas.0605873103.

[125] The A Level Biologist - Your Hub |. 2017. *Carbohydrates (AQA) | The A Level Biologist - Your Hub* (2017). Retrieved February 15, 2024 from https:// thealevelbiologist.co.uk/carbohydrates-3/.

[126] Alfred Thomas. 2003. Fats and Fatty Oils. In *Ullmann's Encyclopedia of Industrial Chemistry*. Wiley. DOI: https://doi.org/10.1002/14356007.a10_173.

[127] Renata Toczyłowska-Mamińska. 2017. Limits and perspectives of pulp and paper industry wastewater treatment – A review. *Renewable and Sustainable Energy Reviews* 78, 764–772. DOI: https://doi.org/10.1016/j.rser.2017.05.021.

[128] Giorgio Tofani, Iris Cornet, and Serge Tavernier. 2021. Estimation of hydrogen peroxide effectivity during bleaching using the Kappa number. *Chem. Pap.* 75, 11, 5749–5758. DOI: https://doi.org/10.1007/s11696-021-01756-y.

[129] B. Tollens. 1882. Ueber ammon-alkalische Silberlösung als Reagens auf Aldehyd. *Ber. Dtsch. Chem. Ges.* 15, 2, 1635–1639. DOI: https://doi.org/10.1002/cber.18820150243.

[130] 2011. *Ullmann's encyclopedia of industrial chemistry* (7. comp. rev. ed.). Wiley-VCH, Weinheim.

[131] M. van den Mooter, H. Maraite, L. Meiresonne, J. Swings, M. Gillis, K. Kersters, and J. de Ley. 1987. Comparison Between Xanthomonas campestris pv. manihotis (ISPP List 1980) and X. campestris pv. cassavae (ISPP List 1980) by Means of Phenotypic, Protein Electrophoretic, DNA Hybridization and Phytopathological Techniques. *Microbiology* 133, 1, 57–71. DOI: https://doi.org/10.1099/00221287-133-1-57.

[132] Vladimir I. Vernadskij. 1998. *The biosphere*. A Peter N. Nevraumont Book. Copernicus, New York, Heidelberg.

[133] Joran Verspreet, Sami Hemdane, Emmie Dornez, Sven Cuyvers, Annick Pollet, Jan A. Delcour, and Christophe M. Courtin. 2013. Analysis of storage and structural carbohydrates in developing wheat (Triticum aestivum L.) grains using quantitative analysis and microscopy. *Journal of agricultural and food chemistry* 61, 38, 9251–9259. DOI: https://doi.org/10.1021/jf402796u.

[134] Alain A. Vertès, Ed. 2010. *Biomass to biofuels*. *Strategies for global industries*. Wiley, Chichester.

[135] Donald Voet and Judith G. Voet. 2011. *Biochemistry* (4. ed.). Wiley, Hoboken, NJ.

[136] Kurt P. C. Vollhardt and Neil E. Schore. 2020. *Organische Chemie* (6. Auflage). Wiley-VCH Verlag GmbH & Co. KGaA, Weinheim.

[137] William H. Welker. 1915. A Disturbing Factor in Barfoed's Test. *J. Am. Chem. Soc.* 37, 9, 2227–2230. DOI: https://doi.org/10.1021/ja02174a036.

[138] Roy L. Whistler, James N. BeMiller, and Eugene F. Paschall. *Starch*. *Chemistry and technology* (2nd ed.). Food science and technology (Academic Press).

[139] Theodorus C. Wijsman. 1989. Glycogen and galactogen in the albumen gland of the freshwater snail Lymnaea stagnalis: Effects of egg laying, photoperiod and starvation. *Comparative Biochemistry and Physiology Part A: Physiology* 92, 1, 53–59. DOI: https://doi.org/10.1016/0300-9629(89)90740-8.

[140] Wikipedia. 2024. *Column chromatography* (2024). Retrieved February 15, 2024 from https://en.wikipedia.org/w/index.php?title=Column_chromatography&oldid=1198209274.

[141] Wikipedia. 2024. *High-performance liquid chromatography* (2024). Retrieved February 15, 2024 from https://en.wikipedia.org/w/index.php?title=High-performance_liquid_chromatography&oldid=1207338922.

[142] M. Wilchek and I. Chaiken. 2000. An overview of affinity chromatography. *Methods in molecular biology (Clifton, N.J.)* 147, 1–6. DOI: https://doi.org/10.1007/978-1-60327-261-2_1.

[143] H. F. Zobel. 1988. Molecules to Granules: A Comprehensive Starch Review. *Starch Stärke (Starch - Stärke)* 40, 2, 44–50. DOI: https://doi.org/10.1002/star.19880400203.